ACTIVE SITE MUTANTS OF ESCHERICHIA COLI CITRATE SYNTHASE

by

Daniel Sousa Pereira

A Thesis Submitted to

The Faculty of Graduate Studies

In Partial Fulfillment of

The Requirements for the Degree of

Master of Science

Department of Chemistry

University of Manitoba

June 24, 1991

ISBN 0-315-76884-3

Canada

ACTIVE SITE MUTANTS OF ESCHERICHIA COLI CITRATE SYNTHASE

BY

DANIEL SOUSA PEREIRA

A thesis submitted to the Faculty of Graduate Studies of the University of Manitoba in partial fulfillment of the requirements of the degree of

MASTER OF SCIENCE

I

You hear with new ears,
after being experienced.

– Jimi Hendrix

ACKNOWLEDGEMENTS

Dr. Harry W. Duckworth, for his sincerity and helpful criticism during the past two years. I have benefited from your experience ... thank you.

Dr. Lynda Donald, of this laboratory, for taking me under her wing. I am very grateful to you, not only as a colleague, but as a friend. Thanks for everything.

Dr. Jamieson and the members of his laboratory.

The Departments of Chemistry and Microbiology, for use of equipment.

TABLE OF CONTENTS

LIST OF FIGURES

LIST OF TABLES

ABSTRACT

Escherichia coli citrate synthase (CS) is an allosteric, hexameric enzyme which is activated by KCl and inhibited by NADH. This enzyme catalyzes the first reaction of the TCA cycle, the condensation of OAA and AcCoA to form citrate and CoA-SH. Although the three-dimensional structure for *E. coli* CS is not yet available, its amino acid sequence is similar to that of the dimeric pig heart CS, whose structure is known; the similarity is especially close at the active site.

The aim of the research presented in this thesis was to determine whether the roles of *E. coli* CS active site residues coincided with the predicted roles of their pig heart CS counterparts. Oligonucleotide-directed *in vitro* mutagenesis was used to create four mutant *E. coli* citrate synthase enzymes designated CS R407L, CS F383A, CS D362A, and CS H264A. The effect these mutations had on the catalytic efficiency and allosteric nature of the enzyme was determined.

CS R407L, CS D362A, and CS H264A exhibited dramatic decreases in their respective kcat values. The removal of the positively charged Arg-407 residue, which is predicted to interact with the 4-carboxyl group of OAA, was associated with a 33 and 11 fold increase in the K_{iOAA} and K_{OAA} parameters. An 84 fold decrease in the kcat value implys that Arg-407 is needed to align OAA properly in the active site for reaction with AcCoA. Asp-362 and His-264 are residues believed to be involved in the enolization of AcCoA. When the residues were mutated to alanine; a 940 and 620 fold decrease in the kcat parameters for CS D362A and CS H264A, respectively, were observed in the presence of KCl.

CS D362A, CS H264A, and CS F383A enzymes exhibited changes in their allosteric nature. Kinetic (lower Km values for both substrates, lower KCl activation ratio, weakened binding of NADH) and physical (OAA induced ultraviolet difference spectra, in the absence and presence of KCl) evidence suggested that the CS D362A and CS H264A enzymes had their allosteric equilibria shifted towards the R state, before addition of ligands.

Phe-383 is a conserved *E. coli* active site residue. A role for the pig heart equivalent of Phe-383, namely Phe-397, has not been predicted. However, since an "edge-on" interaction of the phenyl ring with the substrates was observed in pig heart citrate synthase, it was of interest to mutate Phe-383 to alanine (CS F383A). As compared to the CS H264A results, CS F383A exhibited opposite, yet similar kinetic and physical evidence suggesting that CS F383A had its allosteric equilibrium shifted towards the T state, in the absence of ligands.

INTRODUCTION

CITRATE SYNTHASE

INVOLVEMENT IN CELLULAR RESPIRATION

Citrate synthase is a regulatory enzyme that catalyzes the first reaction of the tricarboxylic acid (TCA) cycle, the condensation of acetyl-CoA (AcCoA) with oxaloacetate (OAA). The condensation of the methyl carbon of AcCoA's acetyl group with the carbonyl group of OAA results in the formation of citrate and coenzyme A (CoA-SH). The TCA cycle (Figure 1), occurring after glycolysis and before the electron transport chain, serves two purposes in aerobic cell respiration. Catabolically, the first role of the TCA cycle is to oxidize metabolites entering the cycle as AcCoA to carbon dioxide (CO_2). In total, the TCA cycle generates 3 molecules of NADH, 1 molecule of $FADH_2$, and 1 molecule of ATP for each AcCoA molecule. Biosynthetically, the cycle's second responsibility is to supply precursors for the creation of macromolecules.

The glyoxylate cycle (Figure 2), which also utilizes citrate synthase as its first enzyme, is a modified form of the TCA cycle. It is not nearly as efficient an energy producing cycle as the TCA cycle, but it allows plants and certain microorganisms to utilize acetate and fatty acids as their sole source of carbon. Interestingly, the glyoxylate cycle is not present in animals since the enzymes isocitrate lyase and malate synthase are absent.

Citrate synthase is also involved in the non-cyclic TCA pathway (Figure 3) common to some facultative anaerobes such as *E. coli*. Upon need, this anaplerotic pathway creates TCA cycle intermediates for the creation of other macromolecules.

All in all, the cyclic and non-cyclic TCA pathways as well as the glyoxylate cycle, act in harmony to maintain the cell's energetic and biosynthetic needs.

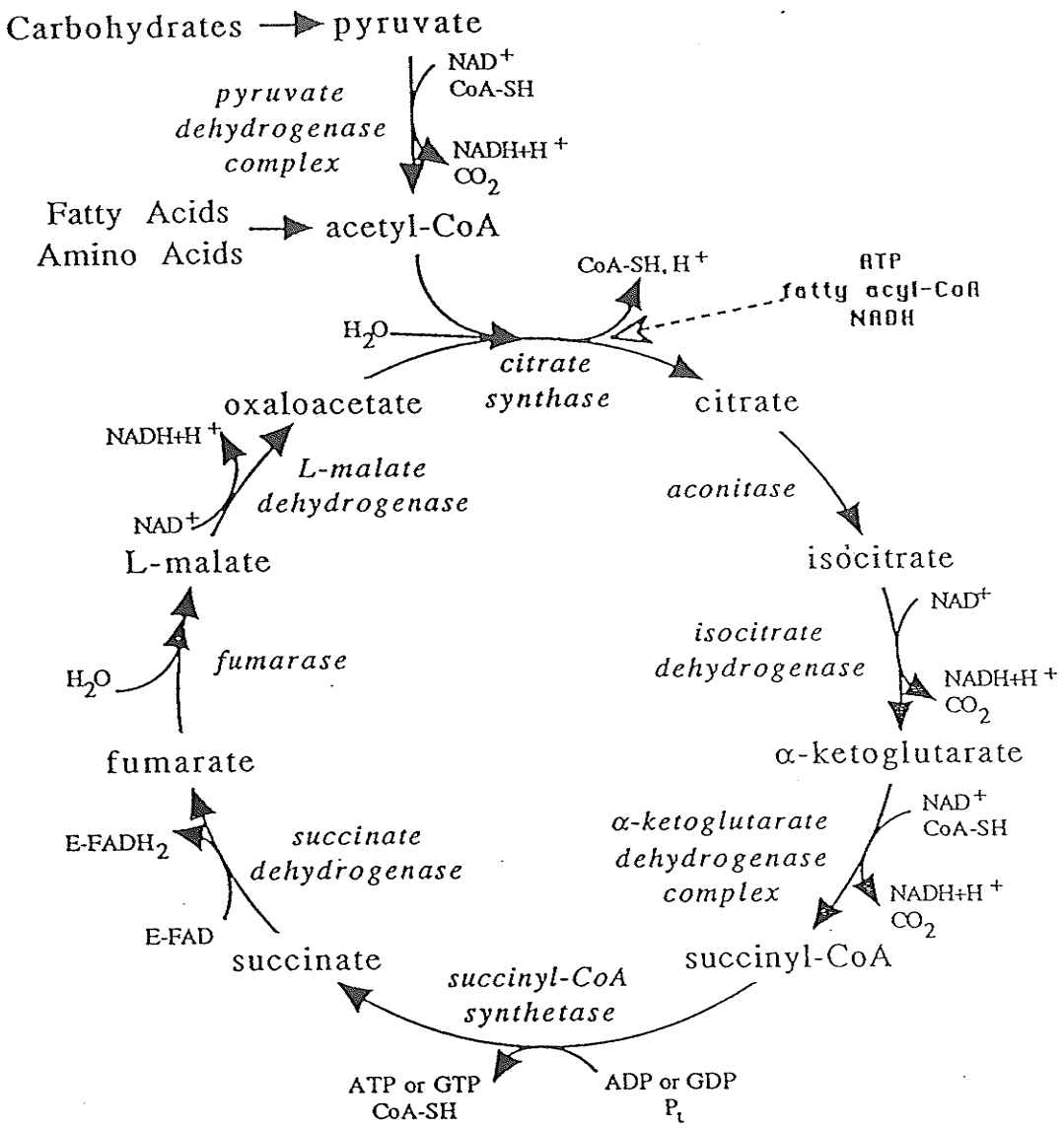

FIGURE 1: THE TRICARBOXYLIC ACID (TCA) CYCLE (TAKEN FROM MOLGAT, 1990)

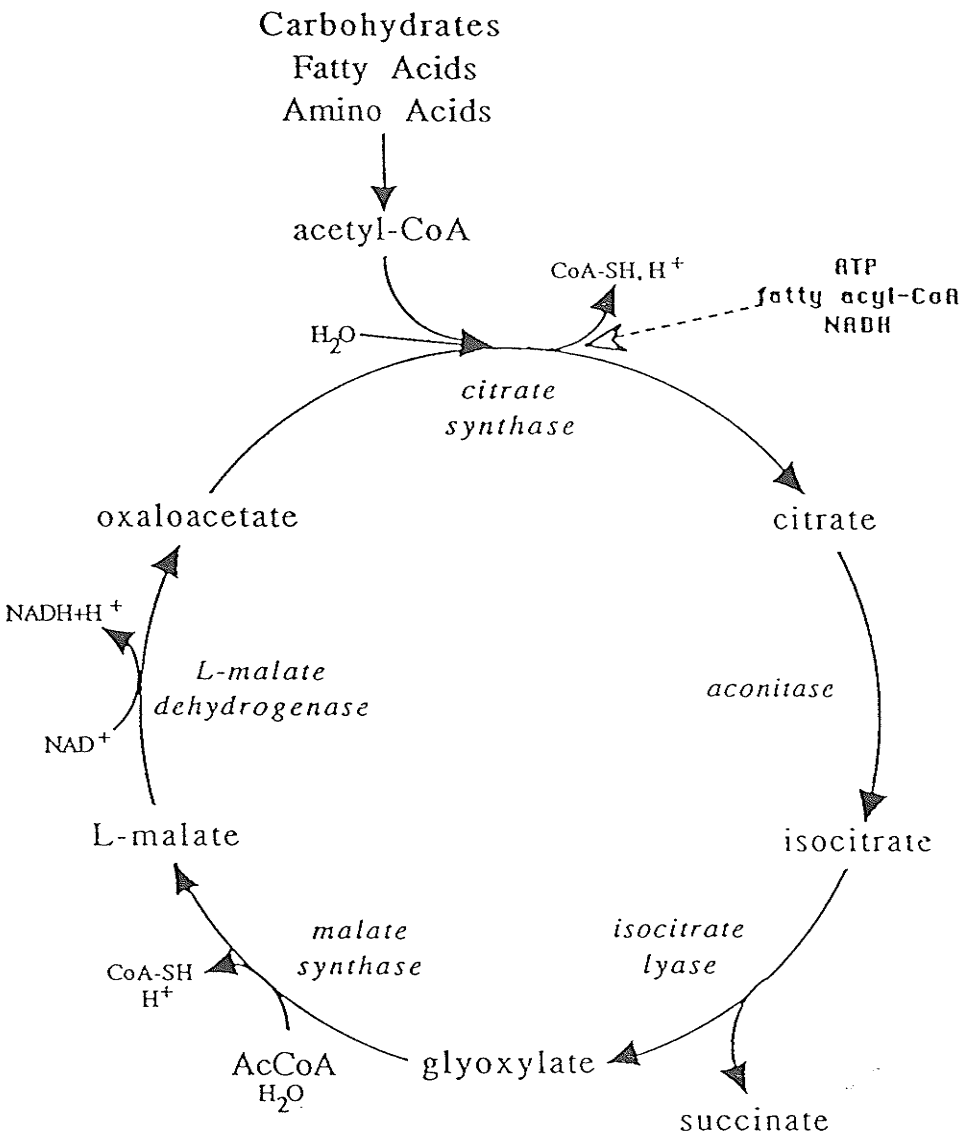

FIGURE 2: THE GLYOXYLATE CYCLE
(TAKEN FROM MOLGAT, 1990)

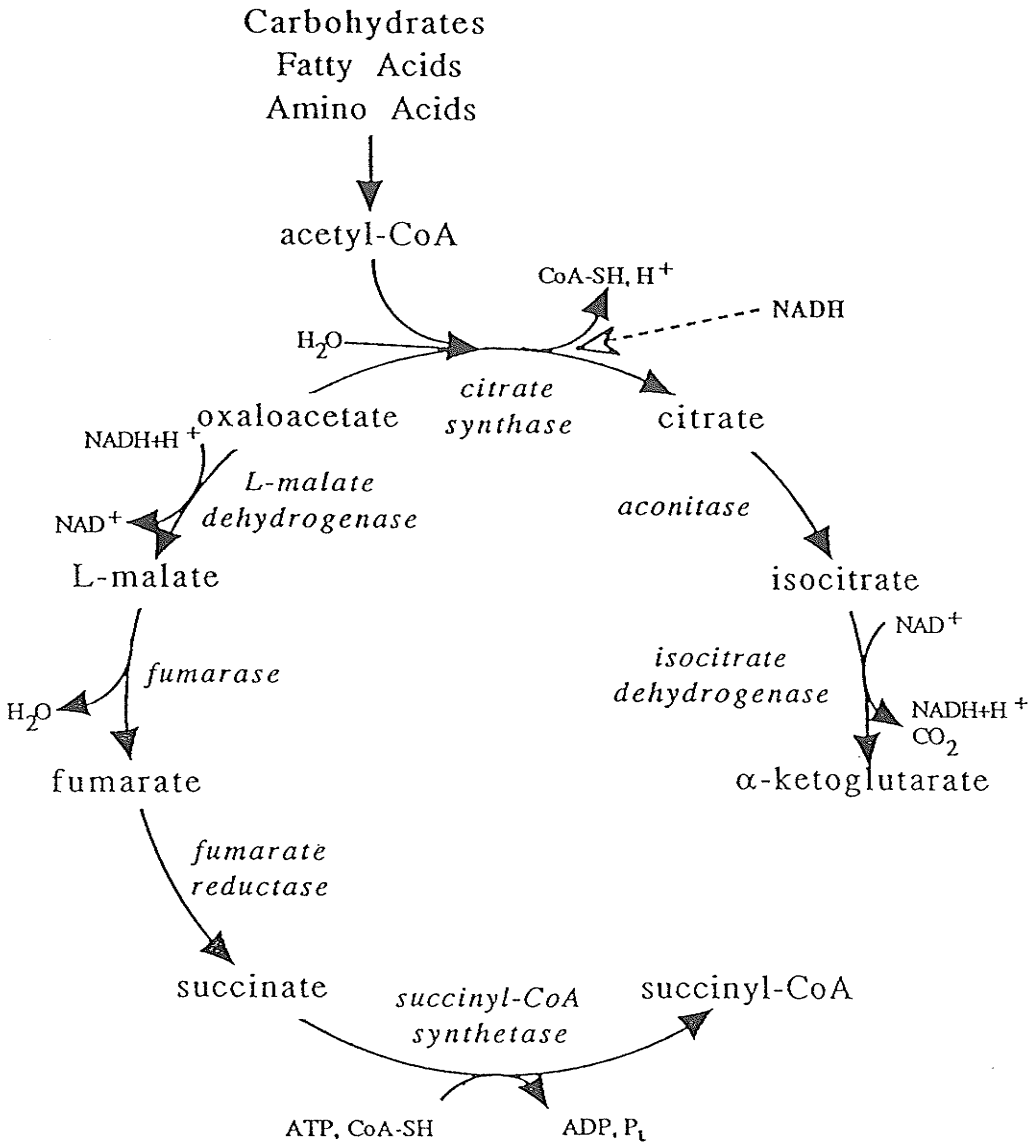

FIGURE 3: THE NON-CYCLIC TRICARBOXYLIC ACID PATHWAY (TAKEN FROM MOLGAT, 1990)

ALIGNMENT AND SEQUENCE COMPARISONS

Currently, four eukaryotic and five prokaryotic citrate synthase amino acid sequences are known. The eukaryotic sequences are from pig heart (Bloxham et al., 1982), two from baker's yeast (Suissa et al., 1984; Rosenkrantz et al., 1986), and a pea plant, *Arabidopsis thaliana* (Unger et al., 1989). *Escherichia coli* (Ner et al., 1983; Anderson and Duckworth, 1988), *Acinetobacter anitratum* (Donald & Duckworth, 1987), *Pseudomonas aeruginosa* (Donald et al., 1989), *Rickettsia prowazekii* (Wood et al., 1987), and *Acetobacter aceti* (Fukaya et al., 1990) are the sources of the prokaryotic sequences. It should be noted that the pig heart and *E. coli* citrate synthases were confirmed by protein sequencing. Donald & Duckworth, 1989, compared the above mentioned sequences on the basis that the functionally essential active site amino acids are totally conserved among all the known citrate synthases. As a result, alignment of these functionally essential amino acids permits regions of sequence similarity between the pig heart (437 residues; Bloxham et al., 1981) and *E. coli* (426 residues; Ner et al, 1983) citrate synthases to be noticed. Actually, approximately 30% sequence similarity exists between *E. coli* and pig heart citrate synthase. Furthermore, these alignments illustrate that every residue suggested to be important for enzyme interaction with OAA and 13 of a possible 25 putative CoA and citrate interacting residues are conserved between pig heart and *E. coli* citrate synthases.

PIG HEART CITRATE SYNTHASE X-RAY STRUCTURE

The pig and chicken heart citrate synthases are the only citrate synthases which have been crystallized. The three dimensional structures of the pig and chicken heart enzymes were resolved using X-ray crystallography at 1.7 and 2.7 Å respectively (Remington, Wiegand, & Huber, 1982).

The pig heart citrate synthase subunit (Figure 4) is "comma" shaped and is composed of a larger and a smaller domain (Remington et al., 1982). Twenty α-helices, labelled A to T, are distributed between the four domains of the pig heart citrate synthase dimer. Fifteen α-helices are found in the large domains while five exist in the small domains. The domains of each subunit are hinged by two passes of the polypeptide backbone, between helices M and N and R and S. The two subunits bind antiparallel to each other. They bind large domain to large domain, on the subunit face of the active site. The helices involved in the antiparallel contact are F, G, M, and L on either subunit.

The pig heart citrate synthase has been crystallized with OAA, CoA (AcCoA analogue), and citrate. As a result, 3 conformations have been observed (Wiegand and Remington, 1986). The three conformations are: open conformation (containing citrate); a partially closed conformation (in the presence of OAA or CoA); and a fully closed conformation (in the presence of both citrate and CoA). An 18.5 Å rotation between the large and small domains, and a total shift of as much as 15 Å by other atoms is the largest change observed between the open and closed conformers (Wiegand & Remington, 1986). Furthermore, the two closed forms are structurally similar despite minor changes observed at their active sites.

Interestingly, when OAA is added to the open form, the crystals fracture (Remington et al., 1982). This finding suggests that OAA, found in the partially

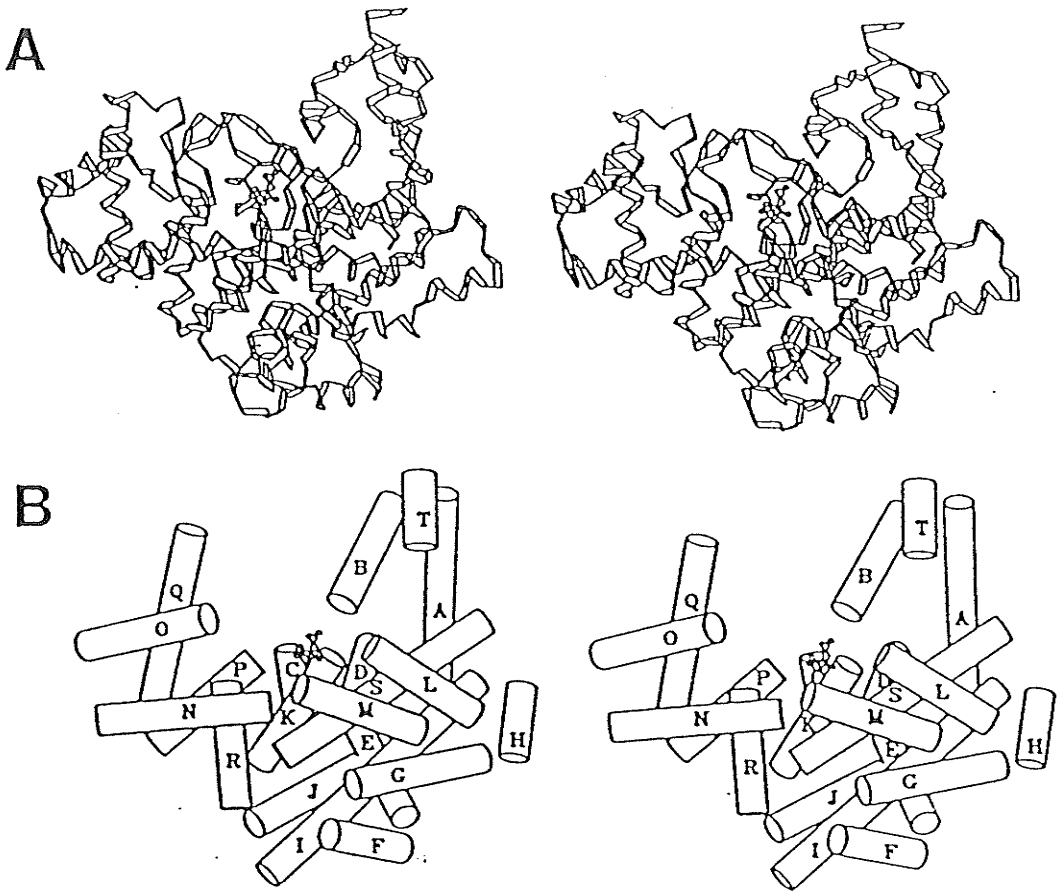

FIGURE 4: STEREO DRAWINGS OF A PIG HEART CITRATE SYNTHASE SUBUNIT IN ITS CITRATE-BOUND OPEN CONFORMATION (WIEGAND & REMINGTON, 1986). THE RIBBON (A) AND CYLINDERIC (**B**) REPRESENTATIONS OF THE SECONDARY STRUCTURE ARE VIEWS OF THE DIMER INTERFACE.

closed form, induces the conformational shift observed between the open and partially closed forms. It is believed that the binding of OAA creates minute changes in the orientations of amino acid side chains which translate into small yet significant adjustments and rotations of helices within both domains (Lesk & Chothia, 1984). In addition, in the open conformation, the small domain does not make contact with the other subunit. However, in the closed conformations, the small domain of one subunit does meet the large domain of the other. The CoA binding site found in closed conformation does not exist until conversion from the open conformation to the closed conformation occurs.

The pig heart crystal structure shows that the active site is located in a cleft between the large and small domains (Remington et al, 1982). The active site is composed of amino acids from both domains of a single subunit and three residues from the large domain of the opposite subunit. Therefore, each dimer has two active sites, which are complete only when the two subunits unite to form the dimer. As a result, it has been suggested that the enzyme is active only when the dimer is created (Else et al., 1988).

THE MODEL OF *E. coli* CITRATE SYNTHASE

Usually, to create an accurate structural model of an enzyme, its three dimensional X-ray structure must be known. The three dimensional X-ray structure of *E. coli* citrate synthase is not known. However, because an approximate 30% sequence similarity between *E. coli* and pig heart citrate synthases exist, a three dimensional working model for *E. coli* citrate synthase (Figure 5) has been created by building its sequence into the structure of the pig heart enzyme (Duckworth et al, 1987). The *E. coli* citrate synthase model is

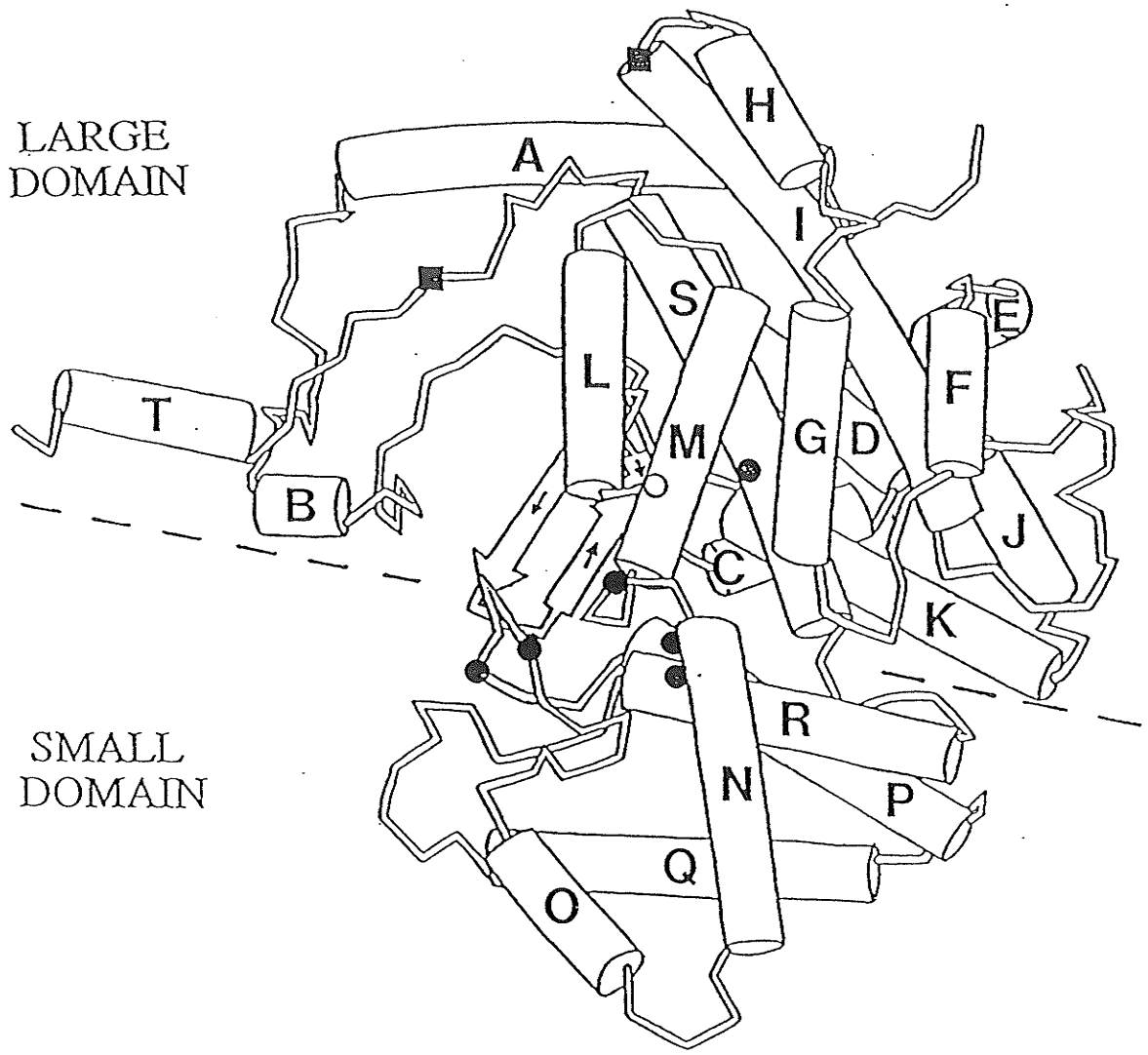

FIGURE 5: THE THREE DIMENSIONAL WORKING MODEL OF AN *E. coli* CITRATE SYNTHASE SUBUNIT (MODIFIED - DUCKWORTH et al., 1987). THE MODEL PROPOSES A SINGLE SECTION OF β-SHEET (ARROWS) AND 20 α-HELICES (15 IN THE LARGE DOMAIN (A TO M, S AND T) & 5 IN THE SMALL DOMAIN (N TO R)). ACTIVE SITE RESIDUES ARE REPRESENTED BY SOLID DOTS (HIS-229 BY A HOLLOW DOT SINCE BEHIND M-HELIX). ACTIVE SITE RESIDUES CONTRIBUTED FROM OTHER SUBUNIT ARE REPRESENTED BY SOLID SQUARES.

structurally similar to the pig heart structure. There are twenty α-helices (A to T) and a three stranded section of antiparallel β-sheet. The large domain has the A to M, S and T helices, while N to R comprise the small domain helices. In addition, the conserved M-N and R-S inter-helical regions "hinging" the domains are present in the *E. coli* citrate synthase model. Presence of the "hinge" region was demonstrated when two chimeric citrate synthases were created by domain exchange between the *E. coli* and *A. anitratum* enzymes (Molgat, Thesis, 1990).

Because NADH does not bind to nor inhibit pig heart citrate synthase, efforts to locate the NADH binding site in the *E. coli* model cannot be accomplished by sequence comparisons. Chemical modification studies of *E. coli* citrate synthase have identified Cys-206 as being at or near the putative NADH binding site (Duckworth et al, 1987). This finding is associated with the fact that the Ellman's reagent - DTNB (5,5'-dithiobis-(2-nitrobenzoic) acid) reacts with a cysteine (probably Cys-206) to abolish citrate synthases sensitivity to NADH (Talgoy et al., 1979).

REACTION MECHANISM OF *E. coli* & PIG HEART CITRATE SYNTHASE

As stated earlier, citrate synthase catalyzes the condensation of AcCoA with OAA to produce citrate and CoA-SH. It should be noted that citrate synthase is the only TCA cycle enzyme capable of assisting in the formation of a carbon-carbon bond between its substrates. The proposed reaction mechanism is based on kinetic (Johansson & Pettersson, 1974) and X-ray (Remington et al., 1982; Wiegand & Remington, 1986; Karpusas et al, 1990) studies conducted on pig heart citrate synthase as well as kinetic studies of *E.*

coli (Wright & Sanwal, 1971) citrate synthase. These studies of *E. coli* and pig heart citrate synthases as well as similarities in their protein sequences, especially at the active site, imply a common reaction mechanism. Table 1 lists the predicted roles of active site amino acids in the pig heart and *E. coli* citrate synthases.

It is believed that the reaction mechanism is governed by an Ordered Bi Bi equation (Cleland, 1963) as seen in Figure 6. The foundation of the equation is that OAA binds to citrate synthase before AcCoA does.

The specifics of the proposed reaction mechanism are shown in the *E. coli* citrate synthase reaction mechanism scheme (Figure 7). It should be noted that visualization and description of the amino acids involved in the reaction mechanism was made possible by viewing the pig heart citrate synthase dimer/OAA complex using the Silicon Graphics Personal IRIS molecular graphics system.

When OAA binds to the active sites in each dimer of citrate synthase, the dimers are in their partially closed conformation. The carbonyl carbon of OAA appears to be centered at the end of a narrow tunnel. AcCoA approaches the carbonyl carbon through the tunnel and binds to the active site in the vicinity of OAA. Step One shows the deprotonated form of Asp-362 abstracting a proton from the methyl carbon of the acetyl group of AcCoA. The negative charge of the enol oxygen is then stabilized by protonation by His-264. As a result, the enol form of AcCoA arises. Nucleophilic attack by the enol on the *si* face of the carbonyl group of OAA constitutes the condensation portion of the reaction mechanism (see Step Two). The nucleophilic attack occurs readily since Arg-314 and His-305 polarize the carbonyl group of OAA. His-305 protonates the carbonyl oxygen of OAA, forming citryl-CoA (a thioester). Step Three shows Asp-362 in its deprotonated form attacking the carbonyl carbon

of citryl-CoA. Consequently, His-264 protonates the negative charge of the carbonyl oxygen which causes a tetrahedral intermediate to be formed. His-264 then deprotonates the hydrogen used to stabilize the negative charge of the carbonyl carbon and causes free CoA-SH to be released. Breakdown of the tetrahedral intermediate results (see Step Four) and is followed by the formation of a mixed anhydride which is proposed to interact with one of two water molecules found in the pig heart citrate synthase crystal. The water molecule is believed to attack the carbonyl carbon. As a result, the negative charge of the oxygen is stabilized when His-264 protonates it. The outcome is a tetrahedral anhydride hydrolysis intermediate (see Step Five). Finally, Step Six displays proton abstraction by His-264, which allows Asp-362 to be released and restored as citrate is formed and released.

The citrate synthase reaction mechanism accounts for the three conformations found in pig heart citrate synthase. The open form exists when citrate is present in the active site. The partially closed conformation arises once OAA binds. It is possible that the fully closed conformation does not result when AcCoA binds, but results following the enolization and condensation portions of the reaction mechanism. In other words, the conversion from the partially to fully closed conformation happens as citryl-CoA is formed.

Conformational changes in *E. coli* citrate synthase are a result of interactions between active site amino acids and substrates, inhibitors, or activators. These interactions and the conformational changes caused by them are governed by the laws of allostery.

TABLE 1: PREDICTED ROLES OF ACTIVE SITE AMINO ACIDS IN PIG HEART AND *E. coli* CITRATE SYNTHASES

PIG HEART CITRATE SYNTHASE RESIDUE	EQUIVALENT *E. coli* CITRATE SYNTHASE RESIDUE	ROLE
ARG-421❶†	ARG-407❶†	- BINDS 4-CARBOXYL OF OAA AS WELL AS CITRATE
ARG-401†	ARG-387†	- BINDS 1-CARBOXYL OF OAA AS WELL AS CITRATE
ASP-375❷†❖	ASP-362❷†❖	- ASSISTS IN THE PROTON ABSTRACTION AND ENOLIZATION OF AcCoA - FOLLOWING THE ALDOL CONDENSATION, ATTACKS THE CARBONYL OF CITRYL-CoA
ARG-329†	ARG-314†	- BINDS 1-CARBOXYL AND POLARIZES THE CARBONYL OF OAA AS WELL AS BINDS CITRATE
HIS-320❷†	HIS-305❷†	- BINDS 4-CARBOXYL AND POLARIZES THE CARBONYL OF OAA ENHANCING ATTACK BY AcCoA. ALSO BINDS CITRATE
HIS-274❷†	HIS-264❷†	- ABSTRACTS PROTON FROM ENOL FORM OF AcCoA AS WELL AS THE MIXED ANHYDRIDE INTERMEDIATE
HIS-238†	HIS-229†	- BINDS 4-CARBOXYL OF OAA AS WELL AS CITRATE
PHE-397†	PHE-383†	- UNKNOWN
Me_3-LYS-368✙	LYS-355✙	- BINDS 5'-DIPHOSPHATE OF AcCoA'S CoA GROUP
ASP-327✙	ASP-312✙	- BINDS CITRATE
ARG-324✙	LYS-309✙	- BINDS 5'-DIPHOSPHATE OF AcCoA'S CoA GROUP
ARG-164❶†	ARG-157❶†	- BINDS 3'-DIPHOSPHATE OF AcCoA'S CoA GROUP
ARG-46❶†	ARG-32❶†	- BINDS 5'-DIPHOSPHATE OF AcCoA's CoA GROUP

❶ - RESIDUES CONTRIBUTED BY OTHER SUBUNIT

❷ - RESIDUES INVOLVED IN CATALYSIS

† - WIEGAND ET AL., 1986

✙ - REMINGTON ET AL., 1982

❖ - KARPUSAS ET AL., 1990

$$\text{Enzyme} + \text{OAA} \underset{k_2}{\overset{k_1}{\rightleftarrows}} \text{Enzyme–OAA}$$

$$\text{Enzyme–OAA} + \text{AcCoA} \underset{k_4}{\overset{k_3}{\rightleftarrows}} \text{Enzyme–OAA–AcCoA}$$

$$\text{Enzyme–OAA–AcCoA} \rightleftarrows \text{Enzyme–Citrate–CoA}$$

$$\text{Enzyme–Citrate–CoA} \underset{k_6}{\overset{k_5}{\rightleftarrows}} \text{Enzyme–Citrate} + \text{CoA}$$

$$\text{Enzyme–Citrate} \underset{k_8}{\overset{k_7}{\rightleftarrows}} \text{Enzyme} + \text{Citrate}$$

FIGURE 6: THE ORDERED BI BI EQUATION (CLELAND, 1963) AS APPLIED TO CITRATE SYNTHASE

FIGURE 7: CITRATE SYNTHASE REACTION MECHANISM

STEP ONE

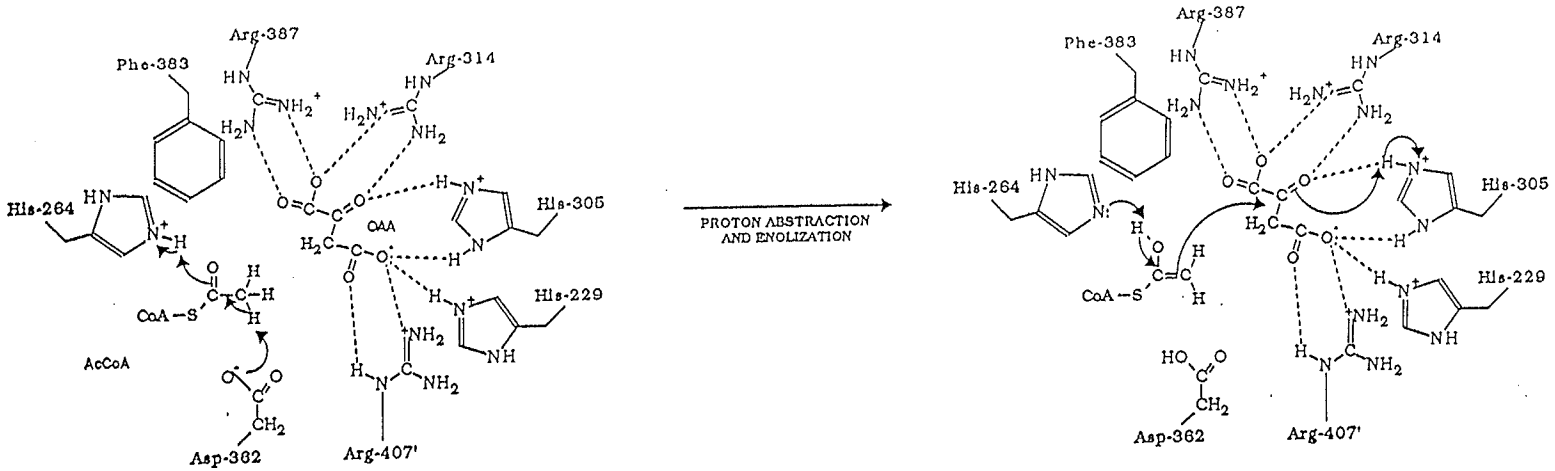

ASPARTATE-362 INDUCED ACTIVATION OF AcCoA

STEP TWO

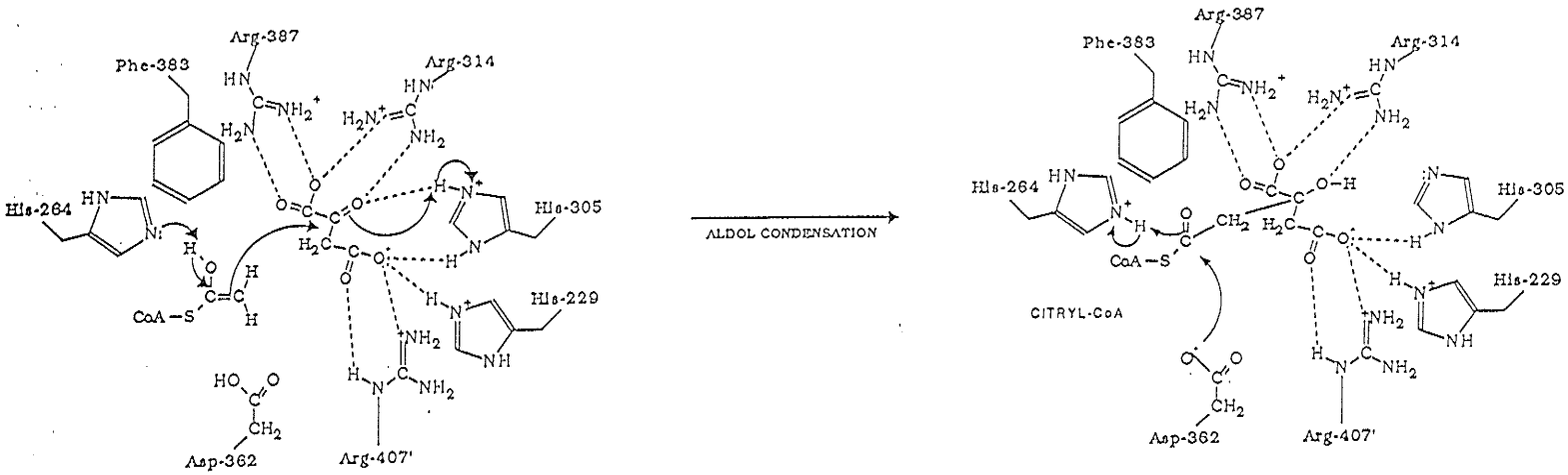

CITRYL-CoA FORMATION VIA ALDOL CONDENSATION

STEP THREE

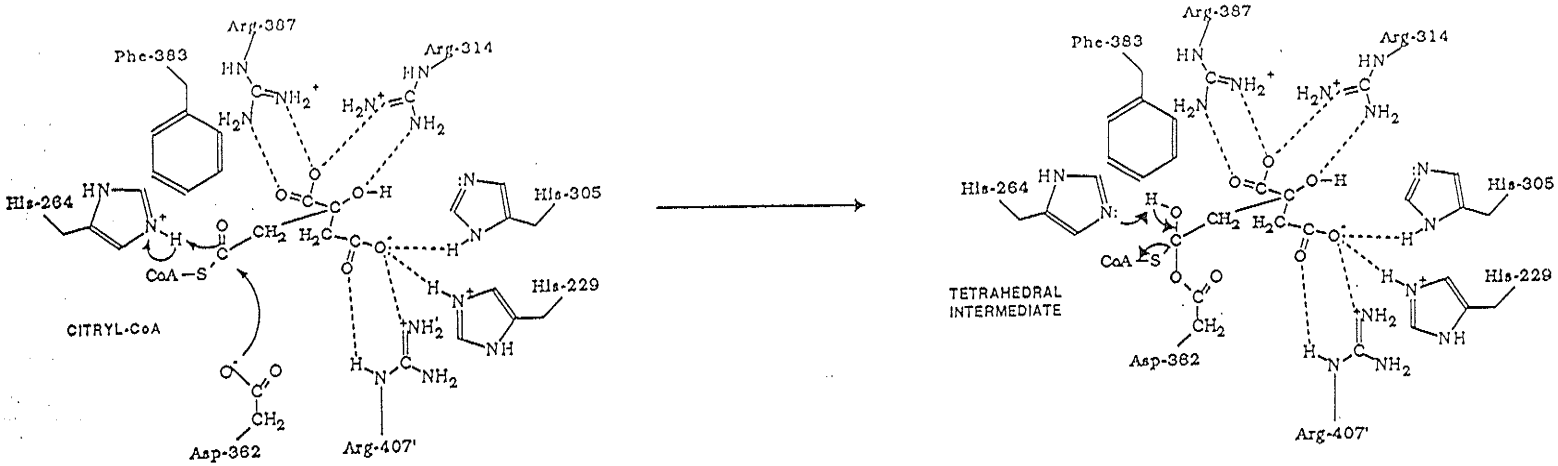

TETRAHEDRAL INTERMEDIATE FORMATION

STEP FOUR

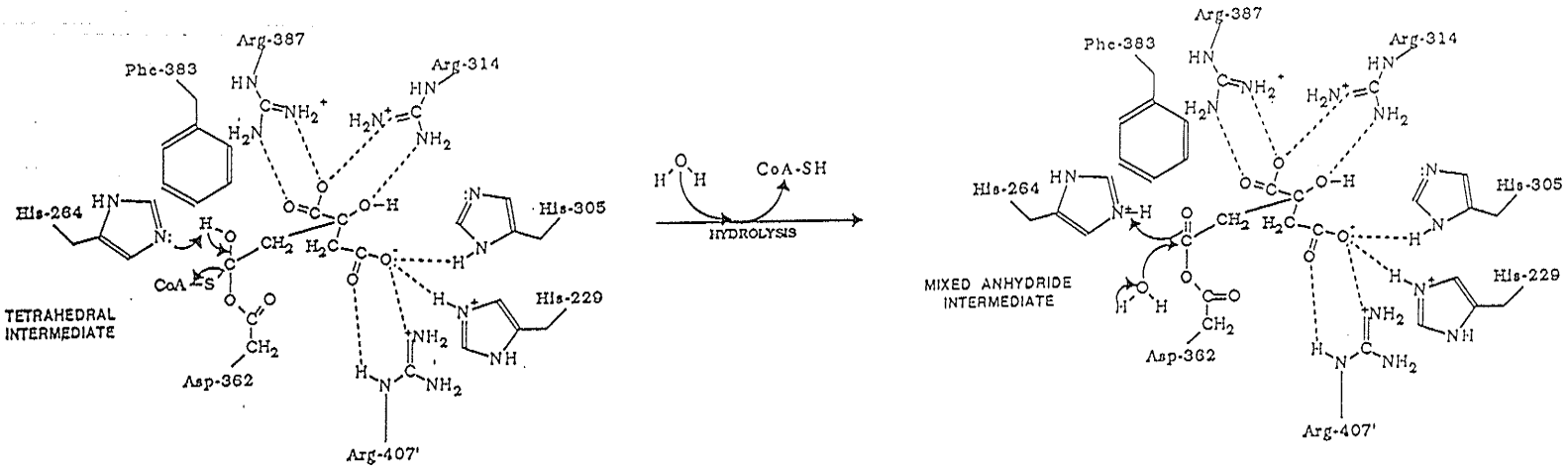

FORMATION OF MIXED ANHYDRIDE INTERMEDIATE
VIA TETRAHEDRAL INTERMEDIATE BREAKDOWN

STEP FIVE

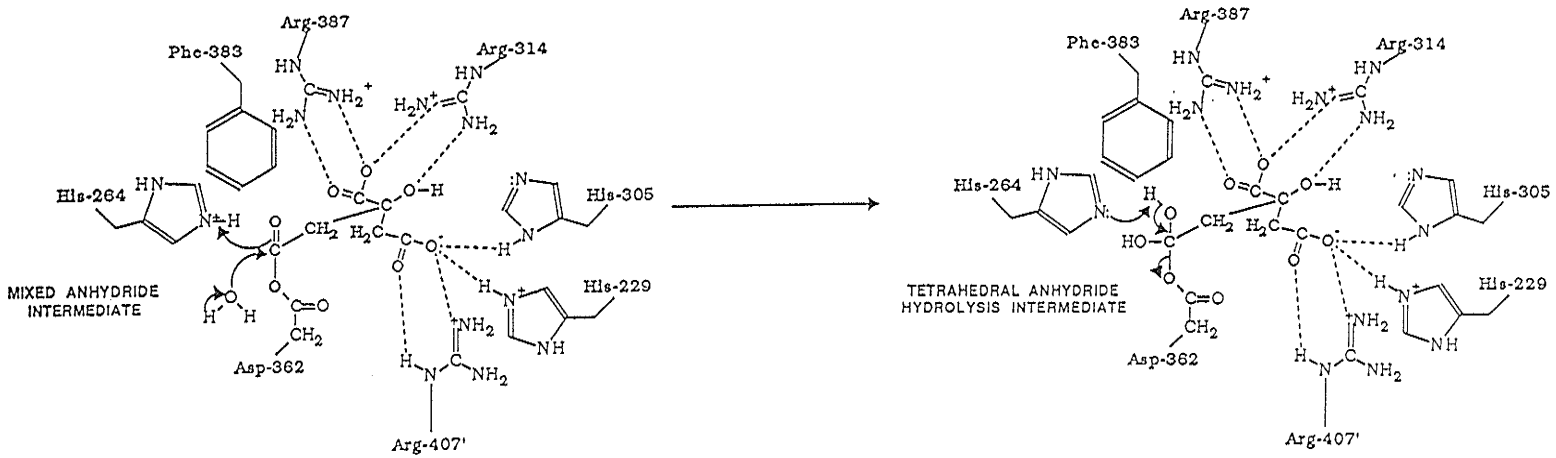

FORMATION OF TETRAHEDRAL ANHYDRIDE HYDROLYSIS INTERMEDIATE

STEP SIX

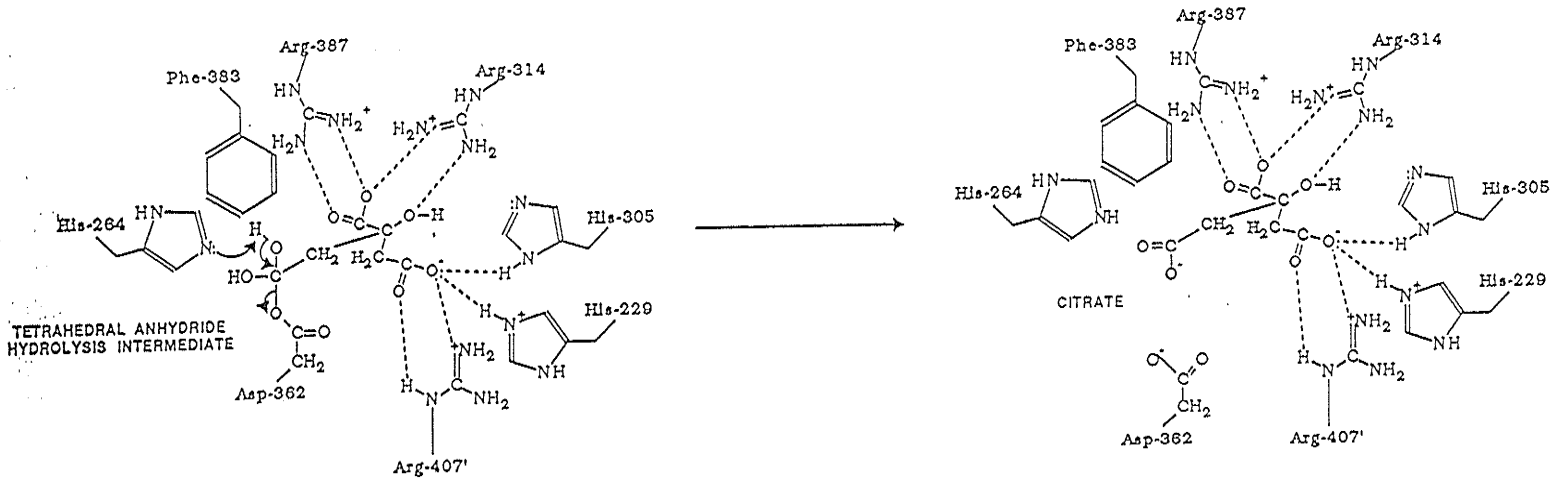

CITRATE FORMATION VIA TETRAHEDRAL
INTERMEDIATE BREAKDOWN

ALLOSTERY

E. coli citrate synthase is an allosteric enzyme. Allosteric enzymes are composed of multiple subunits (6 in the case of *E. coli* citrate synthase) bound together (oligomeric). Their interactions are responsible for allosteric effects. These enzymes possess a regulatory site, distinct from the active site, where positive or negative effector molecules bind non-covalently. The allosteric effect refers to a process where effector molecules induce a change in the active site which in turn affects the catalytic rate and efficiency of the enzyme by either increasing or decreasing the enzyme's potential to bind to its substrates. In the case of *E. coli* and other "large" citrate synthases, the effector molecule is called a positive modulator (potassium (K^+) and other monovalent cations (Faloona & Srere, 1969)) when the catalytic efficiency is improved, and a negative modulator (NADH (Weitzman, 1966)) when the catalytic efficiency is reduced. Obviously, the system is designed to accommodate feedback inhibition by the effector molecules.

One model for explaining the allosteric effect is the Monod-Wyman-Changeux (MWC) Theory (Monod et al., 1965) (Figure 8). Assumptions made by this theory are crucial and as follows: All subunits in oligomeric allosteric enzymes are symmetrically organized in equivalent positions. Allosteric enzymes exist in equilibrium between their active (R) and inactive (T) conformational states. This equilibrium is governed by the allosteric constant (L) which is a value representing the ratio of the T-states to the R-states in the absence of ligands. The R and T states represent different inter-subunit binding states since at any given time not only are all the subunits in the same state, but no mixed states exist. This idea is paralleled by the General Model of Allostery (Eigen, 1967) depicted in Figure 9, which proposes that the R to T and

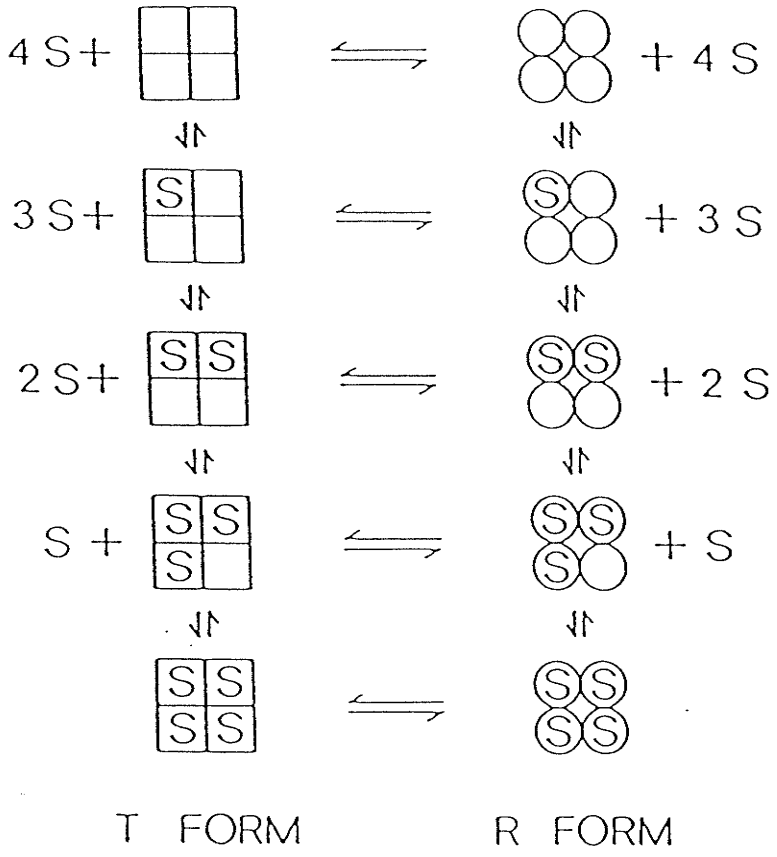

FIGURE 8: THE MONOD-WYMAN-CHANGEUX MODEL FOR BINDING OF LIGANDS TO A TETRAMERIC PROTEIN (FERSHT, 1985). S=SUBSTRATE, R=RELAXED (ACTIVE), T=TAUT (INACTIVE)

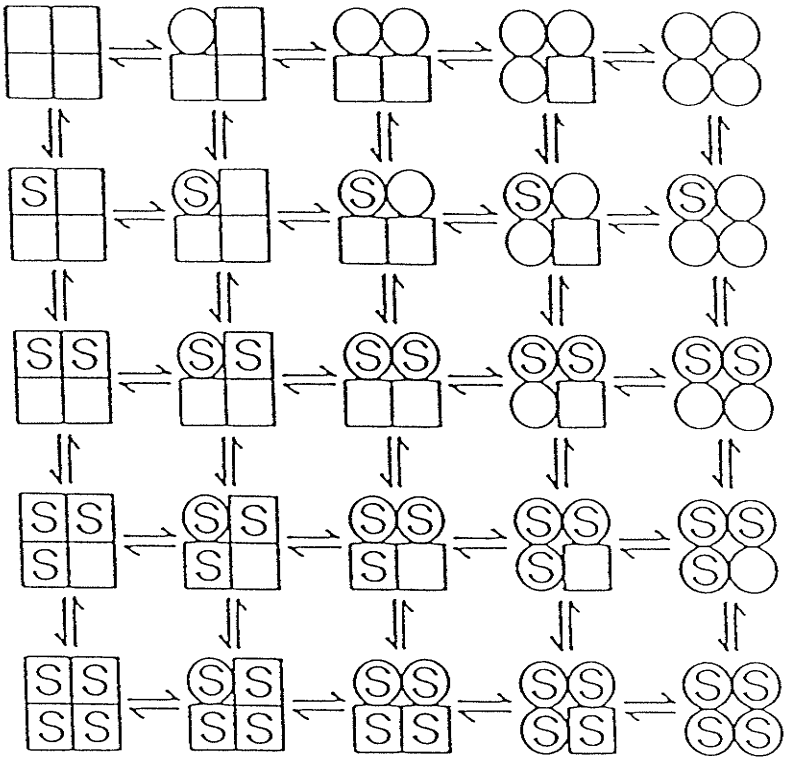

FIGURE 9: EIGEN'S GENERAL MODEL FOR THE BINDING OF LIGANDS TO A TETRAMERIC PROTEIN (FERSHT, 1985). CIRCLES REPRESENT THE R OR RELAXED (ACTIVE) STATE WHILE SQUARES REPRESENT THE T OR TAUT (INACTIVE) STATE. S=SUBSTRATE.

T to R conversions occur between individual subunits. The next MWC assumption is that equivalent substrate binding sites, and binding constants, exist in each subunit. However, the binding constants differ between the T and R states. The fact that the R state has a higher affinity for the substrate(s) is the final assumption of the MWC theory for allosteric enzymes.

Allosteric regulation observed for *E. coli* citrate synthase is both homotropic and heterotropic allosteric regulation.

Homotropic allosteric regulation happens when *E. coli* citrate synthase is allosterically modulated by its own substrate, AcCoA (at low salt concentrations). As OAA binds to the active site, a conformational change in the active site occurs. Since saturation by OAA is hyperbolic, it is likely that the OAA induced conformational change occurs independently at each active site, and is not communicated from one active site to another. Consequently, and assuming absence of NADH, *E. coli* citrate synthase adopts a new conformation favoring the binding of subsequent substrate molecules (AcCoA). A second conformational change, resulting from AcCoA binding occurs cooperatively. Saturation by AcCoA is sigmoidal.

Heterotropic allosteric regulation results when interactions between sites of different kinds occurs, such as active sites interacting with the binding sites for allosteric regulators. KCl, the activator, abolishes cooperativity in AcCoA saturation, presumably by stabilizing the R state. Thus, the conformational equilibria of citrate synthase is shifted in the direction of the R state. When NADH (the inhibitor) binds, AcCoA binding weakens. It is presumed that NADH binds selectively to the T state, which has a decreased affinity for AcCoA. Therefore, the conformational equilibrium shifts in the direction of the T state.

Finally, it is important to note that shifts in the equilibrium between the R and T states occur not only in the presence of enzyme activators and inhibitors, but also when specific R or T state stabilizing amino acid residues are removed by site-specific mutagenesis. The shift can result in either state predominating, as was observed in studies of mutant hemoglobin proteins (Bonaventura & Riggs, 1968; Bunn et al, 1974). Hemoglobin is a protein of red blood cells capable of binding oxygen. When oxygen is bound, the protein is in its R state and designated oxyhemoglobin. Deoxyhemoglobin represents the protein in its T state, when oxygen is not bound. Creation of a mutant hemoglobin protein designated, $Hb_{Kempsey}$, caused a deoxyhemoglobin stabilizing interaction to be lost. Thus, the T to R state equilibrium was shifted towards the R or oxyhemoglobin state. A 15-20 fold greater affinity for oxygen was observed. Hb_{Kansas}, a mutant causing a oxyhemoglobin stabilizing interaction to be lost, resulted in a protein with very low affinity for oxygen. The impact of the mutation shifted the T to R state equilibrium towards the T or deoxyhemoglobin state.

Considering the allosteric *E. coli* citrate synthase enzyme, mutations at the active site also affect the equilibrium between the R and T states. These studies will be discussed in the RESULTS section.

OBJECTIVES

The objective of this thesis is to use site-directed mutagenesis to determine whether four *E. coli* citrate synthase active site residues, listed in Table 1, play similar roles in catalysis and substrate binding as their predicted pig heart counterparts. In *E. coli* and pig heart (equivalent residues in brackets) citrate synthases, these four residues are: Arg-407 (Arg-421), (Arg-397), Phe-383 (Phe-397), Asp-362 (Asp-375), and His-264 (His-274). It should be noted that three other *E. coli* citrate synthase active site residues, listed in Table 1 (His-229, His-305, and Arg-314), have already been mutated and kinetically characterized (Anderson & Duckworth, 1988). The effects of the mutations were found to coincide with the roles predicted for the equivalent pig heart residues.

Arg-407 (Arg-421) is a residue predicted to bind citrate and OAA. Moreover, Arg-407 (Arg-421) is believed to bind to the 4-carboxyl group of OAA. When this arginine is mutated to leucine, binding of OAA to *E. coli* citrate synthase is expected to decrease slightly, while a slight drop in catalytic efficiency (kcat) is anticipated.

Asp-362 (Asp-375) and His-264 (His-274) are amino acids believed to abstract and donate protons from the various intermediates arising as citrate is formed from AcCoA and OAA. Elimination of these charged amino acids by mutation to alanine is predicted to cause a drastic decrease in the respective kcat values. The enzyme's affinity for its substrates is likely to decrease. However, the magnitude of this decrease cannot be anticipated.

Lastly, foreseeing the effect of mutating the strongly conserved Phe-383 (Phe-397) to an alanine is not possible since its role in the pig heart enzyme is not possible to predict. This phenylalanine, however, does make an

"edge-on" interaction with the substrates; AcCoA and OAA. Even though the result of this mutation cannot be guessed, a disruption to the integrity of the active site is likely. The effect this disruption may have on the steady state kinetics of this enzyme is also impossible to foresee.

MATERIALS & METHODS

REAGENTS

COMPANY	REAGENT
Aldrich Chemical Company Inc.	DTNB and OAA
Amersham International	T4 polynucleotide kinase
Bethesda Research Laboratories Life Technologists	BamHI, HpaI, and SalI restriction enzymes
Boehringer Mannheim (Canada) Ltd.	T4 DNA ligase
British Drug Houses (Canada) Ltd.	dimethyldichlorosilane, glucose, and magnesium sulphate
Canlab	acetic acid
Dupont	[α-^{32}P]dATP
Eastman Organic Chemicals	N,N,N',N'-tetramethylene-diamine
Fisher Scientific Company	acetic acid, ammonium acetate, ammonium chloride, boric acid, calcium chloride, cesium chloride, chloroform, EDTA, ethanol, hydrochloric acid, isopropanol, lithium chloride, 2-mercaptoethanol, methanol, phenol, polyethylene glycol-6000, potassium chloride, sodium acetate sodium chloride, and sodium hydroxide
Gibco Ltd.	agarose, yeast extract
J. T. Baker Chemical Company	magnesium chloride
Kodak	xylene cyanol and photographic solutions
Matheson, Coleman, and Bell	bromophenol blue
Pharmacia (Canada) Ltd.	acetyl-CoA, agarose-NA, deoxy- & dideoxynucleotides, DNA polymerase I Klenow fragment, Sephadex G-200, and EcoRI, HindIII restriction enzymes

Sigma Chemical Company	ATP, agarose, ampicillin, BSA, chloramphenicol, Coomassie Brilliant Blue R, cytosine, dithioreitol, egg white lysozyme, ethidium bromide, glutamic dehydrogenase, NADH, SDS, thiamine HCl, Trizma base (TRIS), and uridine
Terochem Laboratories Ltd.	acrylamide, methylene bisacrylamide, and urea
Whatman	DE52 (DEAE-cellulose)

Escherichia coli **STRAINS**

STRAIN	GENOTYPE	PURPOSE
E. coli CJ236 (Kunkel et al., 1987)	F+, *dut1, ung1, thi1, relA1/pCJ105* (Cm^r)	- used in the Kunkel mutagenesis protocol for creation of uracil-containing phage DNA
E. coli JM103 (Messing et al., 1983)	F+, *Δlacpro, thi, strA, supE, endA, sbcB15, hsdR4*, F'*traD36, proAB, lacI*^{q}, *ZΔM15*	- used in the Kunkel mutagenesis protocol for mutant selection - used as host for growth of M13 phage derived clones
E. coli MOB154 (Wood et al., 1987)	F-, *gltA6, galk30, pyrD36, relA1, rpsL129, thi-1, λ-, supE44, hsdR*	- used as host for the expression of plasmids containing mutant *E. coli* citrate synthase genes

MEDIA

JM103 host cells were grown on TY liquid culture media composed of 8 grams (g) Bactotryptone, 5 g yeast extract, and 2.5 g NaCl per litre of distilled water adjusted to pH 7.2.

M9 minimal plates composed of 1.5 % agar with M9 salts (6 g Na_2HPO_4, 3 g KH_2PO_4, 1 g NH_4Cl, and 0.5 g NaCl), 246.5 mg $MgSO_4$, 14.7 mg $CaCl_2$, 337 mg thiamine, and 4 mg glucose in one liter of distilled water at pH 7.2, were used to propagate the JM103 cell line.

CJ236, harboring M13 derivatives, used to produce uracil-containing DNA, were grown at pH 7.2 in LB liquid culture media containing 10 g Bactotryptone, 5 g yeast extract, and 10 g NaCl per litre of distilled water, but with 0.25 mg of uridine supplemented per litre.

Propagation of the CJ236 cell line was accomplished using LBC plates, which were created using LB liguid culture media supplemented with 1.5 % agar and 170 mg chloramphenicol in ethanol per litre.

M13 phage and host cells were first placed in H-top agar (10 g Bactotryptone, 8 g NaCl and 8 g agar per litre) and then placed on TYE medium plates composed of 20 g Bactotryptone, 10 g yeast extract, 16 g NaCl with 1.5 % agar per litre of distilled water at pH 7.2.

MOB 154 cells containing mutant plasmids that express active citrate synthases, were grown in LB liquid culture media and then selectively grown on MOBmin minimal plates containing 1.5 % agar with M9 salts, 100 mg thiamine, 4 mg glucose, and 12.5 mg cytosine per litre; adjusted to pH 7.2. When a positive control was needed to assess the growth of MOB154 cells bearing mutant plasmids, 12.5 mg glutamate was added per litre to the MOBmin minimal plates.

LBA liquid culture medium is identical to LB except that 100 mgs ampicillin is added per litre. LBA was used to grow and select for MOB154 cells harbouring mutant plasmids. LBA plates (LB supplemented with 1.5 % agar) were used to propagate these cells.

PLASMIDS AND OLIGONUCLEOTIDES

The *E. coli* citrate synthase gene, *gltA*, including promoters and terminators, was expressed in pES*gltA*, a derivative of pHS*gltA* (Anderson & Duckworth, 1988). M13ES*gltA* was a result of cloning the small EcoRI-SalI restriction fragment from pES*gltA* into the large EcoRI-SalI fragment of M13mp18 RF DNA.

M13 is a bacteriophage that infects bacteria. It harbours two forms of DNA; a circular single-stranded form and a double-stranded form called replicative form DNA (RF DNA). RF DNA is comprised of single-stranded phage DNA and a complementary strand. The Kunkel method of mutagenesis utilizes Messing's (1983) requirement that *gltA* be cloned into a M13 bacteriophage vector of known sequence (M13mp18 for my work). Use of M13mp18, during this project was important since single-stranded DNA isolated from M13mp18 was used in the Kunkel method to prepare single-stranded uracil-containing template which was annealed to the synthetic oligonucleotides coding for mutant *gltA* genes. Furthermore, single-stranded dideoxynucleotide sequencing of the mutant *gltA* strand was possible and necessary to ensure that *gltA* was indeed a mutant form. Once this check was accomplished, RF DNA served as a source of mutant *gltA* which was used to create M13ES*gltA*. The synthetic oligonucleotide primers, listed in Table 2, were synthesized at and purchased from the University of Calgary's DNA Custom Synthesis Center.

They were created to be complementary to the anti-sense *gltA* strand. Priming sites are numbered from the first base in the initiator methionine codon.

TABLE 2: SYNTHETIC OLIGONUCLEOTIDES USED FOR MUTAGENESIS AND SEQUENCING STUDIES

SYNTHETIC OLIGONUCLEOTIDE	5'→3' BASE SEQUENCE	5'→3' PRIMING SITES (MUTANT SITE)
oligo L407 ●	GACGCGGAAGGGCAATC	1536→1520 (1528)
oligo L387 ●	AACGGTAAGTGCCATTG	1475→1459 (1468)
oligo PR384 ❂	TCCAGCCAACGGTACGT	1482→1466
oligo A383 ●	ATTGCGGCAATGACGGT	1462→1446 (1456→55)
oligo A362 ●	AGTAGAAAGCGACGTTC	1401→1385 (1393)
oligo PR329 ❂	TCATCCTTCGTGCCCAG	1309→1293
oligo A264 ●	CCGCCGGCCGCAGGTCC	1105→1089 (1099→98)
oligo PR260 ❂	AGGTCCCGCCAGTGAAG	1094→1078
oligo PR221 ❂	ATCAGAATAAGGTCCAT	979→963
oligo PRTERM ❂	GCCATATGAACGGCGGG	1637→1621
● = SYNTHETIC OLIGONUCLEOTIDES USED FOR MUTAGENESIS		
❂ = SYNTHETIC OLIGONUCLEOTIDES USED FOR SEQUENCING		
UNDERLINED BASES = MUTATED BASES USED IN MUTAGENESIS		

THE KUNKEL MUTAGENESIS PROCEDURE

THEORY

The Kunkel method of oligonucleotide-directed *in vitro* mutagenesis (Figure 10), is the basis for the flowchart of procedures utilized to create and analyze mutant *E. coli* citrate synthases (see Figure 11). The Kunkel method, which utilizes small synthetic fragments of DNA (12-30 nucleotides long) called oligonucleotides, is a modification of the original mutagenesis procedure invented by Zoller and Smith, 1982. The oligonucleotides are constructed so that they will be complementary to the template DNA in every way except for the mismatch. For my work, the template DNA, M13ES*gltA*, contained the *E. coli* citrate synthase gene, *gltA*, subcloned into the M13mp18 bacteriophage vector (Anderson, 1988). The Kunkel method requires that the template contain uracil. This is possible when M13ES*gltA* is transformed into *E. coli* CJ236, a host cell deficient in the enzymes dUTPase and uracil glycosyl transferase. The lack of dUTPase allows dUTP to accumulate since the formation of dUMP from dUTP will not happen. A small portion of the excess dUTP's will lead to the incorporation of some uridines into the M13 template in place of thymidines, a process normally counteracted by the action of uracil glycosyl transferase. Once the single-stranded uracil-containing M13ES*gltA* template is created, it must be annealed to a phosphorylated mutagenic oligonucleotide. The mutagenic oligonucleotide must be phosphorylated so that DNA ligase can ligate its ends after primer extension by the large Klenow fragment of DNA polymerase I. Consequently, a covalently closed circular heteroduplex is formed which can be transformed into JM103, a host cell possessing uracil glycosyl transferase. The uracil-containing strand of the

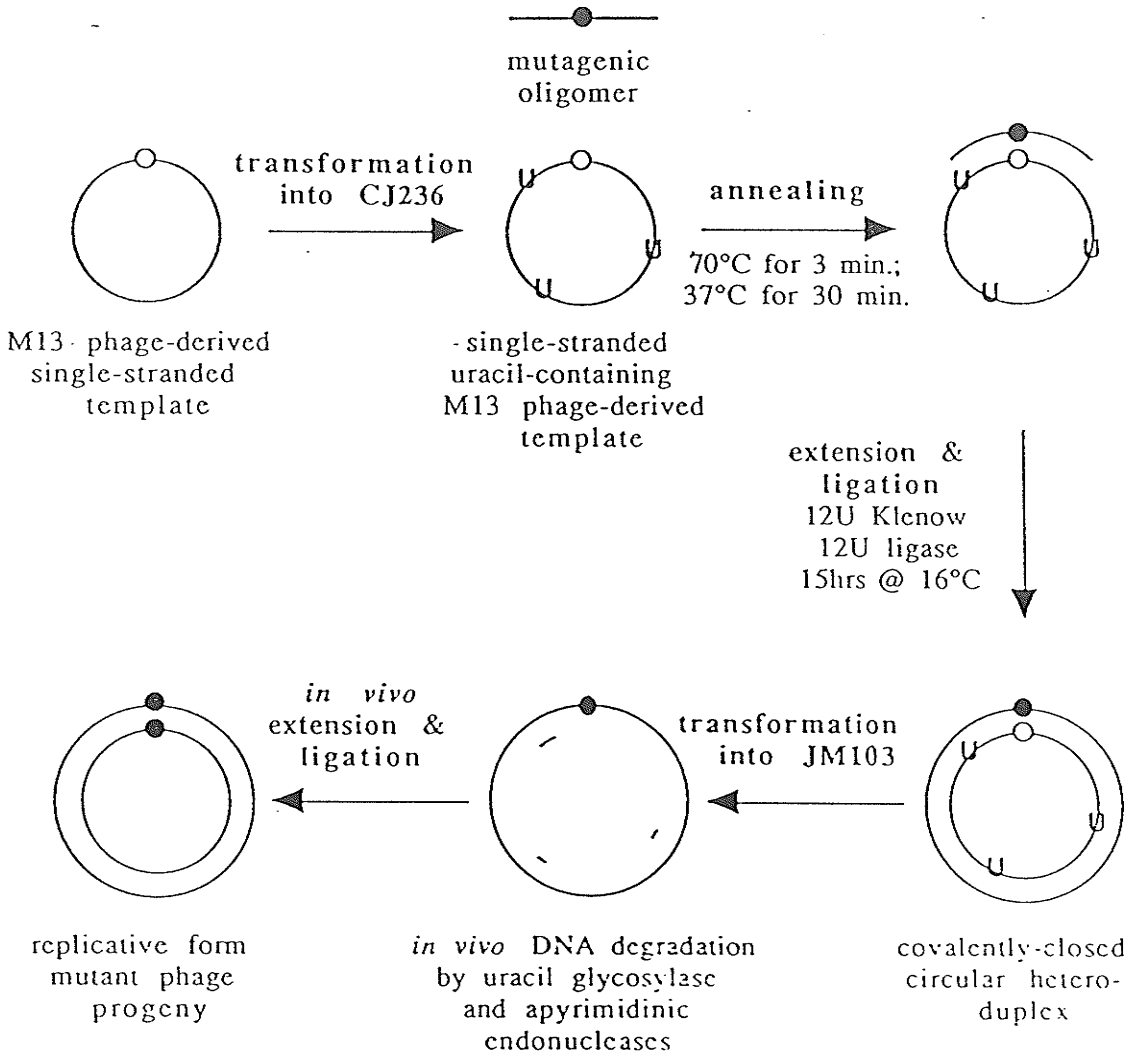

FIGURE 10: THE KUNKEL METHOD OF OLIGONUCLEOTIDE-DIRECTED *IN VITRO* MUTAGENESIS (TAKEN FROM MOLGAT, 1990)

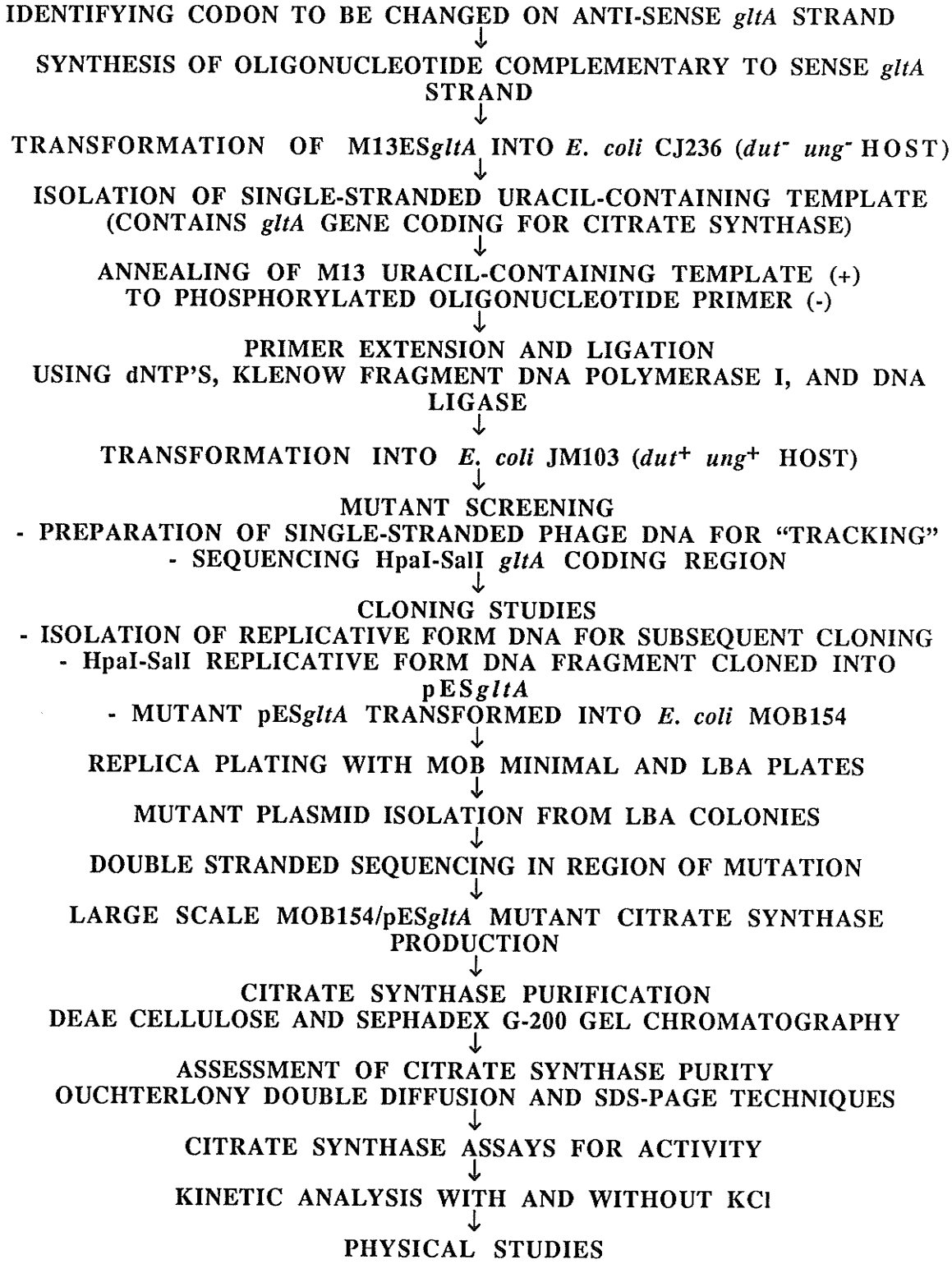

FIGURE 11: FLOWCHART OF PROCEDURES UTILIZED TO CREATE AND ANALYZE MUTANT *E. coli* CITRATE SYNTHASES

heteroduplex is then degraded *in vivo* by this uracil glycosyl transferase. *In vivo* extension and ligation occurs to form mutant M13 RF *gltA* DNA.

CONSTRUCTION OF SINGLE-STRANDED URACIL TEMPLATE

A M13ES*gltA*/JM103 plaque was transferred to 1 ml LB liquid culture media (LB) and incubated for 5 minutes at 60°C to kill the JM103 cells. The cells were pelleted and 100 µL of the supernatant was added to 100 mL of LB supplemented with 10 µL of a 2.5 mg/mL uridine stock. Five microlitres of mid-log phase CJ236 was transferred to the mixture and incubated at 37°C for 5 hours with vigorous shaking. After incubation, the CJ236 cells were pelleted following centrifugation at 5K for 10 minutes. The viral supernatant was suspended in a quarter volume of 20% PEG-6000/2.5 M NaCl and placed on ice for 24 hours. Precipitation of phage resulted. Following centrifugation at 10K for 10 minutes, the viral pellet was suspended in 2.5 mL of TE buffer in order that single-stranded phage DNA be prepared following the protocol of Sanger et al., 1981. To this solution, an equal volume of 1:1 (w:v) phenol/chloroform was added, followed by five minute vortexing and centrifugation periods. To the separated aqueous layer, 0.1 volume of 3M NaOAc (pH 6) and 2.5 volumes of ethanol were added. To induce precipitation of the single-stranded uracil template, the solution was placed at -20°C for at least an hour.

MUTAGENESIS

Once the single-stranded uracil template was isolated, a phage titre was conducted to determine if the template had at least a 10^5 fold greater survival

in CJ236 than JM103. The phosphorylated mutagenic oligonucleotide was then annealed to the single-stranded uracil containing template.

Two hundred picomoles of the mutagenic oligonucleotide were incubated with 3 μL 1 M Tris buffer (pH 8), 1.5 μL 200 mM $MgCl_2$, 1.5 μL 100 mM DTT, 3 μL 10 mM ATP and 5 units of polynucleotide kinase at 37°C for 1 hour. Dilution with sterile water yielded a 20 μg/mL stock solution of phosphorylated mutagenic oligonucleotide. Five microlitres of this 20 mg/mL stock was incubated at 65°C for 5 minutes with 10 μL of single-stranded uracil template (1 μg/μL), 1.7 mL of 20X SSC and 17.3 mL of water. To ensure annealing, this mixture was slowly cooled to 4°C. Extension of the phosphorylated mutagenic oligonucleotide to form a covalently closed circular heteroduplex with the uracil template occurred when 20 μL 100 mM Tris buffer (pH 8), 50 mM $MgCl_2$, 20 μL 10 mM DTT, 10 μL 10 mM ATP, 5 μL of each of the four dNTP stocks (10 mM), 12 units of the large Klenow fragment of DNA polymerase I and 12 units of T4 DNA ligase was added to the above mixture and left at 4°C for 24 hours. The heteroduplex was used to transform JM103 cells, which were mixed with H-top agar and plated on TYE plates (see MEDIA section). A 24 hour incubation at 37°C followed. *In vivo* degradation of the single-stranded uracil template occurred resulting in M13 RF mutant progeny.

MUTANT SCREENING

Following the Kunkel mutagenesis procedure, single-stranded phage DNA was prepared, from the potential M13 clones containing mutated *gltA*, in a scaled down version of Sanger's protocol (1981) utilized to prepare single-stranded uracil-containing template DNA. Screening of these clones was accomplished by single-track sequencing (Zoller and Smith, 1983; Sanger et

al., 1977) of the mutation region (1098-1528). Once a mutant was "tracked", final confirmation that the mutation induced by the oligonucleotide was the only one present was obtained from sequencing of the entire *gltA* HpaI-SalI restriction fragment of DNA. This task was accomplished using five specific synthetic oligonucleotide primers designated oligos 221, 260, 329, 384, and TERM (see Figure 12). Since the HpaI-SalI restriction fragment (759-1589) contains a large portion of the *gltA* coding sequence and is the only sequence produced by primer extension using the large Klenow fragment of DNA Polymerase I, sequencing is required to ensure that no random mutations occurred because of the action of the large Klenow fragment of DNA polymerase I. Portions of the *gltA* sequence outside of the HpaI-SalI region need not be sequenced since subcloning eliminates this portion from the DNA synthesized by Klenow DNA polymerase I.

CLONING TECHNIQUES

Isolation of mutant replicative form DNA was accomplished using the Alkaline-SDS method of Birnboim & Doly, 1979. Restriction enzyme digests, agarose gel electrophoresis, cloning, preparation and transformation of competent cells using calcium chloride, and replica plating were performed as described by Maniatis et al., 1982.

Mutant pES*gltA* plasmids were constructed by digesting mutant replicative form DNA (M13ES*gltA*) and wild type pES*gltA* with the restriction enzymes HpaI and SalI. Agarose gel electrophoresis of these digests was conducted and separate fragments isolated. The smaller M13ES*gltA* HpaI-SalI *gltA* fragment was cloned into the larger pES*gltA* HpaI-SalI fragment. The result, as illustrated in Figure 13, is mutant pES*gltA*.

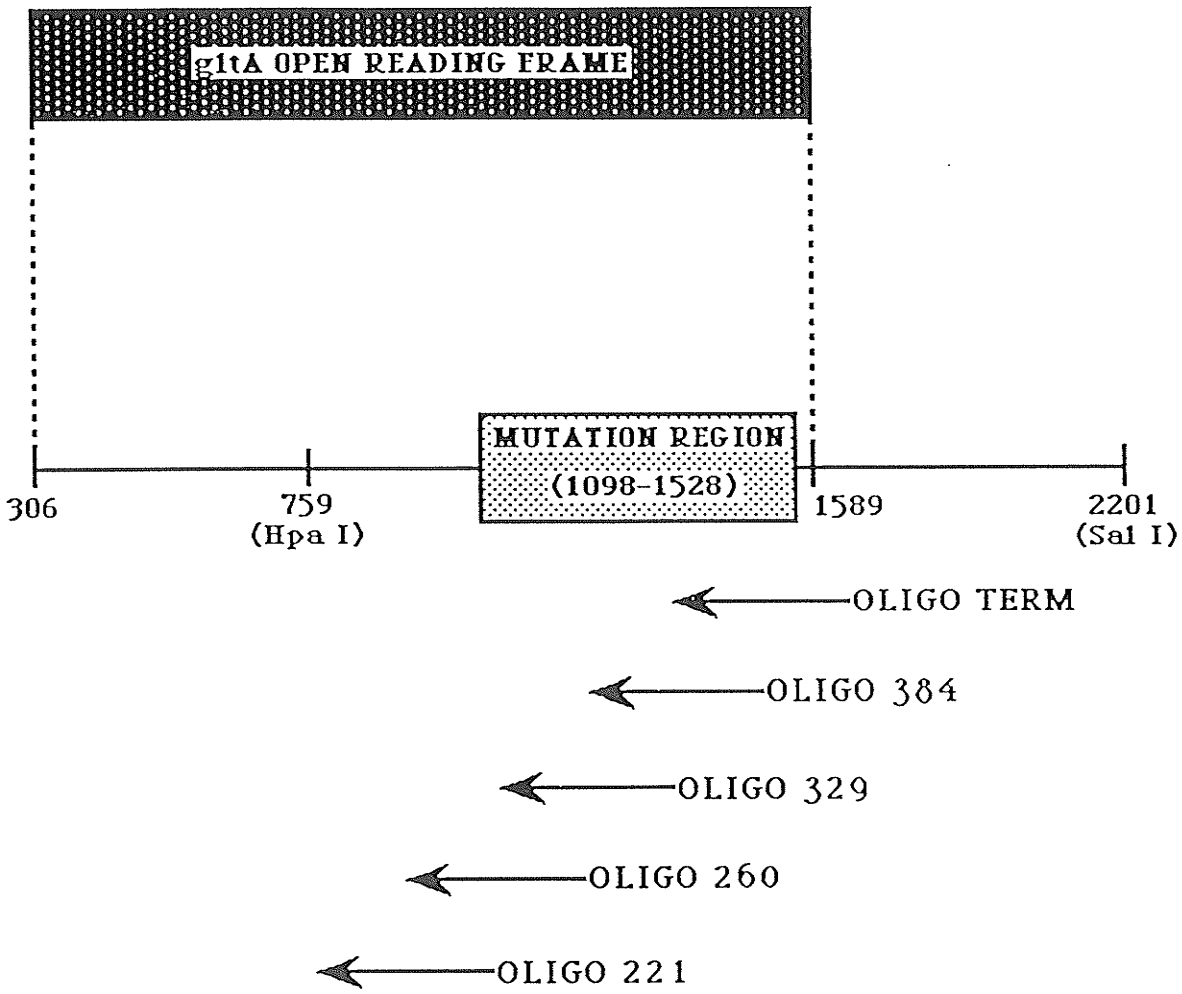

FIGURE 12: SEQUENCING STRATEGY OF *gltA*

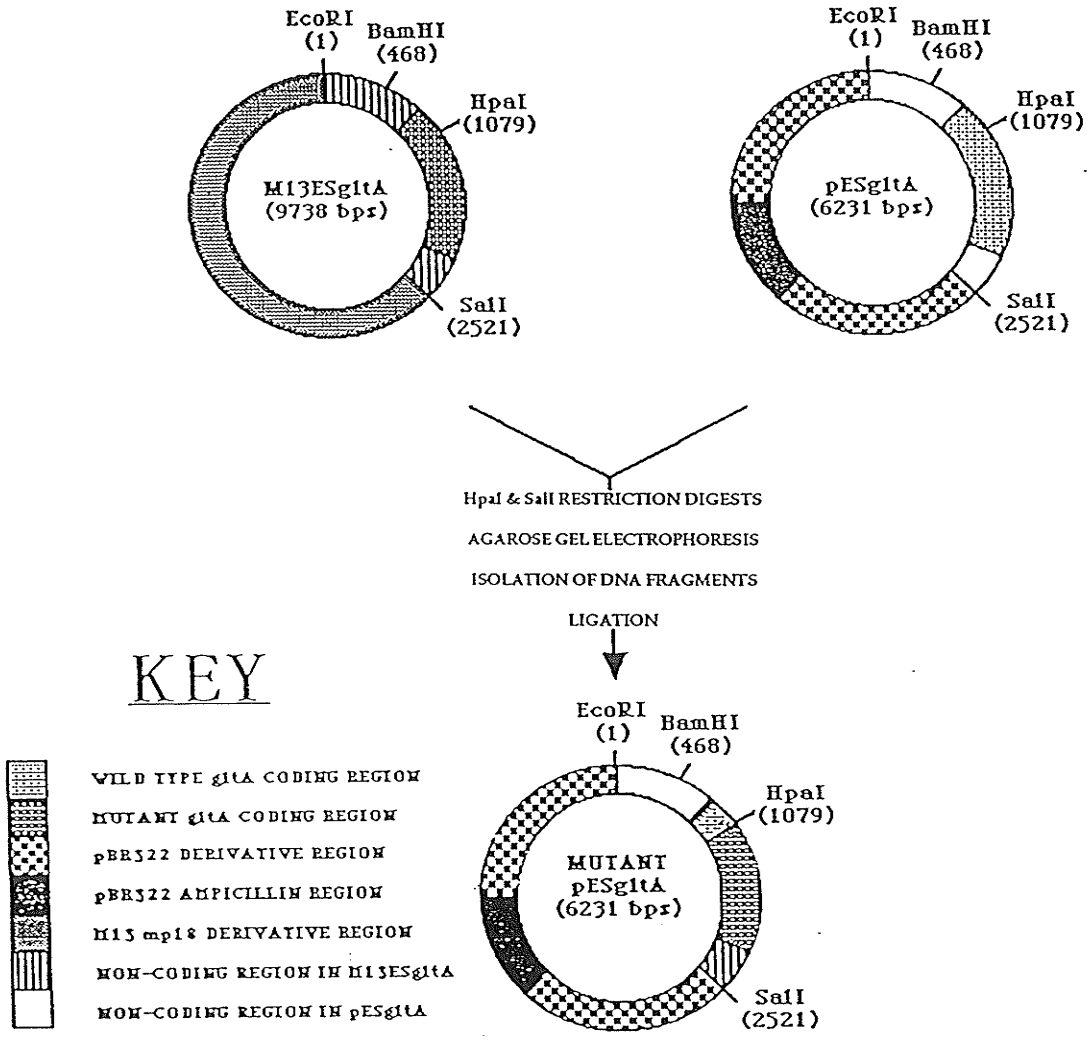

FIGURE 13: CLONING STRATEGY FOR CONSTRUCTING MUTANT pES*gltA*

Testing the effect of the mutation on citrate synthase properties requires transformation of these plasmids into competent host cells lacking native citrate synthase. *E. coli* MOB154 cells were the host cells used for this purpose.

The procedure known as replica plating revealed whether ampicillin resistance from the larger pES*gltA* HpaI-SalI fragment existed. Assuming pES*gltA* coded for an active mutant *E. coli* citrate synthase enzyme, use of MOBmin minimal plates (see MEDIA section) with (positive control for growth) and without glutamate, ensured that mutant *gltA* was expressing. Final and definite proof that the mutant *E. coli* citrate synthases obtained were indeed derived from mutant *gltA* genes, arose from double-stranded sequencing of the mutant plasmids (Mierendorf and Pfeffer, 1987) in the region of the mutation.

MUTANT *Escherichia coli* CITRATE SYNTHASE PRODUCTION AND PURIFICATION

Following verification of the presence of the mutation by plasmid sequencing, one colony was transferred into 5 mL of LBA liquid culture media. The entire culture was used to inoculate 500 mL of LB liquid media containing 5 mL of an ampicillin stock solution (20 mg/mL). MOB 154 harbouring a mutant plasmid from the 500 mL culture was grown in twelve flasks, each containing one liter of LB and 5 mL of ampicillin (20 mg/mL) at 37°C for 24 hours. After 8 hours, an additional 5 mL of ampicillin solution was added to each of the twelve flasks. Once the cultures were grown (16 hours later), the cells were harvested using a Sharples centrifuge (7000 rpm) and ruptured in a French pressure cell (17000 psi.). The resultant extract was centrifuged at 15000 rpm for 1 hour. The supernatant possessing citrate synthase and other proteins

was purified by ion-exchange column chromatography, using the anion exchange resin diethylaminoethyl (DEAE) cellulose and gel chromatography using Sephadex G-200, according to the method of Duckworth and Bell, 1982. The DNase treatment and ammonium sulphate precipitation steps were omitted.

ASSESSMENT OF *E. coli* CITRATE SYNTHASE PURITY

Two procedures, employed to assess the purity of mutant *E. coli* citrate synthases created during this project, were: SDS polyacrylamide gel electrophoresis (Laemmli, 1970) and Immunodouble diffusion precipitin reaction (Ouchterlony, 1953).

Ouchterlony immunodouble diffusion supporting medium was composed of 1.0% agar, 147 mM sodium chloride, 0.02% sodium azide, and 10mM Tris buffer (pH 7.4). Each plate had a center well and five surrounding wells punched into the supporting medium where antibody and antigen were placed respectively. The diffusion process was allowed to proceed at 37°C for 24 hours.

The Ouchterlony immunodouble diffusion precipitation reaction was done with individual and "pooled" fractions collected from DEAE-celluose and Sephadex G-200 chromatographic columns in order to detect the presence of *E. coli* citrate synthase. Diffusion of twenty microlitres of undiluted rabbit anti-wild type polyclonal *E. coli* citrate synthase antiserum (gift from Dr J. Jamieson), placed in the center well, and twenty micrograms of appropriately diluted potential *E. coli* citrate synthase, placed in surrounding wells, near their equivalence point resulted in the formation of a cross-linked immunoprecipitate. The immunoprecipitate only formed if the antigen was *E. coli* citrate synthase. In addition, identity between antigens was implied when

precipitin arcs, formed between the single antibody and surrounding wells, were totally fused.

Sodium Dodecyl Sulphate (SDS) Polyacrylamide Gel Electrophoresis (PAGE) was conducted on column chromatography fractions. Standards used were bovine serum albumin (BSA) (68 000 g/mol), glutamic dehydrogenase (56 000 g/mol) and ovalbumin (44 000 g/mol). Following electrophoresis, *E. coli* citrate synthase (subunit molecular weight = 48000 g/mol) was found to migrate to a point between glutamic dehydrogenase and ovalbumin. Use of 10 and 50 microgram preparation sizes determined whether the *E. coli* citrate synthase preparations were pure and free of significant amounts of contaminating proteins respectively.

CITRATE SYNTHASE ASSAYS

The objective of an enzyme assay is to detect the presence of citrate synthase and its activity. Citrate synthase utilizes the substrates, OAA and AcCoA to form citrate and CoA-SH. Because CoA-SH contains a free sulfhydryl group, it can react with 5,5'-dithiobis-(2-nitrobenzoic acid) (DTNB), also known as Ellman's reagent, to form 2-nitro-5-thio-benzoic acid-CoA and 2-nitro-5-thio-benzoic acid anion (E_{412}=13600 M^{-1} cm^{-1}). Figure 14 illustrates DTNB's reaction with coenzyme A. Since the formation of CoA-SH is the rate-limiting step, rate of appearance of yellow color must be equal to the rate of the reaction catalyzed by citrate synthase. DTNB also reacts with a sulfhydryl group (Cys-206) of *E. coli* citrate synthase (Talgoy et al., 1979). Since the concentration of protein under assay conditions is insignificant, contribution of the protein reaction to the amount of 2-nitro-5-thio-benzoic acid anion

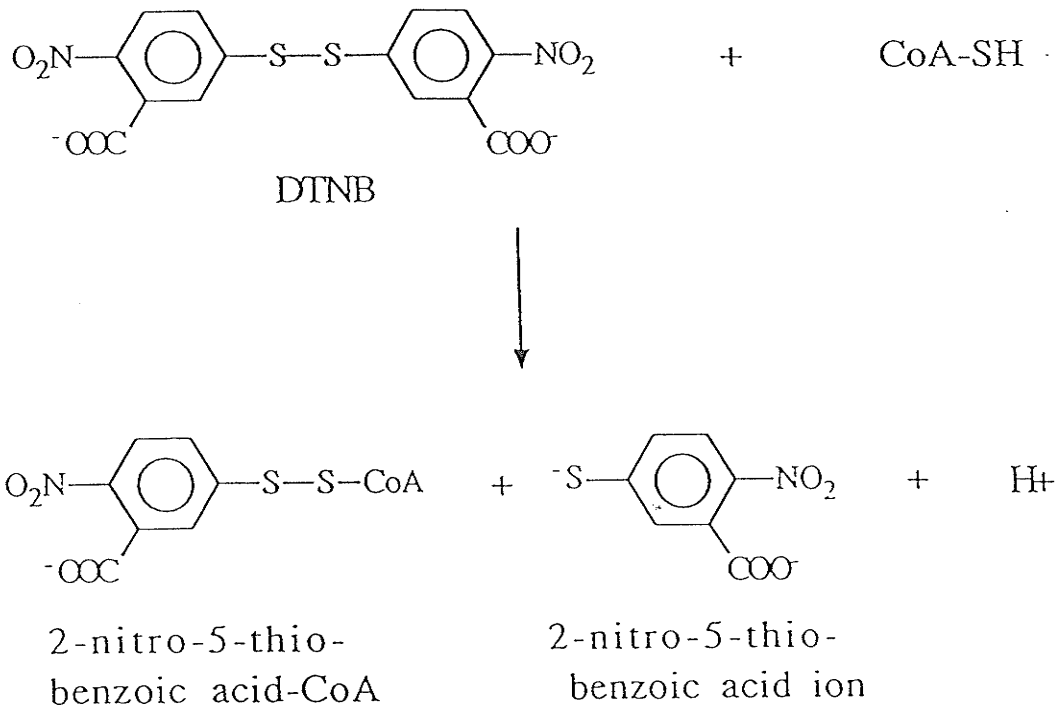

FIGURE 14: REACTION OF DTNB WITH CoA-SH (TAKEN FROM MOLGAT, 1990)

produced will also be insignificant. The reaction between DTNB and CoA-SH can be followed spectrophotometrically, at 412nm, in a Gilford 2400-2 single beam spectrophotometer using the method of Srere et al., 1963.

Citrate synthase assays were performed in 1 cm cuvettes in total volumes of 1 ml and 600 µL. Standard *E. coli* citrate synthase assay conditions required 940 µl of Tris buffer (TB) (20mM Tris-Cl, pH=7.8, 1mM EDTA), 10 µL of suitably diluted enzyme, and 50 µL of Tris buffer containing 2.0 mM AcCoA, 2.5 mM OAA, and 1.0 mM DTNB. Assays were carried out at room temperature.

Under standard assay conditions, one unit of citrate synthase activity is defined as the amount of enzyme required to produce 1.0 µmol of product per minute at room temperature, and is determined using the following formula:

$$\frac{\mu\text{mol product/min}}{\text{mL extract}} = \frac{(\Delta\text{Abs@412nm/min})}{\varepsilon@412} \times \frac{10^{-3}\text{ L}}{\text{mL}} \times \frac{10^{6}\mu\text{mol}}{\text{mol}} \times \frac{V}{E} \times D$$

where ε is the extinction coefficient of 2-nitro-5-thio-benzoic acid anion (13 600 $M^{-1}cm^{-1}$), E is µL of enzyme assayed, V is assay volume, D is the dilution factor.

Specific activity is defined as units of activity divided by milligrams of citrate synthase (determined by absorbance values at 278nm) assayed.

STEADY STATE KINETICS OF *E. coli* CITRATE SYNTHASE

Following standard enzyme assays, activities were determined for various combinations of OAA and AcCoA concentrations in the presence and absence of 0.1M KCl. Relationships between specific activities and substrate concentrations were plotted in Lineweaver Burk double-reciprocal form. Sets

of data obeying the Ordered Bi Bi equation (Cleland, 1963) were fitted into the equation by the GENLSS program of DeTar, 1972. The GENLSS program determines best values for the four parameters (Vmax, K_{OAA}, K_{iOAA}, K_{AcCoA}) by independently placing each data point into the Michaelis-Menten hyperbolic curve equation. In addition, assignment of a standard deviation to each parameter is accomplished. Vmax is the maximum velocity of the reaction in the presence of saturating amouts of OAA and AcCoA. When AcCoA is saturating, K_{OAA} is the concentration of OAA yielding half the Vmax. K_{iOAA} is the dissociation constant for OAA in the absence of AcCoA. When OAA is saturating, K_{AcCoA} is the concentration of AcCoA yielding half the Vmax.

In the absence and, at times, presence of KCl, Lineweaver-Burk plots (specific activity^{-1} versus [AcCoA]$^{-1}$) of mutants created during the course of this project, exhibited curved as opposed to straight lines. When such sigmoid curvature occurred, the y-intercepts (Vmax values) for the various OAA concentrations were collected and used to create Hill plots (log (v/Vmax-v) versus log [AcCoA]), where v represented the specific activity of citrate synthase at that particular OAA/AcCoA concentration combination. The slopes of the lines represent the Hill numbers, which were averaged for each OAA concentration and reported as a common Hill number for the mutant enzyme. The anti-log of the slopes divided by the y-intercepts are the $S_{0.5AcCoA}$ values, which were also averaged to report a common $S_{0.5AcCoA}$ value for the mutant enzyme. Values for the apparent Km of OAA were determined from specific activity^{-1} versus [OAA]$^{-1}$ Lineweaver-Burk plots which were always linear. For each AcCoA concentration, the x-intercepts of these sets of data represented the apparent Km for OAA at that particular AcCoA concentration. The apparent Km for the mutant enzyme is reported as that of the highest AcCoA concentration.

ACTIVATION & INHIBITION STUDIES

Activation and inhibition studies pertaining to *E. coli* citrate synthase involve the enzyme's activator, KCl, and inhibitor, NADH.

Determining the effect of KCl on the enzyme's activity requires that a series of standard citrate synthase assays be performed with increasing amounts of KCl. Maximum activation of wild type *E. coli* citrate synthase occurs at approximately 100 mM KCl. KCl concentrations exceeding 100 mM commonly result in a decrease of activity.

To determine the inhibitory effect of NADH on enzyme activity, standard citrate synthase assays, in the absence of KCl, were performed with increasing amounts of NADH. Since KCl abolishes the inhibitory effect of NADH on *E. coli* citrate synthase (Talgoy & Duckworth, 1979), it was omitted from assays of NADH inhibition.

Citrate synthase activity is also subject to competitive inhibition with respect to oxaloacetate, at the active site, by α-ketoglutarate (α-KG) (Wright & Sanwal, 1967). Because α-KG is an analogue of OAA, it will bind to the active site (Anderson & Duckworth, 1988), but not be utilized by the enzyme. As a result, the enzyme is inhibited by increasing amounts of α-KG. In practical terms, the standard citrate synthase assay is performed in the presence and absence of KCl using constant OAA concentrations and varying α-KG concentrations. The outcome is inhibition curves for the different OAA concentrations.

Determination of the maximum percent activation and Km, KCl values as well as the maximum percent inhibition and Ki, NADH or Ki, α-KG values, required creation of Lineweaver-Burk plots of KCl activation and NADH or α-

KG inhibition curves. The y-intercept yielded $1/(V_0-V_\infty)$ and $1/(V_\infty-V_0)$ values for inhibition and activation plots respectively. V_0 represented specific activity values when KCl, NADH, and α-KG concentrations were equal to zero. V_∞ represented specific activity values with an "infinite" amount of additional ligand present. The maximum percent activation by KCl was determined using the following calculation, $(V_\infty-V_0)$ x 100. Maximum percent inhibition by NADH or α-KG was found using (V_0-V_∞) x 100. The x-intercepts of Lineweaver-Burk plots were determined by subjecting the data to the GENLSS program. As a result, Km, KCl, K_{iNADH} and $K_{i\alpha\text{-}KG}$ values were determined along with their associated standard deviations.

FLUORESCENT LIGAND BINDING STUDIES

ANS DISPLACEMENT

ANS displacement studies, conducted during the course of this project, were executed using a Gilford Fluoro IV Model 1452X11 Spectrofluorimeter and 1cm Canlab fluorescence cuvettes. The method of Talgoy & Duckworth, 1979, was followed. ANS or 8-anilino-1-naphthalenesulfonic acid is a fluorescent ligand that binds to *E. coli* citrate synthase. In the presence and absence of KCl, ANS/citrate synthase complexes were titrated with the ligands OAA and AcCoA in order to determine whether they displaced ANS from the enzyme. The concentration range in which displacement occurs, reflects the enzyme's affinity for its substrates. Changes in fluorescence (ΔF_{obs}) occurring as a function of ligand concentrations ([L]) were plotted as Scatchard plots (ΔF_{obs}/[L] versus ΔF_{obs}). When saturation with ligand is hyperbolic (linear scatchard plot), ΔF_{obs} is represented by the equation: ΔF_{obs} =

$(\Delta F_{max}[L])/(K_D^{app} + [L])$ (Talgoy & Duckworth, 1979). ΔF_{obs} is the change in fluorescence observed at any [L]. ΔF_{max} represents the maximal change in fluorescence obtained at saturation, while K_D^{app} is the concentration of ligand (nucleotide) required to get half the maximal fluorescence change. Data giving linear scatchard plots were fitted to the above equation for a rectangular hyperbola, using DeTar's GENLSS program, and values for ΔF_{max} and K_D^{app} were obtained along with their respective errors. Sigmoid saturation data were fitted to the equation $\Delta F_{obs} = (\Delta F_{max}[L])/([L_{0.5}]^2+[L]^2)$, which is the Hill equation with n=2. $L_{0.5}$ represents the ligand concentration needed to achieve half minimal fluorescence changes. Once again, the GENLSS program was employed to determine the ΔF_{max} and $L_{0.5}$ values and their errors.

NADH BINDING

NADH binding was measured using the fluorescence enhancement technique of Duckworth & Tong, 1976. The aim of this technique was to observe the effect the presence of KCl and substrates had on the binding of NADH to both wild type and mutant *E. coli* citrate synthases. A Gilford Fluoro IV Model 1452X11 Spectrofluorimeter using Canlab fluorescence cuvettes (1 cm) was used. Data obtained from NADH binding experiments were treated according to Duckworth & Tong, 1976, and were fitted to the equation for a rectangular hyperbola using DeTar's GENLSS program. Values for K_D, NADH were given along with their associated deviations.

PHYSICAL STUDIES

CIRCULAR DICHROISM SPECTROSCOPY

Ellipticity values generated by circular dichroism spectroscopy of *E. coli* citrate synthase were collected on a JASCO-500A Spectropolarimeter in the range of 210-240 nm using 0.5 cm cuvettes. Concentrations of enzyme solutions used were approximately 0.2 mg/mL. The percentage of α-helix in the enzymes was determined from ellipticity values collected at 222 nm. Prior to determining the percent α-helix content, ellipticity values at 222nm, θ_{222}, were used to determine the molar ellipticity, $[\theta_{222}]_M$, in ° cm2 dmol-1, using the following equation (Adler, 1973):

$$[\theta_{222}]M = \frac{\theta_{222} \times M}{10 \times L \times C}$$

where M is the molecular weight of the protein, C is the protein concentration in milligrams/mL, and L is the path length (5.015 mm). The percent α-helix in mutant citrate synthases, $f\alpha$, was found using the formula,

$$f\alpha = \frac{[\theta_{222}] + 2730}{-28770}$$

where $[\theta_{222}]$ is the mean residue ellipticity calculated by dividing the molar ellipticity by the number of amino acids in the protein.

Comparison of the percent α-helix in wild type to mutant citrate synthases ensured that mutant citrate synthases created during this project retained structural integrity.

ULTRAVIOLET DIFFERENCE SPECTROSCOPY

A Cary 15 double-beam spectrophotometer was employed for collecting ultraviolet difference spectra in the range of 240-340 nm. Double chamber cuvettes were used in which each chamber had a path length of 4.47 mm. The concentration of enzyme solutions was approximately 2.3 mg/mL so that effective absorbance of samples was nearly 1.0. The suspension buffer used was TB buffer (see MEDIA) supplemented with 0.15 M KCl when needed. Since OAA absorbs light at the 240-270 nm range, two double chamber cuvettes (reference and experimental) were used. In the reference cuvette, TB buffer, with and without 0.15 M KCl, was added to both chambers. Subsequently, OAA was added in the first chamber and enzyme solution was added to the second. In the experimental cuvette, TB buffer and protein were placed in the first and second chambers respectively. OAA was added to the second chamber of the experimental cuvette at the same time it was added to the first chamber in the reference cuvette.

It is important to note that because OAA absorbs in the region, 240-270 nm, OAA induced difference spectra, in this region, may in part be due to changes in the absorbance of OAA upon binding to citrate synthase. Furthermore, OAA induced difference spectra of citrate synthase may not necessarily be due to a conformational change caused by OAA binding, but rather to a change in the environment of aromatic amino acids caused by the presence of OAA.

PURIFICATION & STRUCTURAL ANALYSIS

Prior to analyzing the kinetic and physical properties of mutant *E. coli* citrate synthase enzymes created during this project, it was important to determine whether these enzymes were indeed *E. coli* citrate synthases, and furthermore, whether they were properly purified in a manner that retained their structural integrity.

Ouchterlony immunoprecipitation reactions of mutant enzyme preparations with *E.coli* citrate synthase antiserum are shown in Figure 15. Precipitation was due to the presence of *E. coli* citrate synthase domains for each of the mutant enzyme preparations.

SDS-PAGE results of all mutant enzyme preparations (gel not shown) gave a single band of molecular weight about 48000 grams/mole (same as wild type). Contaminating bands were not apparent in lanes of the SDS gel containining excess enzyme sample. Therefore, all mutant enzyme preparations were pure.

In order to determine whether conformations of mutant *E. coli* citrate synthase enzymes were different from wild type *E. coli* citrate synthase, in the absence of substrates or other ligands, circular dichroism (CD) spectra were compared. As an example, the CD spectrum of CS R407L showed no significant difference from the wild type spectrum (see Figure 17). Therefore, no detectable overall conformational change was caused by mutating Arg-407 to leucine. Moreover, quite similar spectra were exhibited by all the other mutant enzymes created (spectra not shown). As stated in the METHODS section, determination of the percentage of α-helix in both wild type and mutant enzymes was possible by using the ellipticity values at 222 nm. Wild type *E. coli* citrate synthase has approximately 50% α-helical content. Since

the α-helical content of the mutants (seen in Table 3) were similar to the wild type value, it was expected that all the mutant enzymes maintained structural integrity despite their mutations.

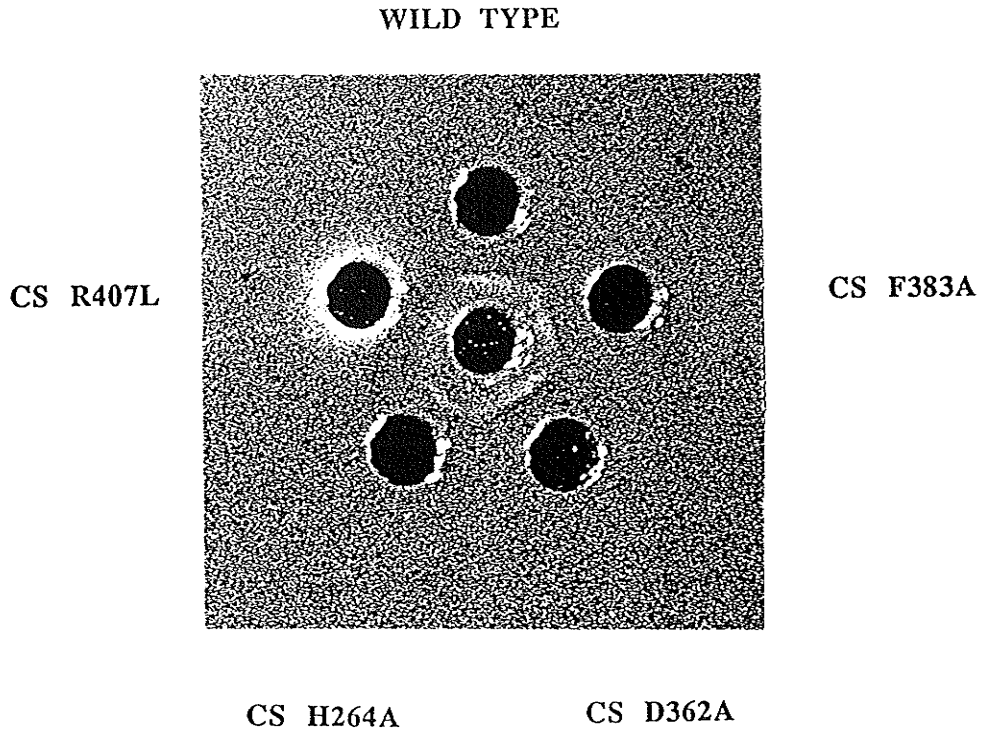

FIGURE 15: OUCHTERLONY DOUBLE-DIFFUSION OF WILD TYPE CITRATE SYNTHASE AND MUTANTS. ALL ENZYME CONCENTRATIONS WERE 82 μg/mL. TO EACH WELL, 20 μL OF SAMPLE AND UNDILUTED ANTISERUM WERE LOADED.

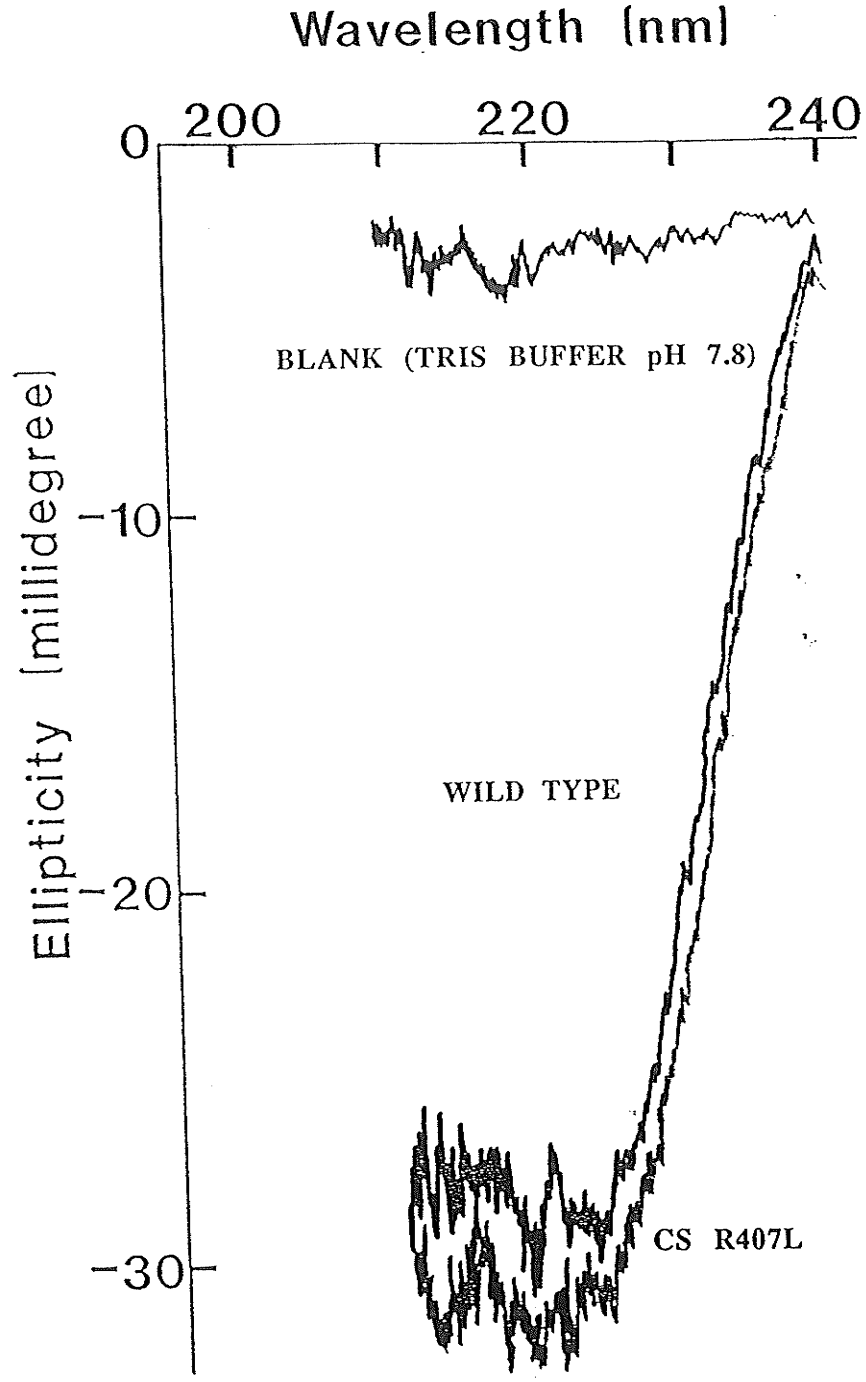

FIGURE 17: CIRCULAR DICHROISM SPECTRA OF WILD TYPE CITRATE SYNTHASE AND CS R407L. THE CONCENTRATION OF BOTH ENZYMES WAS 0.035 mg/mL.

TABLE 3: DETERMINATION OF α–HELICAL CONTENT FOR WILD TYPE CITRATE SYNTHASE AND CS R407L.

ENZYME	ELLIPTICITY (m°)	MOLAR ELLIPTICITY ($°cm^2\ dmol^{-1}$)	MEAN RESIDUE ELLIPTICITY ($°cm^2\ dmol^{-1}$)	PERCENTAGE OF α–HELIX
WILD TYPE	-26	$(-7.1\pm0.1)\times10^6$	$(-1.7\pm0.1)\times10^4$	48.20±0.05
CS R407L	-28	$(-7.7\pm0.1)\times10^6$	$(-1.8\pm0.1)\times10^4$	52.60±0.05

Figure 18 is a three-dimensional illustration of the pig heart citrate synthase active site residues surrounding OAA. Equivalent *E. coli* residues are listed in Table 1. The citrate synthase reaction mechanism (seen in Figure 7) is a result of studying the X-ray data behind Figure 18.

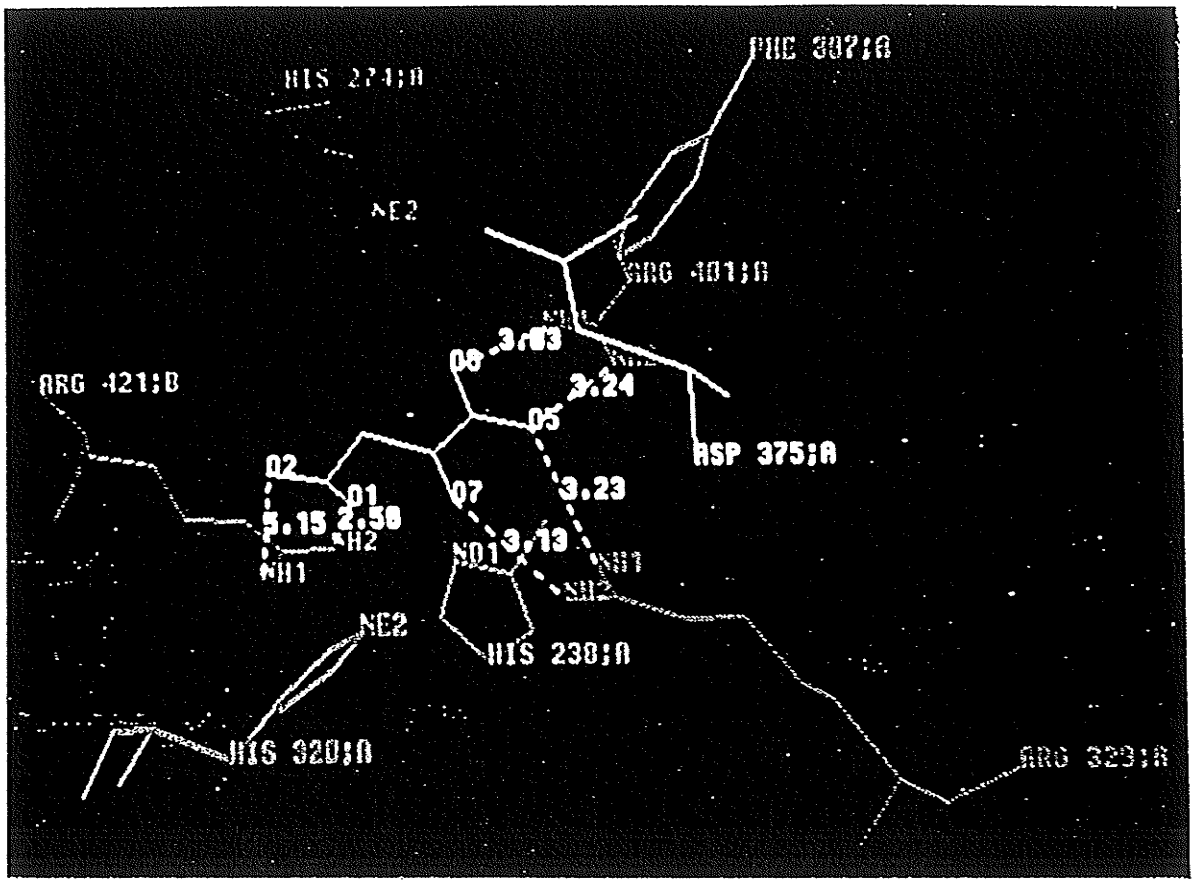

FIGURE 18: THREE-DIMENSIONAL ORIENTATION OF PIG HEART CITRATE SYNTHASE ACTIVE SITE RESIDUES. OAA IS SHOWN IN THE ACTIVE SITE. EQUIVALENT *E. coli* RESIDUES ARE LISTED IN TABLE 1. THE 'A' AND 'B' SYMBOLS, FOLLOWING THE AMINO ACID LABELS, REPRESENT THEIR RESPECTIVE SUBUNIT.

CS R407L

INTRODUCTION

X-ray diffraction studies on pig heart citrate synthase (Wiegand and Remington, 1986) have implicated Arg-421, the residue equivalent to Arg-407 of *E. coli*, in the binding of OAA and citrate to the active site. In fact, it was proposed that this arginine formed either a hydrogen bond or an ion pair with the 4-carboxyl group of OAA. To determine whether this conserved arginine played the same role in the *E. coli* enzyme, I mutated Arg-407 to leucine. The mutant enzyme created was named CS R407L.

Since Arg-407 is implicated in substrate binding and not direct catalysis, it is expected that the kcat parameter for CS R407L will be only slightly lower, while it is expected that the affinity of CS R407L for OAA will decrease, that is, that K_{iOAA} and K_{OAA} will increase.

STEADY STATE KINETIC RESULTS

IN THE PRESENCE OF KCl

CS R407L steady state kinetic parameters are listed in Table 4, and Lineweaver-Burk plots are shown in Figure 19 and 20. The nearly 33 and 11 fold increases in K_{iOAA} and K_{OAA} values respectively, were as expected. Figure 21 illustrates the comparison of K_{iOAA} and K_{OAA} values between CS R407L and wild type citrate synthase. Saturation by AcCoA was hyperbolic and associated with a Hill number of 1.00 (see Figure 24 for AcCoA Hill plot). K_{AcCoA} for CS R407L was comparable to the wild type value. The kcat value for CS R407L was unexpected. It was determined to be nearly 80 fold lower than the wild type value.

IN THE ABSENCE OF KCl

Steady state kinetic data are presented in Table 5, while Lineweaver-Burk plots are shown in Figure 22 and 23. In the absence of KCl, saturation by AcCoA was sigmoid. The Hill number was 1.55 (see Figure 24 for Hill plot). The $S_{0.5}$ value for AcCoA was determined to be almost the same as the wild type value. In the presence of 700 μM AcCoA, the apparent Km for OAA was determined to be 90±20 μM (wild type; 27±5 μM). The kcat value for CS R407L, in the presence of KCl, was 20 fold larger (wild type; 2 fold larger) than in the absence of KCl.

ACTIVATION & INHIBITION RESULTS

Activation and inhibition results are seen in Table 4 and 5 respectively. The Km, KCl value determined for CS R407L was identical to the wild type value within error. Therefore, KCl binds to CS R407L equally as well as it does to wild type *E. coli* citrate synthase. Furthermore, the KCl activation ratio (47±4) was only slightly larger than the wild type value of 39±3.

CS R407L sensitivity to NADH inhibition was unlike that of wild type. The K_i, NADH parameter was approximately 9 fold larger. Maximum percent inhibition by NADH was found to be 85±9% (wild type; 99±1%).

In the presence or absence of KCl, CS R407L did not bind α-KG very well. In the absence of KCl, a 9 fold increase in the amount of α-KG was required to inhibit CS R407L activity, while in the presence of KCl, only a 2.3 fold increase in this amount was necessary. Increased K_{is}, α-KG values, for CS R407L, were not unexpected, since α-KG inhibits by binding at the OAA site.

BINDING RESULTS

NADH BINDING

From NADH binding data collected for CS R407L (see Table 6), it was apparent that NADH binding was similar to wild type, since the K_D, NADH parameter was quite similar. The trend with NADH binding to wild type citrate synthase is that it decreases with increasing amounts of KCl. Although this trend was maintained with CS R407L, KCl inhibited NADH binding to a greater extent. The K_D, KCl value for CS R407L was 37±4 μM (wild type; 90±10 μM).

ANS BINDING

Both the CS R407L and wild type enzymes exhibited saturable decreases in fluorescence of ANS-citrate synthase complexes upon additon of AcCoA and CoA, as indicated by $L_{0.5}$, AcCoA and $L_{0.5}$, CoA values listed in Table 7. As with the wild type enzyme, when 0.2 mM OAA was present, the $L_{0.5}$, CoA values for CS R407L decreased further since OAA tightened CoA binding. A subsequent and similar decrease in respective $L_{0.5}$ values, in the presence of 0.1 M KCl, was observed for both enzymes.

As expected, the K_D, OAA and K_D, α-KG parameters for CS R407L, in the absence of KCl, increased substantially. Obviously, the loss of Arg-407 decreased the ability of this enzyme to bind OAA and α-KG.

PARAMETER	WILD TYPE	CS R407L
k_{cat} (sec^{-1})	81±6	0.959±0.143
K_{AcCoA} (μM)	120±20	130±19
K_{OAA} (μM)	26±5	280±100
K_{iOAA} (μM)	33±7	1100±200
K_{is}, α-KG (μM)	760±250	1800±170
K_m, KCl (mM)	28±4	29±4
KCl ACTIVATION RATIO	39±3	47±4
HILL NUMBER	1.0	1.0

TABLE 4: CS R407L STEADY STATE KINETICS (IN THE PRESENCE OF KCl)

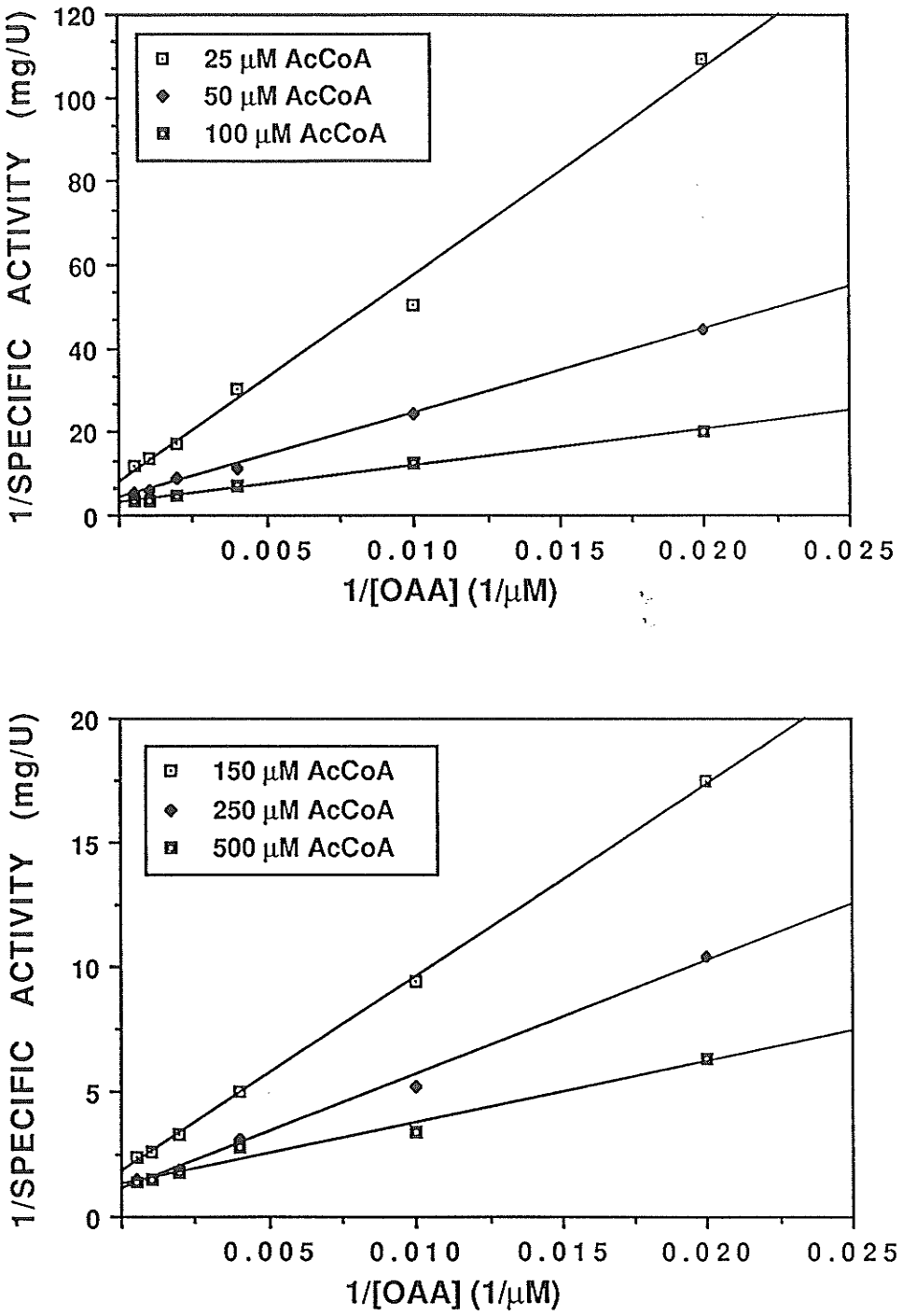

FIGURE 19: LINEWEAVER-BURK PLOTS FOR SPECIFIC ACTIVITY OF CS R407L AS A FUNCTION OF OAA CONCENTRATION AT VARIOUS AcCoA CONCENTRATIONS. KCl PRESENT.

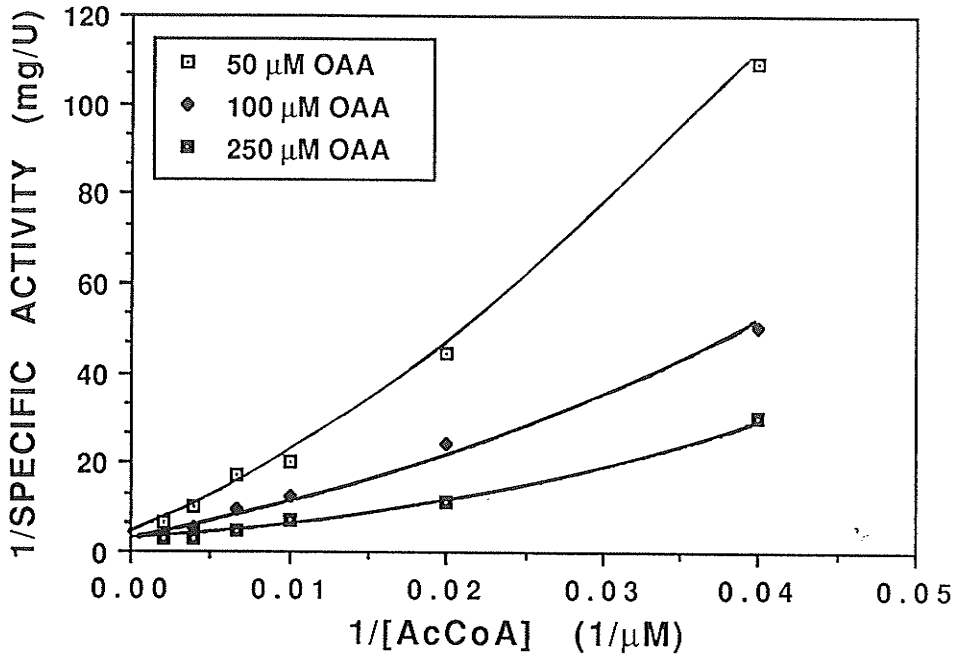

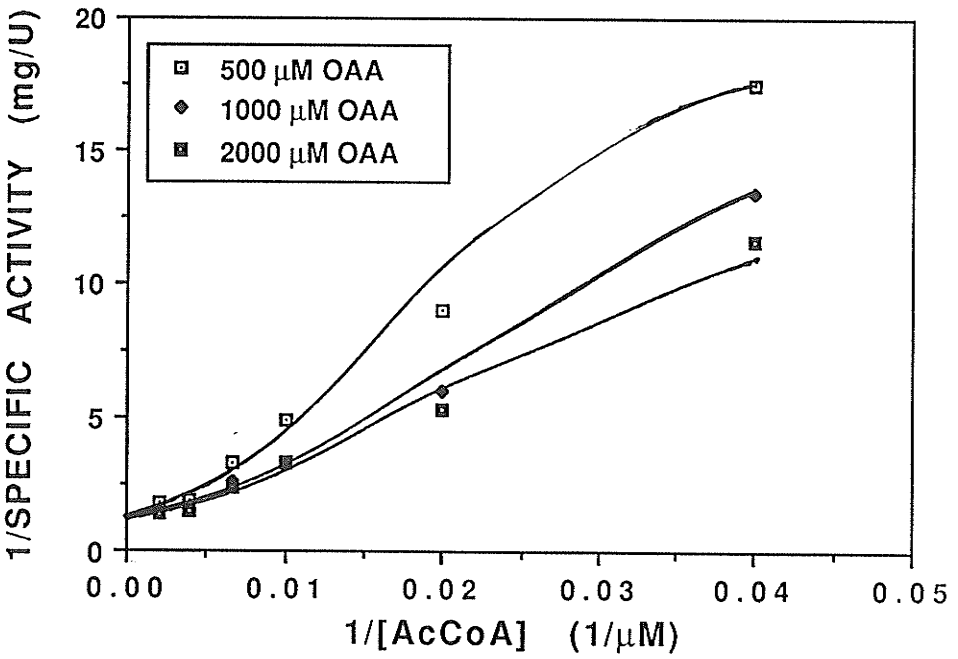

FIGURE 20: LINEWEAVER-BURK PLOTS FOR SPECIFIC ACTIVITY OF CS R407L AS A FUNCTION OF AcCoA CONCENTRATION AT VARIOUS OAA CONCENTRATIONS. KCl PRESENT.

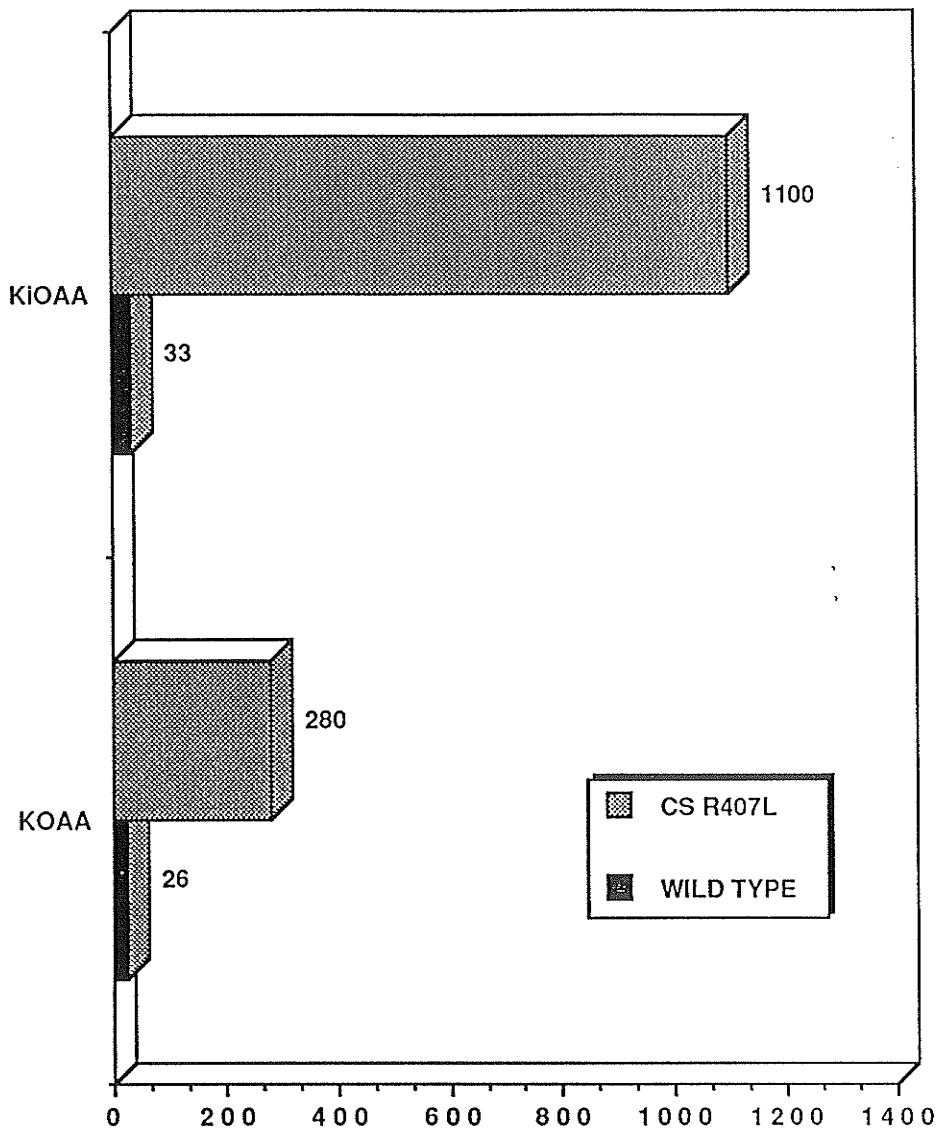

FIGURE 21: COMPARISON OF CS R407L AND WILD TYPE K_{iOAA} AND K_{OAA} PARAMETERS. KCl PRESENT.

PARAMETER	WILD TYPE	CS R407L
k_{cat} (sec^{-1})	44±5	0.046±0.006
$S_{0.5AcCoA}$ (μM)	410±20	500±50
apparent Km for OAA (μM)	27±5 ★	90±20 ☆
K_{is}, α-KG (μM)	93±18	835±330
K_i, NADH (μM)	3.3±0.1	29±5
MAXIMUM % INHIBITION BY NADH	99±1	85±9
HILL NUMBER	1.3	1.55

★ DETERMINED AT 1000 μM AcCoA.
☆ DETERMINED AT 700 μM AcCoA.

TABLE 5: CS R407L STEADY STATE KINETICS (IN THE ABSENCE OF KCl)

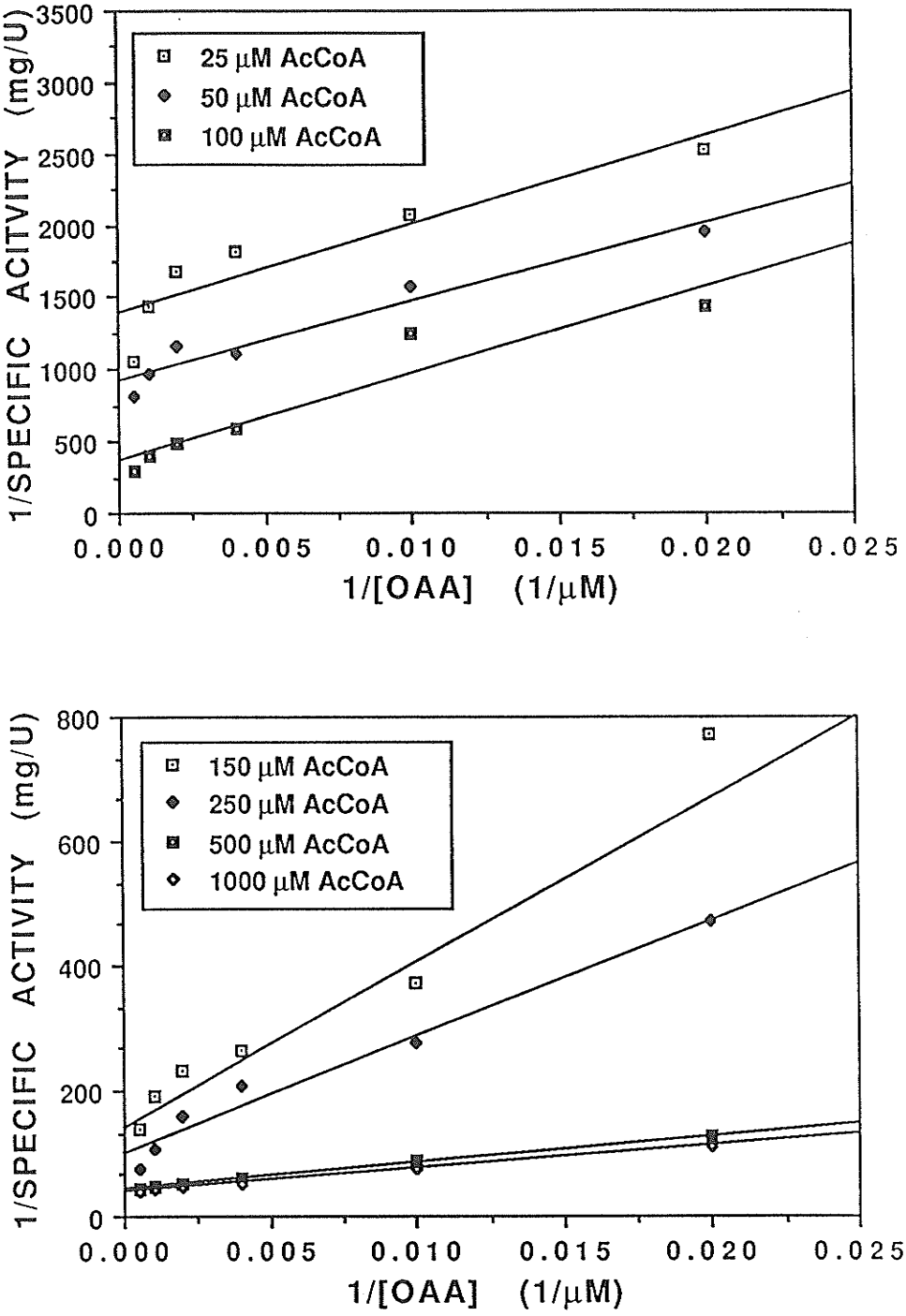

FIGURE 22: LINEWEAVER-BURK PLOTS FOR SPECIFIC ACTIVITY OF CS R407L AS A FUNCTION OF OAA CONCENTRATION AT VARIOUS AcCoA CONCENTRATIONS. KCl NOT PRESENT.

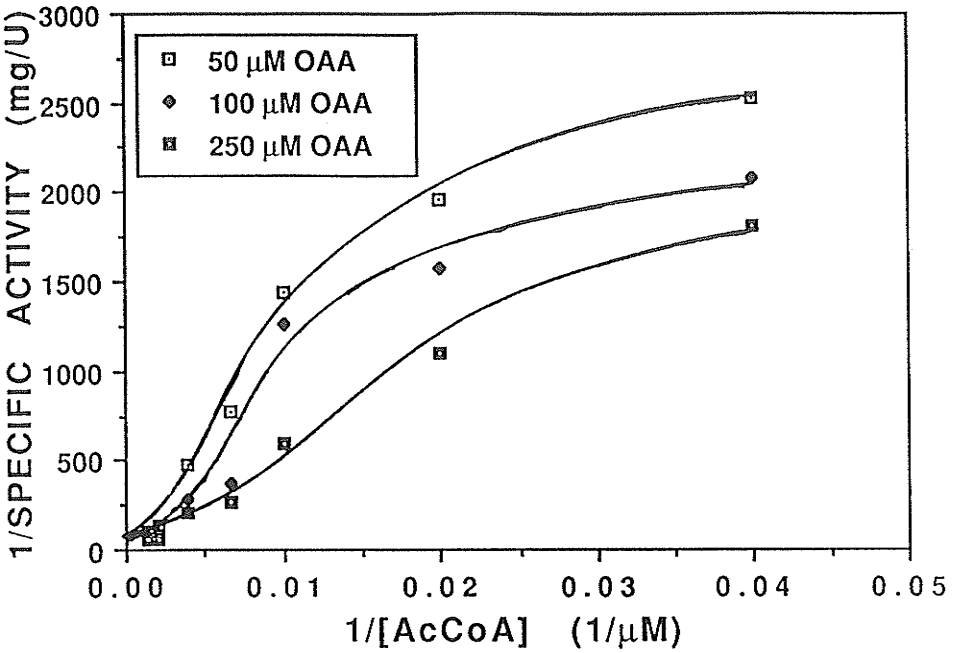

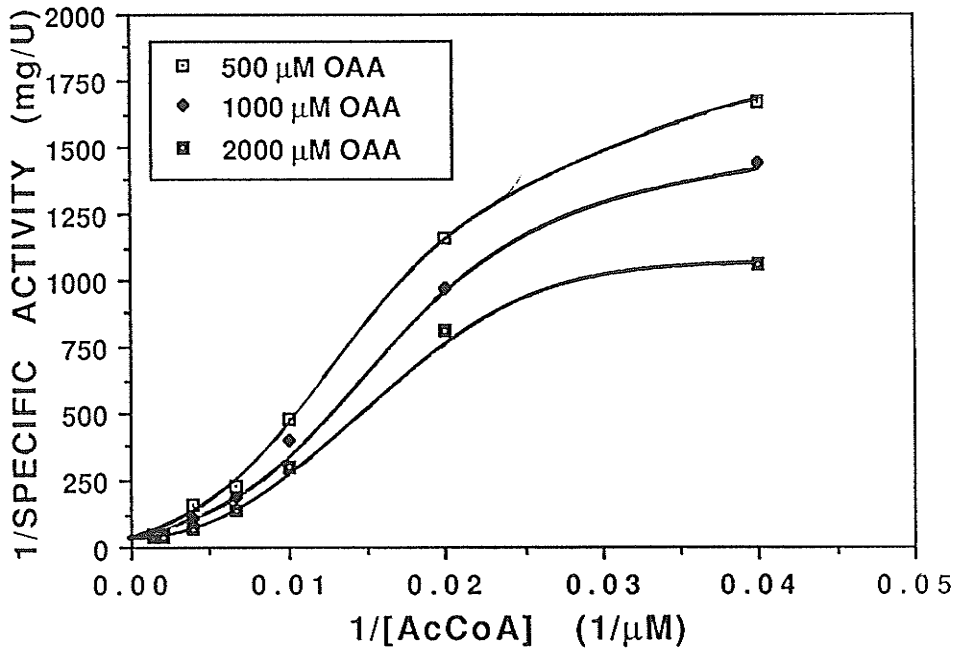

FIGURE 23: LINEWEAVER-BURK PLOTS FOR SPECIFIC ACTIVITY OF CS R407L AS A FUNCTION OF AcCoA CONCENTRATION AT VARIOUS OAA CONCENTRATIONS. KCl NOT PRESENT.

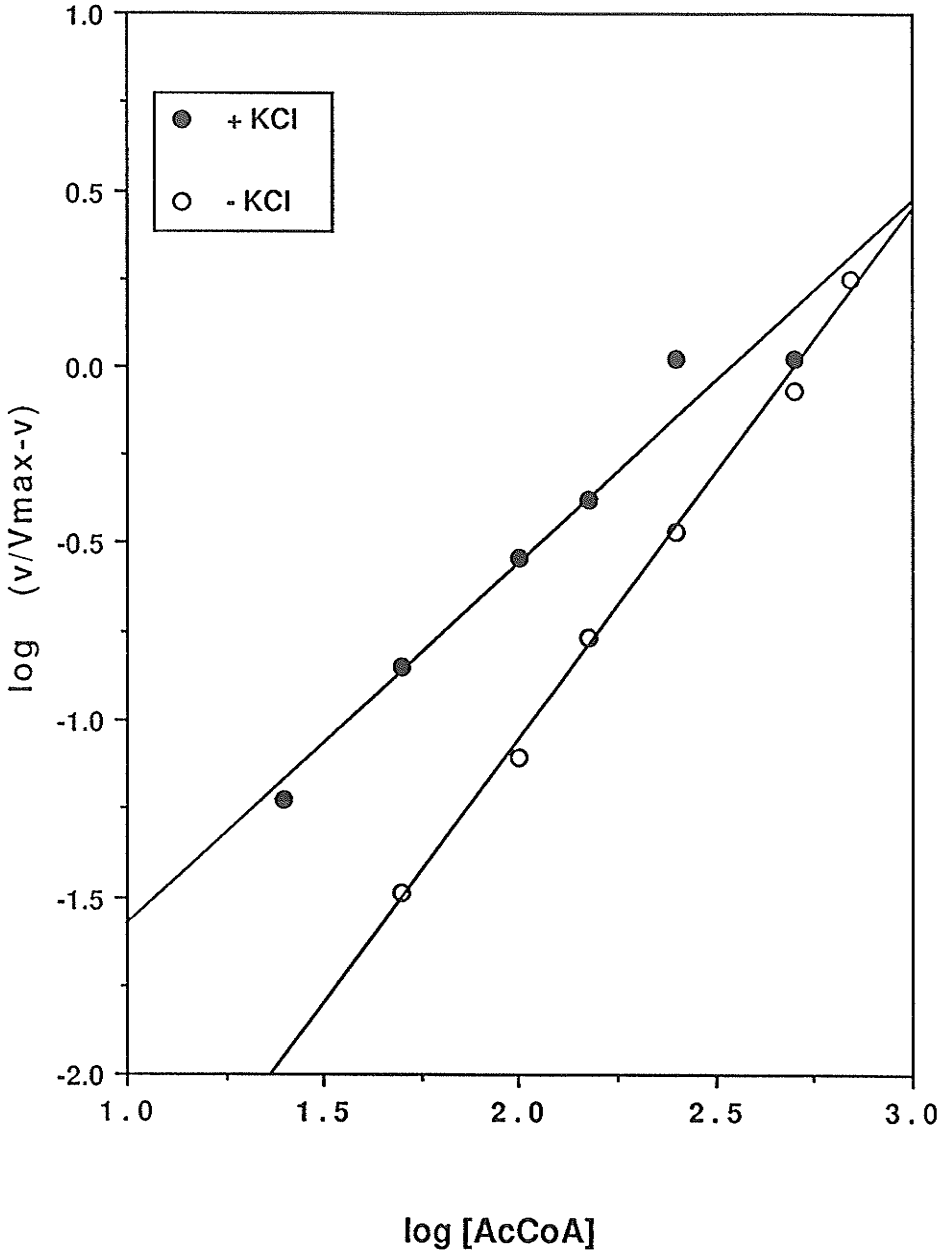

FIGURE 24: HILL PLOTS FOR AcCoA SATURATION OF CS R407L, DETERMINED IN THE PRESENCE (HILL #=1.0) AND ABSENCE (HILL #=1.55) OF KCl, AT 1000 μM OAA.

ENZYME	K_D, NADH (μM) (- KCl)	K_D, NADH (μM) (+ KCl)			K_D, KCl (μM)
		0.1 M	**0.2 M**	**0.3 M**	
WILD TYPE	1.94±0.07 *0.42-0.74*	3.68±0.05 *0.53±0.03*	6.87±0.16 *0.49±0.01*	11.8±0.50 *0.43±0.01*	90±10
CS R407L	2.36±0.29 *0.73±0.03*	7.26±0.51 *0.67±0.03*	12.33±1.30 *0.66±0.05*	16.64±0.39 *0.58±0.01*	37±4

TABLE 6: CS R407L NADH BINDING RESULTS

PARAMETER	WILD TYPE		CS R407L	
(μM)	NO KCl	0.1 M KCl	NO KCl	0.1 M KCl
$L_{0.5}$, AcCoA	260±40	60±3	250±20	70±4
$L_{0.5}$, CoA	270±40	53±3	275±55	75±5
$L_{0.5}$, CoA †	73±3	47±5	158±6	60±7
K_D, OAA ✞	25±1	ND	300±30	ND
K_D, α-KG ✞	76±11	ND	2500±100	ND

† = MEASURED IN PRESENCE OF 0.2 mM OAA
✞ = MEASURED IN PRESENCE OF 0.2 mM CoA
ND = NOT DETERMINED

TABLE 7: CS R407L ANS BINDING RESULTS

CS H264A

INTRODUCTION

Wiegand and Remington (1986) proposed that His-274, a pig heart citrate synthase residue, equivalent to His-264 of the *E. coli* enzyme, was involved in the first step of the citrate synthase reaction mechanism, enolization of AcCoA. This charged residue was believed to donate a proton to the carbonyl oxygen of AcCoA. In addition, His-274 was implicated in proton abstraction. Since citrate synthase converts its substrates into products by sequential protonation and deprotonation, it was of interest to observe the consequences of mutating His-264 to alanine (CS H264A).

The catalytic efficiency of CS H264A is expected to be severely retarded if protonation and deprotonation of substrates by His-264 is lacking. Since many amino acids exist to secure and position the substrates for interaction with His-264, the effect of this mutation on substrate binding may be minimal.

STEADY STATE KINETIC RESULTS

IN THE PRESENCE OF KCl

Steady state kinetic data listed in Table 8 were determined from Lineweaver-Burk plots presented in Figure 25 and 26. In comparison to wild type citrate synthase, a decrease in the kcat value of approximately 620 fold was observed along with a four fold increase in the affinity of the enzyme for OAA and AcCoA. The K_{OAA} and K_{AcCoA} values calculated were 6.7±1.3 μM and 32±7 μM respectively.

IN THE ABSENCE OF KCl

Because the loss of His-264 severely retarded the catalytic efficiency of the enzyme in the presence of KCl, collection of steady state kinetic data in the absence of KCl was not possible. Attempts to assay for activity using a 50 fold increase in protein concentration and an 8 fold increase in AcCoA, as compared to wild type assay conditions, proved unsuccessful. As a result, collection of steady state kinetic and Lineweaver Burk plot data was not feasible. Furthermore, a Hill number was not determined.

ACTIVATION & BINDING RESULTS

Table 8 shows CS H264A activation results. The Km, KCl result (6.2±0.4 mM), for CS H264A, was four fold lower than the wild type value. Therefore, the affinity of CS H264A for KCl, with respect to wild type, increased by a factor of four. Consequently, a 10 fold decrease in the KCl activation ratio was not unexpected. The maximum specific activity observed for this mutant occurred in the presence of 20 mM KCl (see Figure 27 for KCl saturation curve). In contrast, wild type citrate synthase attains maximum specific activity at 100 mM KCl.

Since CS H264A is virtually inactive in the absence of KCl, collection of data from α-KG and NADH inhibition studies was not possible. Inhibition of CS H264A by α-KG, in the presence of KCl, however, proved to be unaffected. The K_{is}, α-KG parameter was identical to the value for wild type citrate synthase.

BINDING RESULTS

NADH BINDING

NADH binding data for CS H264A are outlined in Table 9. In the absence of KCl, the K_D, NADH parameter is 23.24±0.42 μM. Therefore, binding of NADH to CS H264A is decreased by a factor of 12. The presence of 0.1 M KCl, causes a further 1.3 fold decrease in NADH binding (1.9 fold for wild type). As the concentration of KCl increases to 0.2 and 0.3 M, however, a further decrease in NADH binding to CS H264A did not occur as it would have with the wild type enzyme. Finally, the K_D, KCl result for CS H264A was 5.6 fold lower than the wild type value.

ANS BINDING

ANS binding results are listed in Table 10. As with the wild type enzyme, when AcCoA and CoA were added to ANS-CS H264A complexes, saturable decreases in fluorescence resulted. The $L_{0.5}$ AcCoA and CoA values were quite similar to wild type results regardless of whether KCl or OAA were present.

In the absence of KCl, K_D, OAA and K_D, α-KG results were slightly larger than those for wild type.

ULTRAVIOLET DIFFERENCE SPECTROSCOPY

Relative to wild type *E. coli* citrate synthase, the increased affinities (lower Kms) for both substrates, lower Km for KCl activation, and weaker binding of NADH values observed for CS H264A, suggest the possibility that the H264A mutation causes a conformational shift towards the R or active state, as previously postulated for the *E. coli* CS R319L mutant (Anderson et al, 1991). In order to obtain direct evidence for such a change, ultraviolet difference spectra were collected. Previous studies have demonstrated that both OAA and KCl induce characteristic difference spectra in wild type and CS R319L enzymes; the full OAA difference spectrum is obtained with wild type enzyme only in the presence of KCl, while with CS R319L, KCl has no effect (Anderson et al, 1991).

In the absence of KCl, it is possible that the binding of OAA (first substrate to bind) to wild type *E. coli* citrate synthase induced a conformational change which was detected by ultraviolet difference spectroscopy (see Figure 28 A). It is also possible that OAA binding, in the presence of KCl, induced a further conformational change (see Figure 28 B). For CS H264A, Figure 29 shows two ultraviolet difference spectra induced by OAA in the absence (A) and presence (B) of KCl. Because the two spectra were nearly identical, this suggested that KCl had no effect on the conformation of the protein. Therefore, it is possible that OAA binding to CS H264A, in the absence of KCl, induced an enzyme conformation further along in R state than the wild type conformation in the absence of KCl.

PARAMETER	WILD TYPE	CS H264A
k_{cat} (sec^{-1})	81±6	0.130±0.003
K_{AcCoA} (μM)	120±20	32±7
K_{OAA} (μM)	26±5	6.7±1.3
K_{iOAA} (μM)	33±7	69±22
K_{is}, α-KG (μM)	760±250	760±230
K_m, KCl (mM)	28±4	6.2±0.4
KCl ACTIVATION RATIO	39±3	3.5±0.5
HILL NUMBER	1.0	1.0

TABLE 8: CS H264A STEADY STATE KINETICS
(IN THE PRESENCE OF KCl)

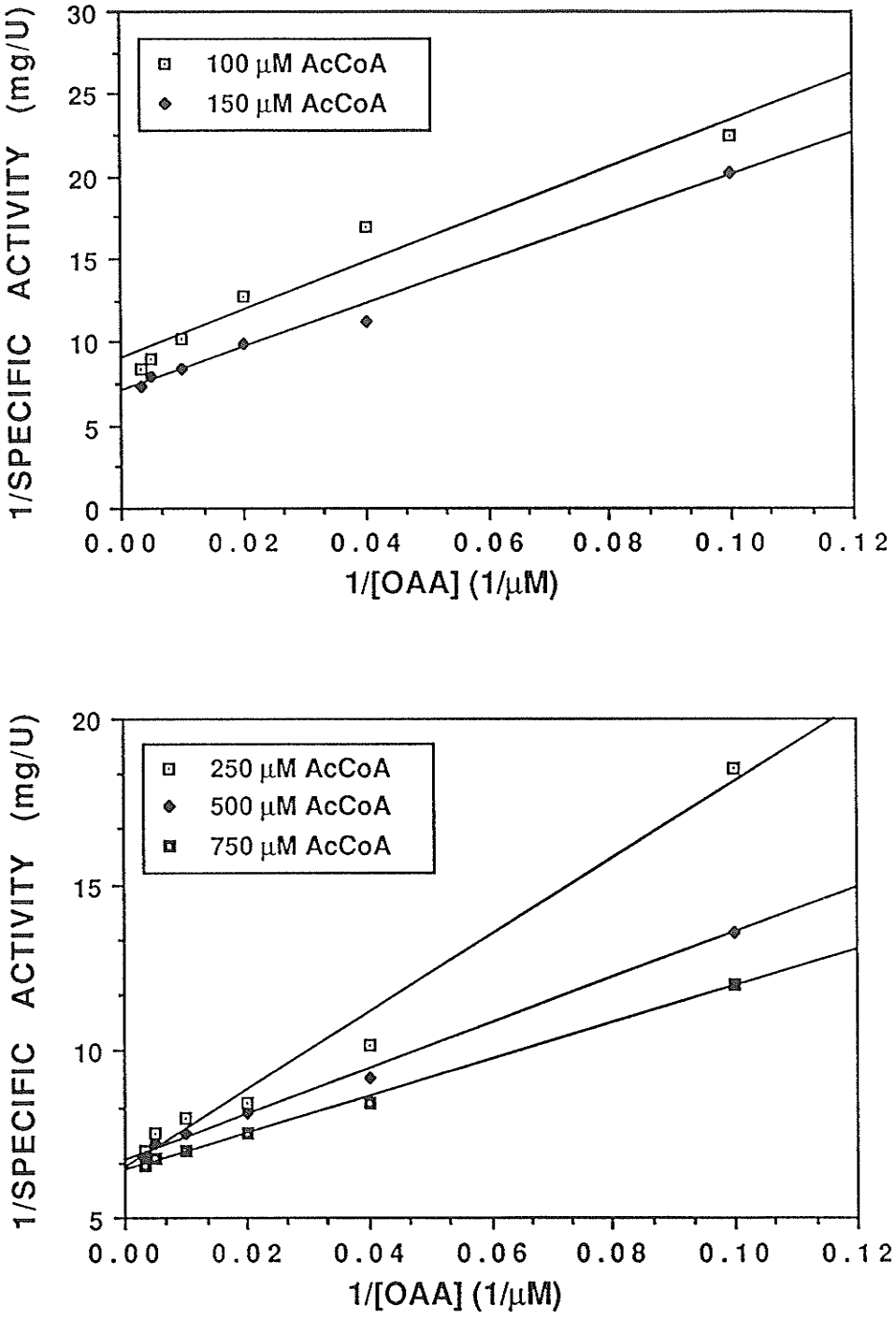

FIGURE 25: LINEWEAVER-BURK PLOTS FOR SPECIFIC ACTIVITY OF CS H264A AS A FUNCTION OF OAA CONCENTRATION AT VARIOUS AcCoA CONCENTRATIONS. KCl PRESENT.

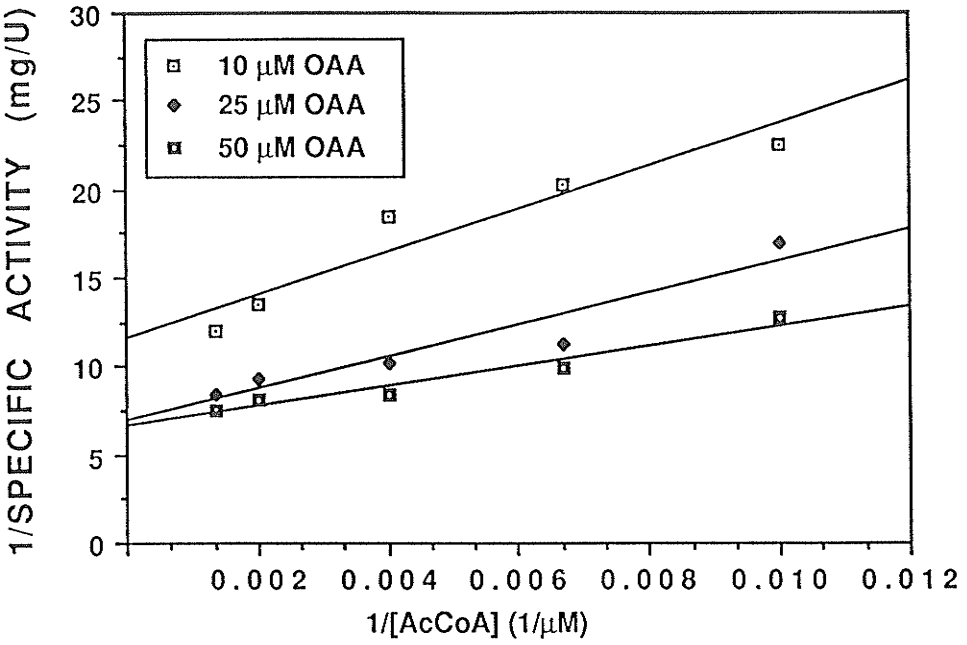

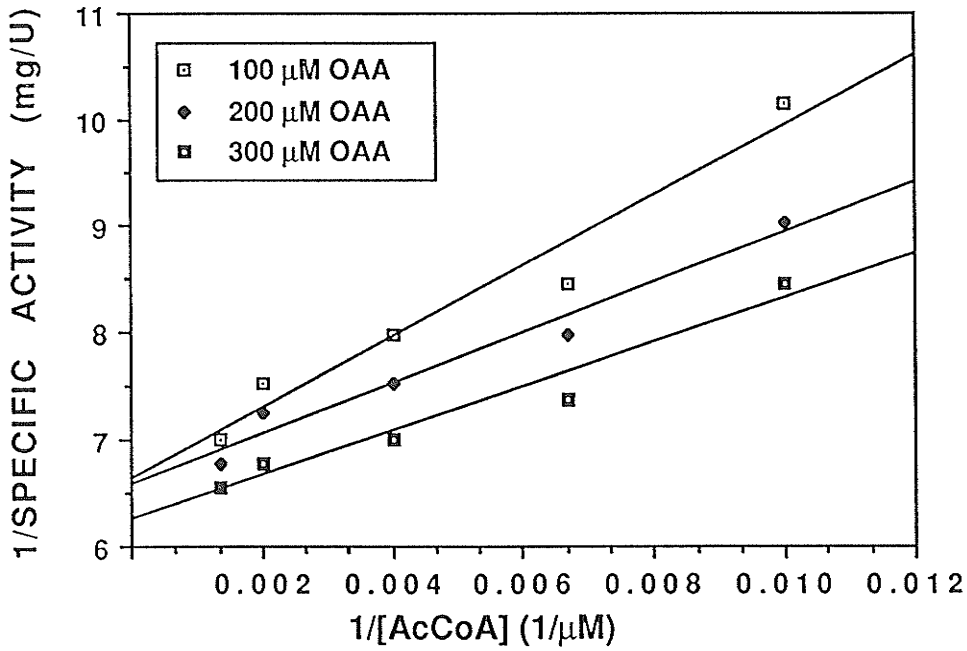

FIGURE 26: LINEWEAVER-BURK PLOTS FOR SPECIFIC ACTIVITY OF CS H264A AS A FUNCTION OF AcCoA CONCENTRATION AT VARIOUS OAA CONCENTRATIONS. KCl PRESENT.

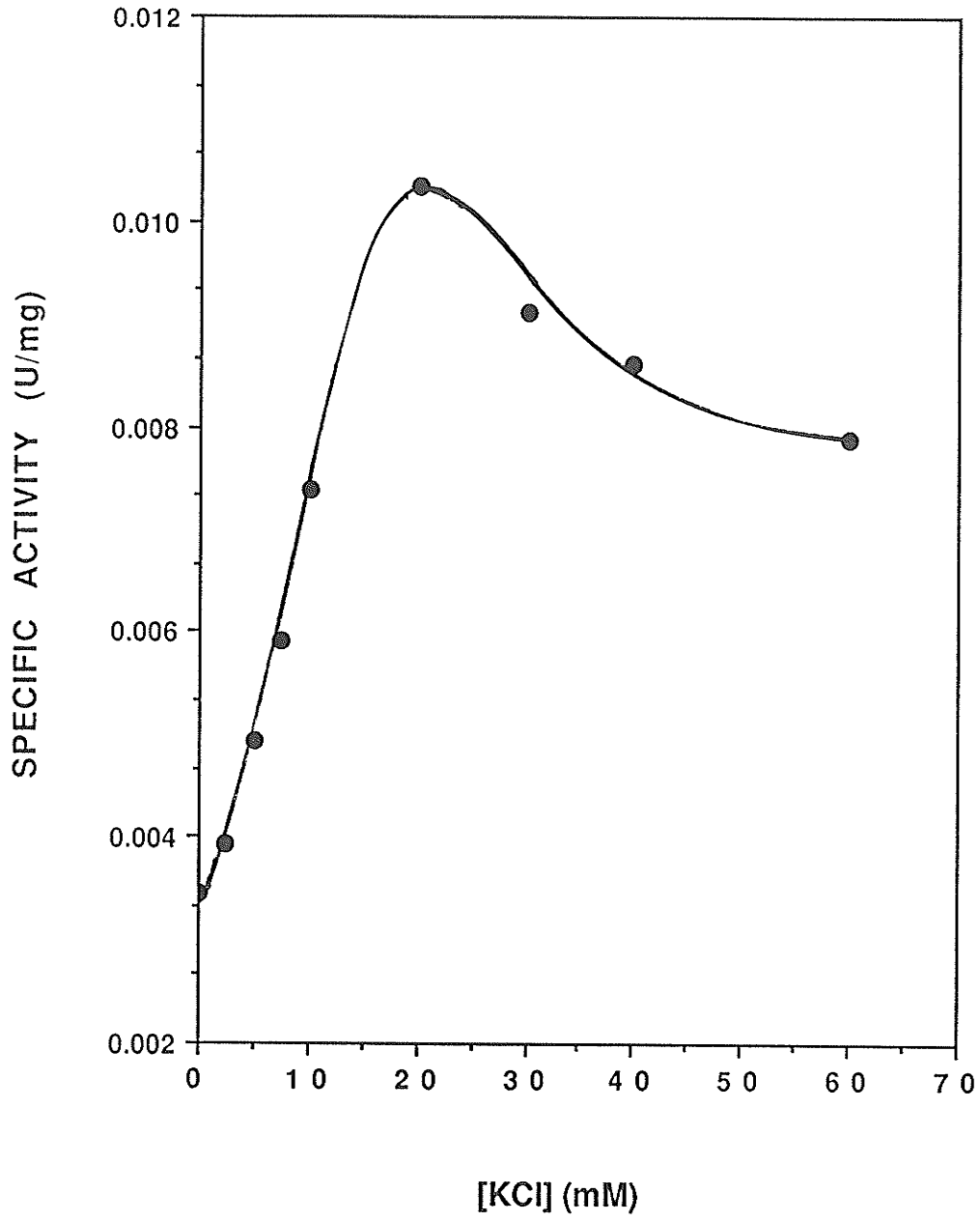

FIGURE 27: KCl SATURATION CURVE FOR CS H264A.

ENZYME	K_D, NADH (μM) (- KCl)	K_D, NADH (μM) (+ KCl)			K_D, KCl
		0.1 M	**0.2 M**	**0.3 M**	
WILD TYPE	1.94±0.07 *0.42-0.74*	3.68±0.05 *0.53±0.03*	6.87±0.16 *0.49±0.01*	11.8±0.50 *0.43±0.01*	90±10
CS H264A	23.24±0.42 *0.62±0.02*	29.11±0.99 *0.68±0.02*	30.14±1.81 *0.63±0.01*	29.86±1.64 *0.57±0.01*	16±4

TABLE 9: CS H264A NADH BINDING RESULTS

PARAMETER	WILD TYPE		CS H264A	
(μM)	**NO KCl**	**0.1 M KCl**	**NO KCl**	**0.1 M KCl**
$L_{0.5}$, AcCoA	260±40	60±3	195±30	61±7
$L_{0.5}$, CoA	270±40	53±3	230±40	56±9
$L_{0.5}$, CoA ✝	73±3	47±5	77±7	49±8
K_D, OAA ✞	25±1	ND	52±4	ND
K_D, α-KG ✞	76±11	ND	120±19	ND

✝ = MEASURED IN PRESENCE OF 0.2 mM OAA
✞ = MEASURED IN PRESENCE OF 0.2 mM CoA
ND = NOT DETERMINED

TABLE 10: CS H264A ANS BINDING RESULTS

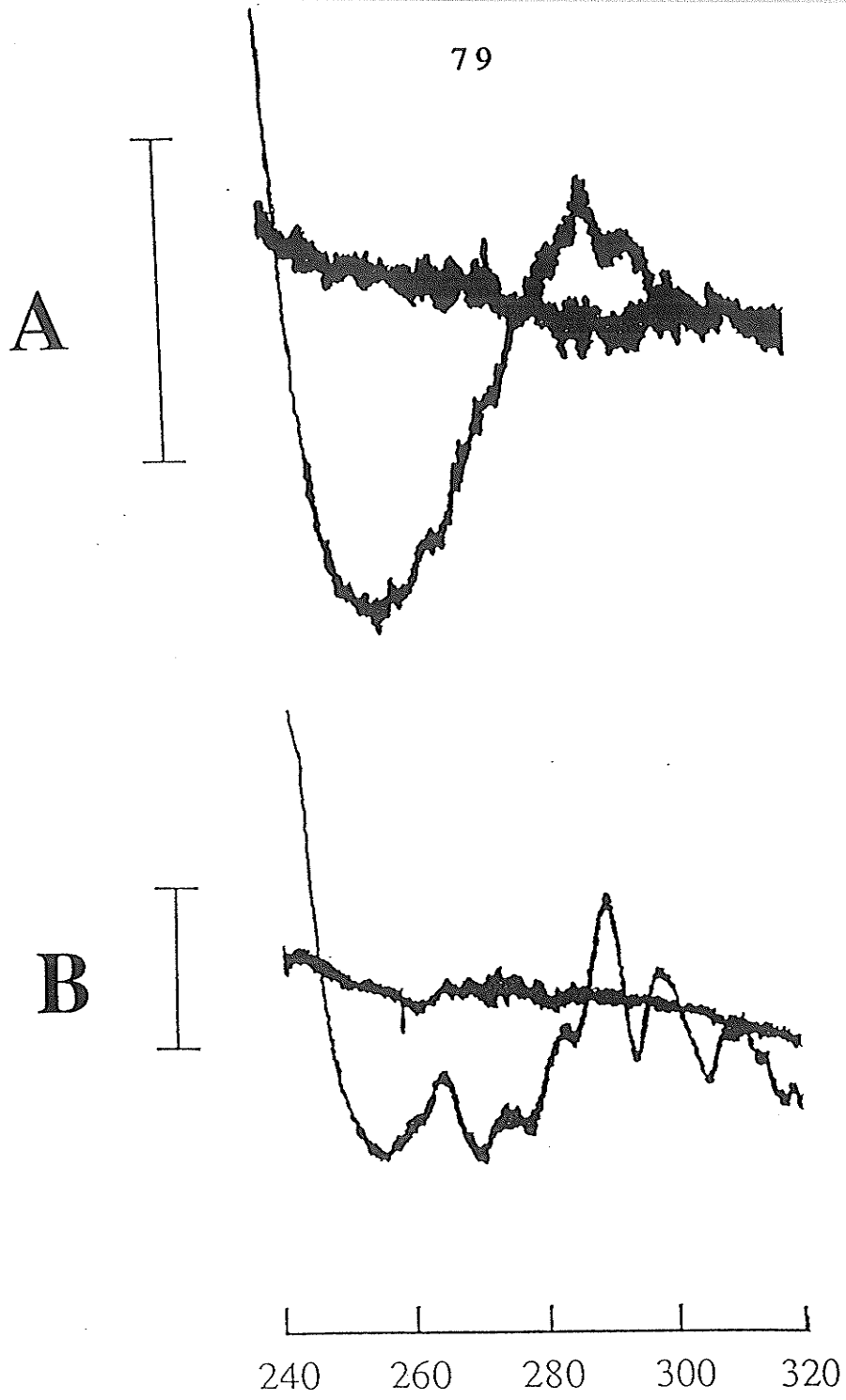

FIGURE 28: DIFFERENCE SPECTRA INDUCED IN WILD TYPE CITRATE SYNTHASE BY OAA, IN THE ABSENCE (A) AND PRESENCE (B) OF KCl. ENZYME, OAA, AND KCl CONCENTRATIONS WERE 41 μM, 0.91 mM, AND 0.15 M RESPECTIVELY. INCLUDED IN BOTH SPECTRA IS A BASE-LINE, & A VERTICAL BAR REPRESENTING 0.05 Å. THE SCALE AT THE BOTTOM IS WAVELENGTH IN NANOMETERS

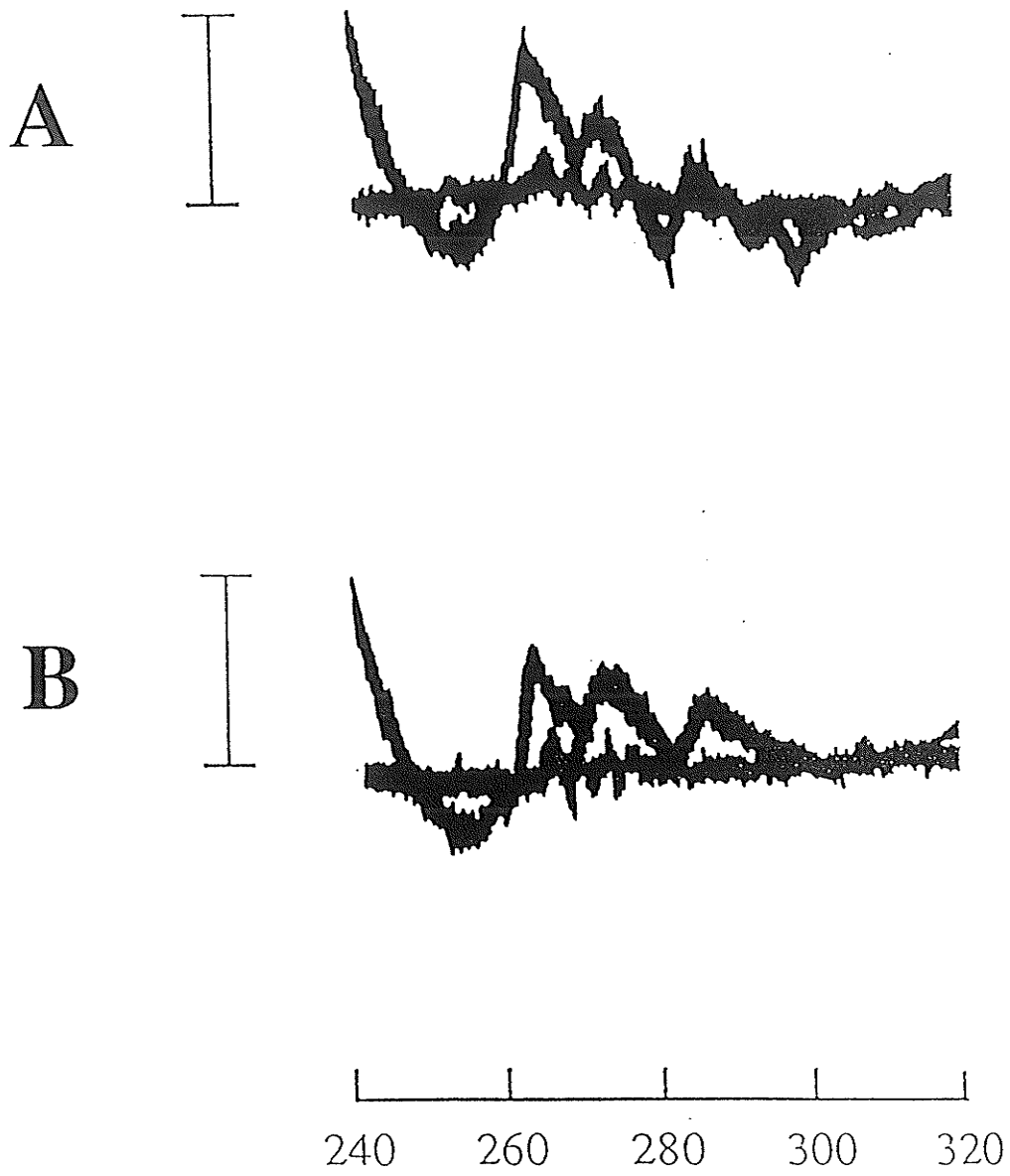

FIGURE 29: DIFFERENCE SPECTRA INDUCED IN CS H264A BY OAA, IN THE ABSENCE (A) AND PRESENCE (B) OF KCl. ENZYME, OAA, AND KCl CONCENTRATIONS WERE 41 μM, 0.91 mM, AND 0.15 M RESPECTIVELY. INCLUDED IN BOTH SPECTRA IS A BASE-LINE, & A VERTICAL BAR REPRESENTING 0.05 Å. THE SCALE AT THE BOTTOM IS WAVELENGTH IN NANOMETERS

CS F383A

INTRODUCTION

Wiegand and Remington (1986) did not predict a role for Phe-397, a pig heart citrate synthase active site residue, conserved in all known citrate synthase sequences and equivalent to Phe-383 of the *E. coli* enzyme. However, the authors did observe an "edge on" interaction of the phenyl ring in the vicinity of the substrates OAA and AcCoA. Because phenylalanine is a stable uncharged amino acid, it was difficult to predict the effect of removing it. Phe-383 may play a role in maintaining the structure of the active site. Acting as a space "filler", Phe-383 may keep other active site residues in their proper orientations for reaction with substrates. Phe-383 was mutated to alanine to determine what effect, if any, the phenyl ring had on catalysis or substrate binding. The mutant enzyme created was designated CS F383A.

STEADY STATE KINETIC RESULTS

IN THE PRESENCE OF KCl

CS F383A steady state kinetics are listed in Table 11, while Lineweaver-Burk plots are shown in Figure 30 and 31. Remarkably, saturation by AcCoA, in the presence of KCl, was sigmoid and associated with a Hill number of 1.85 (see Figure 32 for specific activity versus AcCoA concentration plot and Figure 33 for CS F383A/wild type AcCoA Hill plot). Because kinetic data for CS F383A were sigmoid, values for K_{AcCoA}, K_{iOAA}, and K_{OAA}, could not be extracted. Instead, $S_{0.5,\ AcCoA}$ and apparent Km for OAA values are reported. An $S_{0.5,\ AcCoA}$ value of 2000±100 μM was determined for this enzyme. The apparent Km

for OAA, 30±5, at 2000 μM AcCoA was equivalent to the wild type value (27±5 μM at 1000 μM AcCoA) within error. The kcat value for CS F383A was determined to be about 8 fold lower than the wild type value.

IN THE ABSENCE OF KCl

Table 12 shows the steady state kinetic data for CS F383A in the absence of KCl. When AcCoA saturation of CS F383A was conducted, in the absence of KCl, rates of activity collected were very low. Correction for a blank rate due to CoA in AcCoA, which increases as AcCoA increases, was necessary. However, subtraction of large blank values led to badly scattered data which showed no signs of saturating the enzyme at the highest AcCoA concentration (4000 μM) tested. Therefore, these data were not collected, however, Michaelis-Menten and Lineweaver-Burk OAA saturation plots, in the presence of 2000 μM AcCoA, were collected (see Figure 34). Because AcCoA saturation was not obtained, a Hill number and a value for $S_{0.5,AcCoA}$ could not be determined. From data presented in Figure 34, the apparent Km for OAA was 1000±100 μM at 2000 μM AcCoA, whereas the apparent Km for the wild type enzyme, at 1000 μM AcCoA, is 27±5 μM.

ACTIVATION & INHIBITION RESULTS

Activation and inhibition results are seen in Table 11 and 12 respectively. The Km, KCl value for CS F383A was determined to be twice the wild type value. As a result, the ability for KCl to bind to CS F383A was decreased by a factor of two. The KCl activation ratio (14±1) of this mutant, however, was found to be 3 fold lower than the wild type value of 39±3.

Determining the sensitivity of CS F383A to NADH inhibition was not possible since the enzyme had such low activity in the absence of KCl. Therefore, K_i, NADH and maximum percent inhibition by NADH values were not possible to determine.

In the presence of KCl, a 1.4 fold increase in the K_{is}, α-KG value for CS F383A was observed. Because CS F383A lacked activity in the absence of KCl, determination of a K_{is},α-KG value was not possible.

BINDING RESULTS

NADH BINDING

Based on NADH binding data collected for CS F383A (see Table 10), it was apparent that NADH binding was similar to wild type, since the K_D, NADH parameter was only slightly larger. NADH binding to CS F383A decreased significantly upon addition of increasingly concentrated KCl. The K_D, KCl value for CS F383A was determined to be 16±4 μM (wild type; 90±10 μM).

ANS BINDING

Both the CS F383A and wild type enzymes exhibited saturable decreases in fluorescence of ANS-citrate synthase complexes upon additon of AcCoA and CoA, as indicated by $L_{0.5}$, AcCoA and $L_{0.5}$, CoA values listed in Table 11. However, in comparison to wild type $L_{0.5}$, AcCoA and CoA values, CS F383A values were greater by a factor of two. The presence of 0.2 mM OAA did not appear to tighten CoA binding nor significantly decrease the $L_{0.5}$, CoA values for CS F383A in the absence of KCl. A decrease in the $L_{0.5}$, AcCoA value, in the presence of 0.1 M KCl and 0.2 mM OAA, was observed however.

In the absence of KCl, the K_D, OAA and K_D, α-KG results were 300±30 μM and 3600±200 μM respectively. Thus, the ability of CS F383A to bind OAA and α-KG was hindered.

ULTRAVIOLET DIFFERENCE SPECTROSCOPY

Since a strongly sigmoidal saturation curve for AcCoA, in the presence of KCl, was associated with a $S_{0.5}$, AcCoA value, 17 fold greater than the wild type value, it is believed that this mutant is still in the T conformational state, even in the presence of 0.1 M KCl. Wild type citrate synthase shows non-cooperative kinetics under these conditions. To obtain further evidence for such a conformational change, OAA induced difference spectra were collected for reasons previously explained for the CS H264A mutant.

OAA induced ultraviolet difference spectra for CS F383A in the absence (Figure 35-A) and presence (Figure 35-B) of KCl were different. Response to KCl was similar to the wild type difference spectrum under identical conditions. However, it should be noted that the CS F383A OAA induced difference spectrum, in the presence of KCl, was similar in appearance to the wild type OAA induced spectrum, in the absence of KCl. This may suggest that prior to KCl addition, CS F383A was in a conformation favoring the T-state, but when KCl was present, CS F383A was in a conformation favoring the R-state. In fact, this R-state favoring conformation may have been similar to the conformation of the wild type enzyme in the absence of KCl since the spectra were similar. When comparing CS F383A OAA difference spectra, in the presence of KCl, to the wild type OAA difference spectra, in the absence of KCl, it should be remembered that CS F383A lacks Phe 383 which may contribute to the difference spectrum.

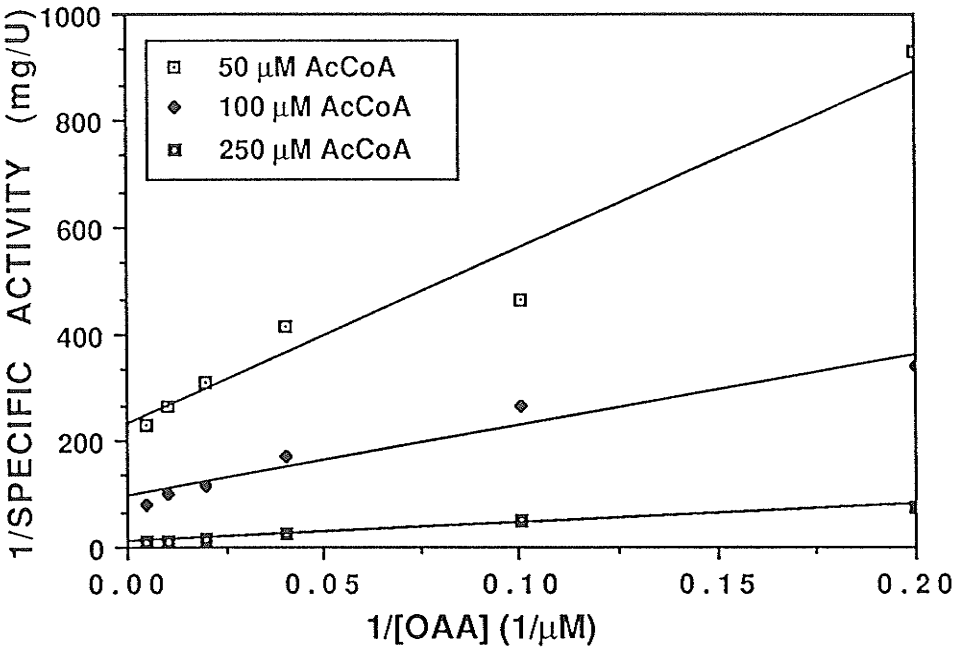

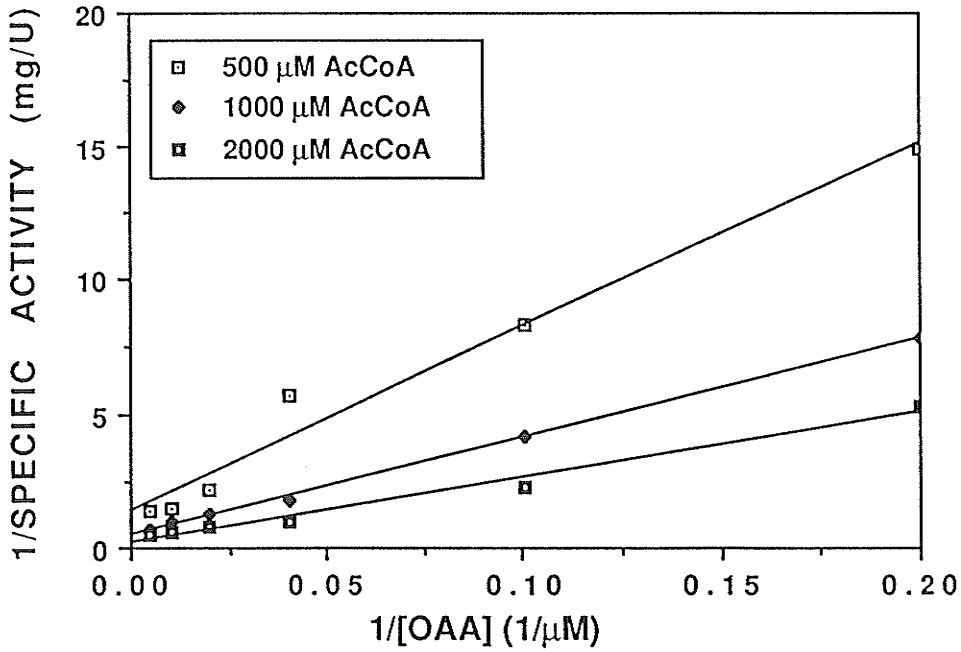

FIGURE 30: LINEWEAVER-BURK PLOTS FOR SPECIFIC ACTIVITY OF CS F383A AS A FUNCTION OF OAA CONCENTRATION AT VARIOUS AcCoA CONCENTRATIONS. KCl PRESENT.

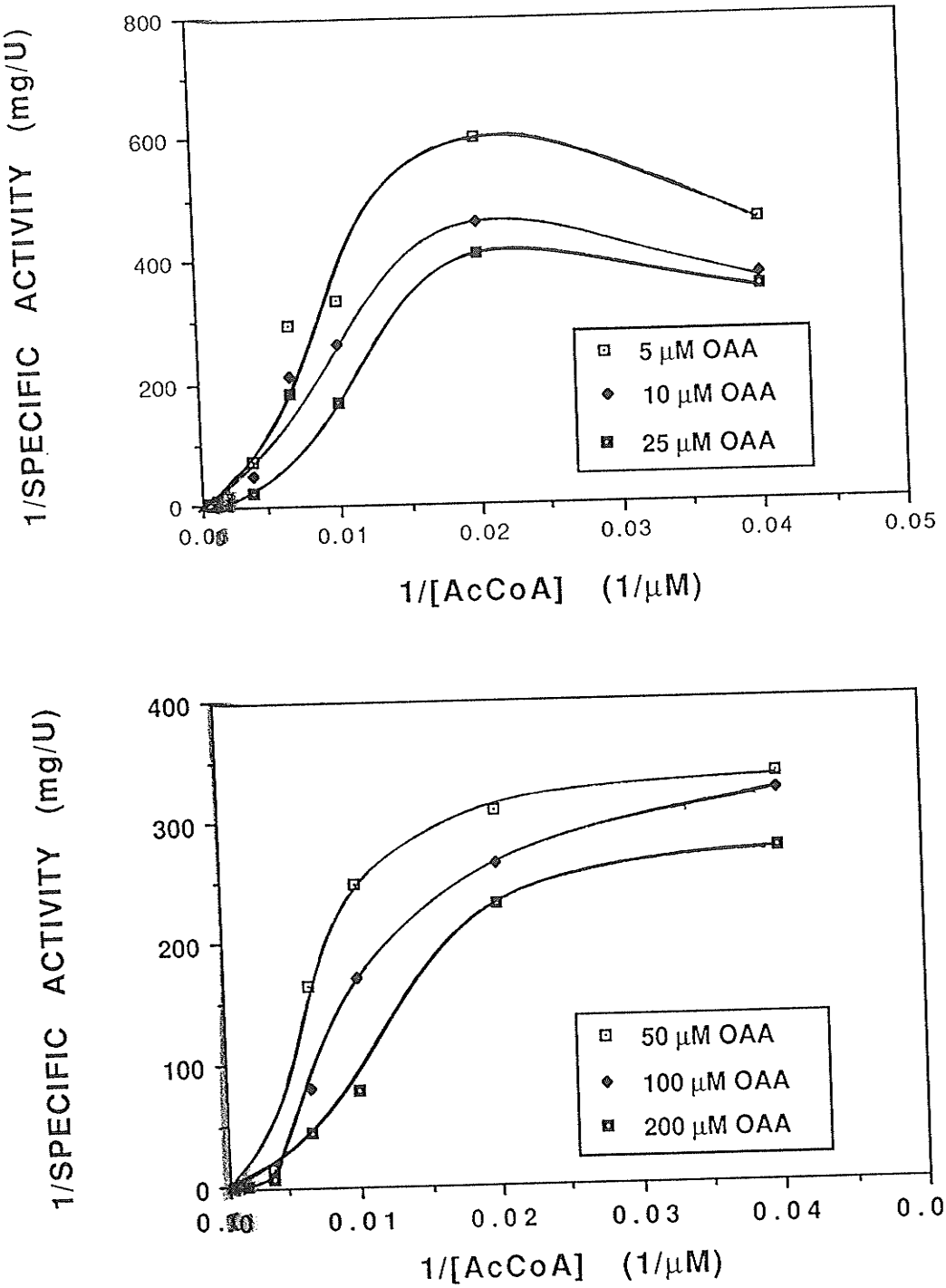

FIGURE 31: LINEWEAVER-BURK PLOTS FOR SPECIFIC ACTIVITY OF CS F383A AS A FUNCTION OF AcCoA CONCENTRATION AT VARIOUS OAA CONCENTRATIONS. KCl PRESENT.

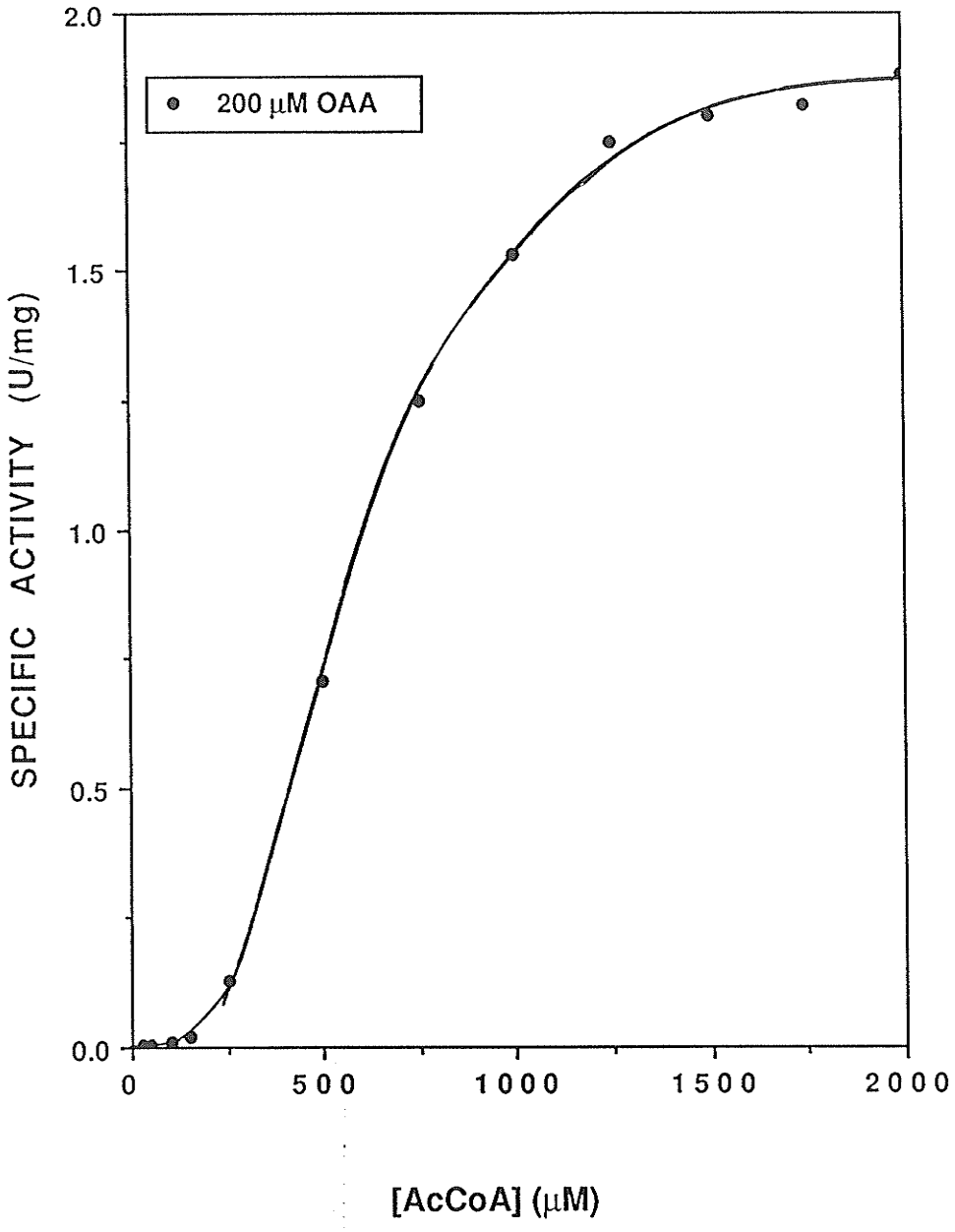

FIGURE 32: MICHAELIS-MENTEN PLOT FOR SPECIFIC ACTIVITY OF CS F383A AS A FUNCTION OF AcCoA CONCENTRATION AT 200 μM OAA. KCl PRESENT.

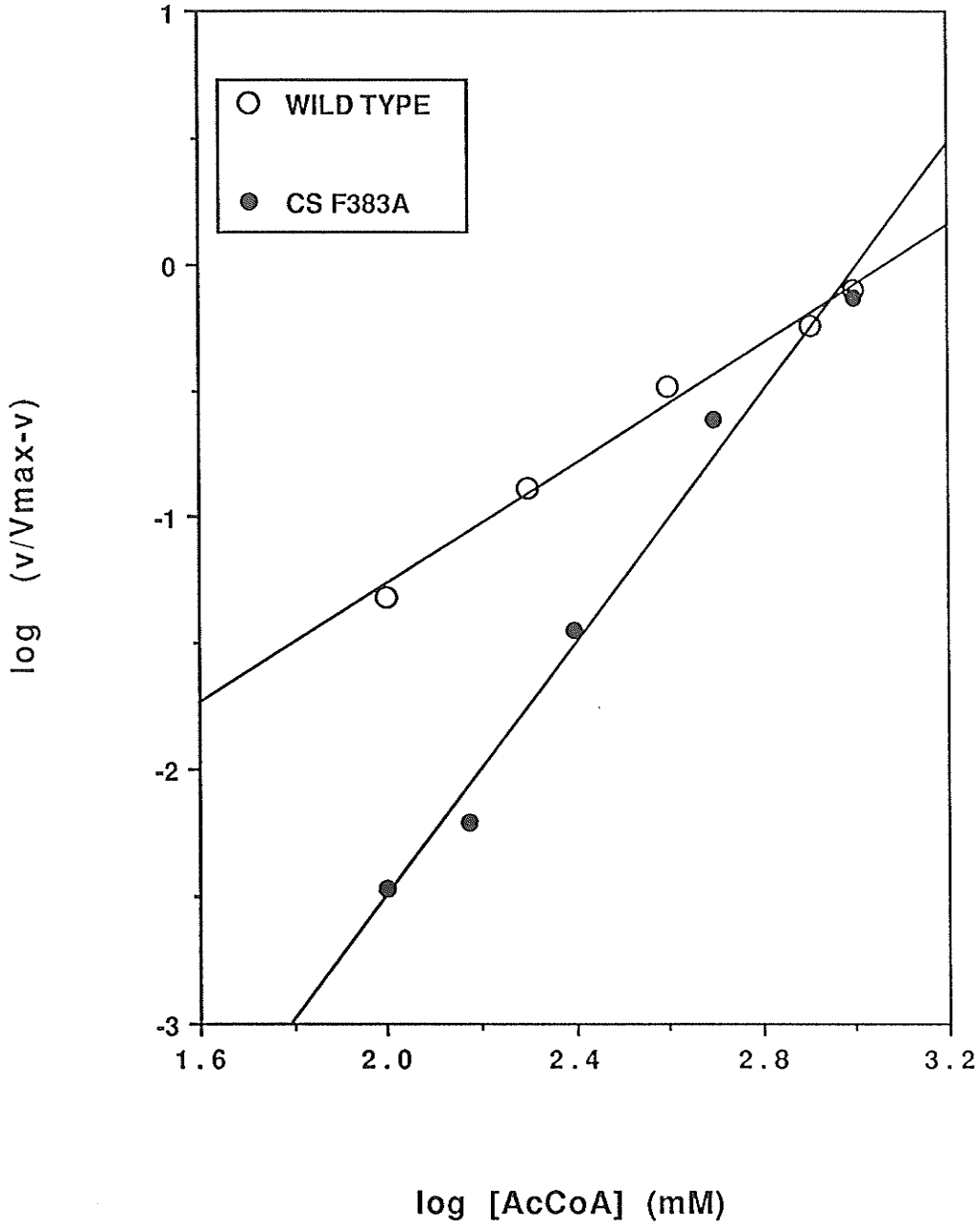

FIGURE 33: HILL PLOTS FOR AcCoA SATURATION OF WILD TYPE CITRATE SYNTHASE (HILL # = 1.0) AND CS F383A (HILL # = 1.85), DETERMINED IN THE PRESENCE OF KCl, AT 300 μM OAA.

PARAMETER	WILD TYPE	CS F383A ▼
k_{cat} (sec^{-1})	44±5	0.139±0.025
$S_{0.5AcCoA}$ (μM)	410±20	NPTD
apparent Km for OAA (μM)	27±5 ★	1000±100 ☆
K_{is}, α-KG (μM)	93±18	NPTD
K_i, NADH (μM)	3.3±0.1	NPTD
MAXIMUM % INHIBITION BY NADH	99±1	NPTD
HILL NUMBER	1.3	NPTD, but >1.85

NPTD = NOT POSSIBLE TO DETERMINE.

★ DETERMINED AT 1000 μM AcCoA.

☆ DETERMINED AT 2000 μM AcCoA.

▼ DATA BASED ON LINEWEAVER-BURK PLOT (SPECIFIC ACTIVITY^{-1} VERSUS $[OAA]^{-1}$) AT 2000 μM AcCoA.

TABLE 12: CS F383A STEADY STATE KINETICS (IN THE ABSENCE OF KCl)

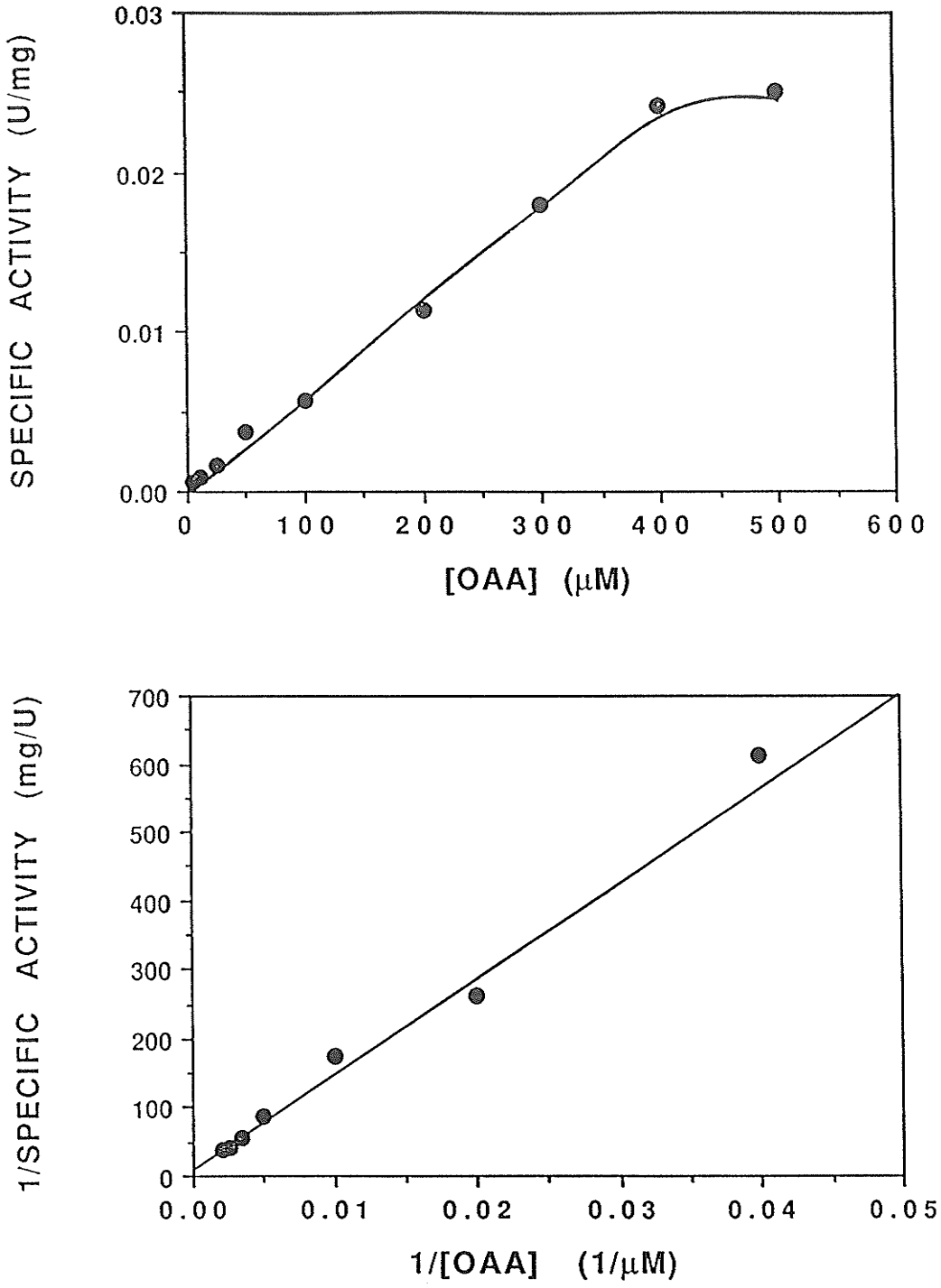

FIGURE 34: MICHAELIS-MENTEN (TOP) AND LINEWEAVER-BURK (BOTTOM) PLOTS FOR SPECIFIC ACTIVITY OF CS F383A AS A FUNCTION OF OAA CONCENTRATION AT 2000 μM AcCoA. KCl NOT PRESENT.

ENZYME	K_D, NADH (μM) (- KCl)	K_D, NADH (μM) (+ KCl)			K_D, KCl
		0.1 M	**0.2 M**	**0.3 M**	
WILD TYPE	1.94±0.07 *0.42-0.74*	3.68±0.05 *0.53±0.03*	6.87±0.16 *0.49±0.01*	11.8±0.50 *0.43±0.01*	90±10
CS F383A	2.75±0.17 *0.82±0.02*	7.17±0.47 *0.78±0.03*	22.03±0.38 *0.93±0.01*	52.41±6.60 *1.57±0.17*	16±4

TABLE 13: CS F383A NADH BINDING RESULTS

PARAMETER	WILD TYPE		CS F383A	
(μM)	**NO KCl**	**0.1 M KCl**	**NO KCl**	**0.1 M KCl**
$L_{0.5}$, AcCoA	260±40	60±3	630±90	440±90
$L_{0.5}$, CoA	270±40	53±3	590±110	400±70
$L_{0.5}$, CoA †	73±3	47±5	510±70	290±45
K_D, OAA ⇧	25±1	ND	300±30	ND
K_D, α-KG ⇧	76±11	ND	3600±200	ND

† = MEASURED IN PRESENCE OF 0.2 mM OAA
⇧ = MEASURED IN PRESENCE OF 0.2 mM CoA
ND = NOT DETERMINED

TABLE 14: CS F383A ANS BINDING RESULTS

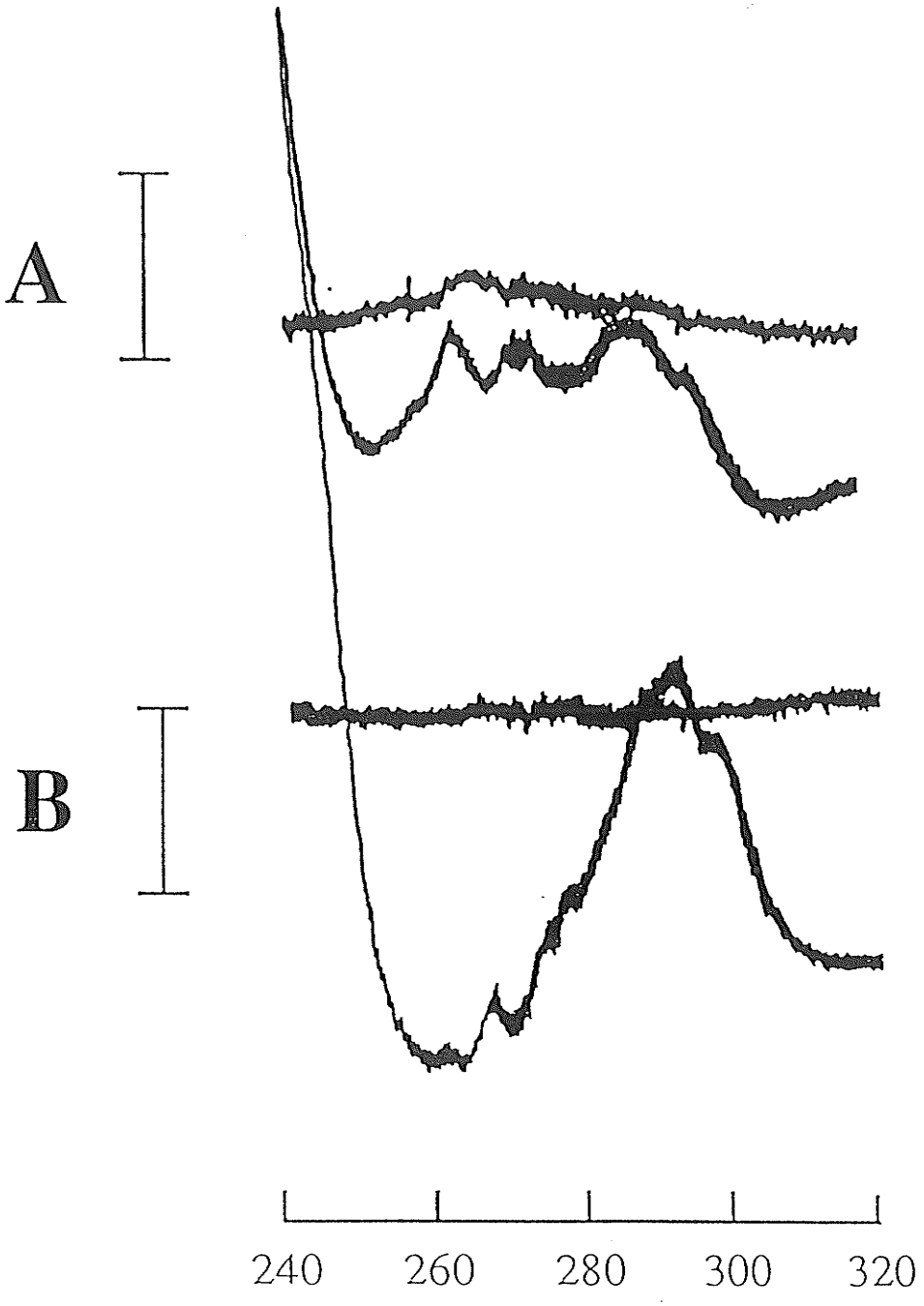

FIGURE 35: DIFFERENCE SPECTRA INDUCED IN CS F383A BY OAA, IN THE ABSENCE (A) AND PRESENCE (B) OF KCl. ENZYME, OAA, AND KCl CONCENTRATIONS WERE 41 μM, 0.91 mM, AND 0.15 M RESPECTIVELY. INCLUDED IN BOTH SPECTRA IS A BASE-LINE, & A VERTICAL BAR REPRESENTING 0.05 ABSORBANCE UNITS. THE BOTTOM SCALE IS WAVELENGTH IN NANOMETERS.

CS D362A

INTRODUCTION

From X-ray diffraction (Wiegand & Remington, 1986; Karpusas, 1990) studies of pig heart citrate synthase, Asp-375 (*E. coli* equivalent, Asp-362), has been implicated in the reaction mechanism as a protonating/deprotonating residue. It is involved in the enolization of AcCoA as well as the formation of a tetrahedral intermediate from citryl-CoA. In order to determine the importance of Asp-362 in catalysis, elimination of this charged residue by mutation to alanine was accomplished.

As with CS H264A, it is expected that the catalytic efficiency of CS D362A will be minimal. Since many amino acids secure and position the substrates for interaction with Asp-362, the effect of this mutation on substrate binding may be minimal.

STEADY STATE KINETIC RESULTS

IN THE PRESENCE OF KCl

Table 15 shows steady state kinetic data determined from Lineweaver-Burk plots presented in Figure 36 and 37. In comparison to wild type citrate synthase, a decrease in the kcat value of approximately 924 fold resulted. The K_{OAA} value for this mutant (20±6 μM) was quite similar to the wild type value, however, the K_{AcCoA} value was 78±22 μM (wild type; 120±20 μM).

IN THE ABSENCE OF KCl

As with CS H264A, the loss of Asp-362 severely retarded the catalytic efficiency of the enzyme. Consequently, collection of steady state kinetic data in the absence of the enzyme's activator, KCl, was not possible. In addition, a Hill number for CS D362A was not determined.

ACTIVATION & INHIBITION RESULTS

Table 15 shows CS D362A activation results. The Km, KCl result found for CS D362A was 2.2 fold lower than the wild type value. As a result, a 4.2 fold decrease in the KCl activation ratio was not unexpected. As with CS H264A, CS D362A attained maximum activity in the presence of 20 mM KCl (see Figure 38 for KCl saturation curve). In contrast, wild type citrate synthase attains maximum specific activity at 100 mM KCl.

Because CS D362A was virtually inactive in the absence of KCl, determination of the K_{is}, α-KG and K_i, NADH parameters was not possible.

BINDING RESULTS

NADH BINDING

NADH binding data for CS D362A is outlined in Table 16. In the absence of KCl, the K_D, NADH parameter is 1.72±0.16 μM. Therefore, binding of NADH to CS D362A was quite similar. When KCl was present, however, a further 7.8 fold decrease in NADH binding (1.9 fold for wild type) resulted. As with the wild type enzyme, when 0.2 and 0.3 M KCl was introduced, a 19.5 and 40.5 fold

decrease in NADH binding to CS D362A was observed respectively. The K_D, KCl result for CS D362A was 2.9 fold lower than the wild type value of 90±10 μM.

ULTRAVIOLET DIFFERENCE SPECTROSCOPY

As with CS H264A, the CS D362A data, presented above, suggested that mutation of Asp-362 to alanine was responsible for the loss of a T-state stabilizing interaction. Once again, OAA induced ultraviolet difference spectroscopy was employed to determine whether the conformation of CS D362A in the absence of KCl was shifted towards the R-state. Figure 39-A shows the OAA induced spectra in the absence of KCl, while Figure 39-B represents the OAA induced spectra in the presence of KCl. The two spectra are only slightly different from one another. The effect KCl has on the OAA induce spectra of CS D362A is small, suggesting that CS D362A is in a conformation favoring the R-state. Interestingly, when comparing the two CS D362A spectra to the two CS H264A spectra (Figure 29-A and -B), it appears that CS D362A's conformation favors the R-state less than the CS H264A conformation.

PARAMETER	WILD TYPE	CS D362A
k_{cat} (sec^{-1})	81±6	0.086±0.005
K_{AcCoA} (μM)	120±20	78±22
K_{OAA} (μM)	26±5	20±6
K_{iOAA} (μM)	33±7	150±40
K_{is}, α-KG (μM)	760±250	VERY LARGE
K_m, KCl (mM)	28±4	12.7±5.4
KCl ACTIVATION RATIO	39±3	9.2±0.9
HILL NUMBER	1.0	1.0

TABLE 15: CS D362A STEADY STATE KINETICS (IN THE PRESENCE OF KCl)

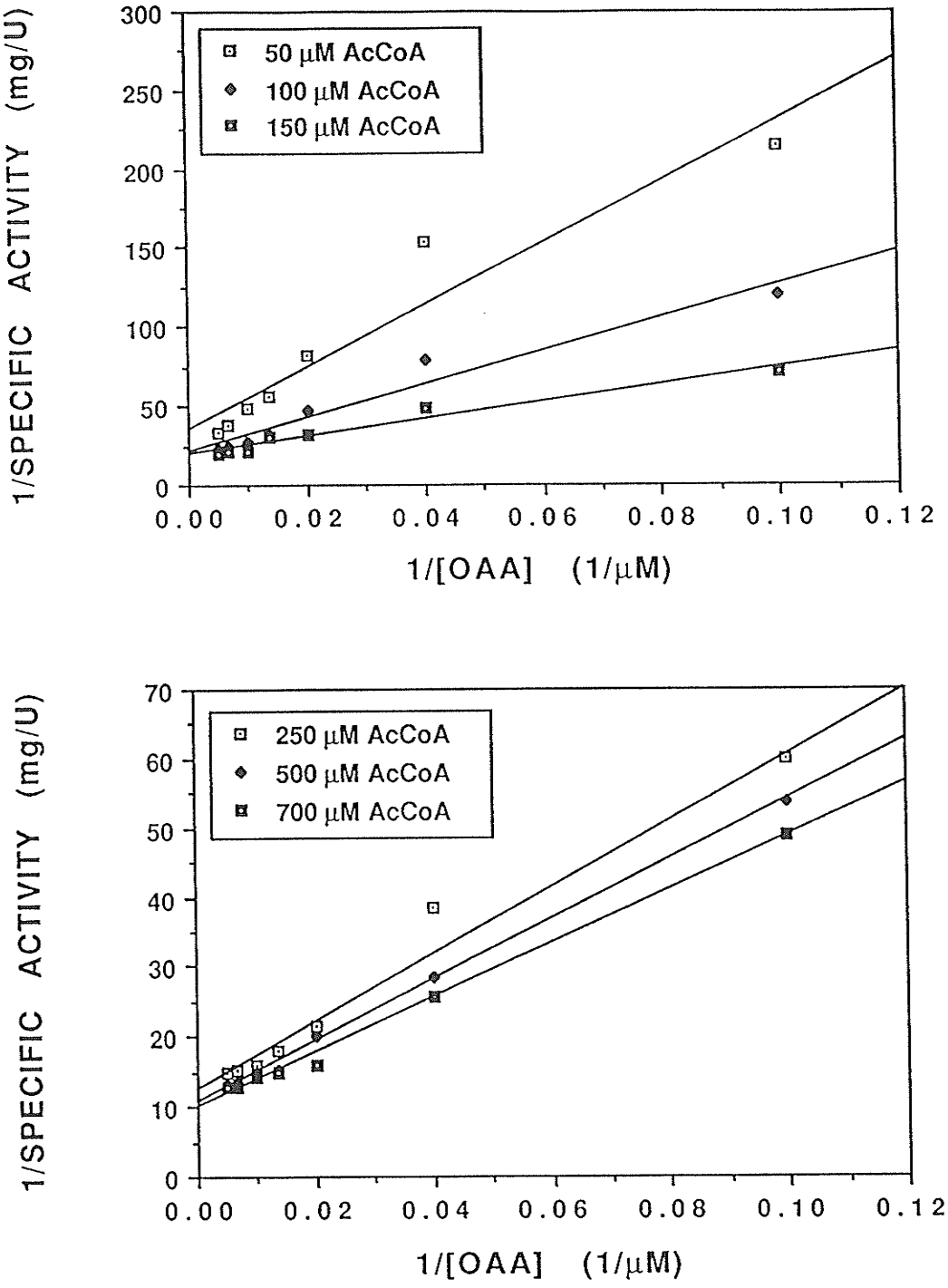

FIGURE 36: LINEWEAVER-BURK PLOTS FOR SPECIFIC ACTIVITY OF CS D362A AS A FUNCTION OF OAA CONCENTRATION AT VARIOUS AcCoA CONCENTRATIONS. KCl PRESENT.

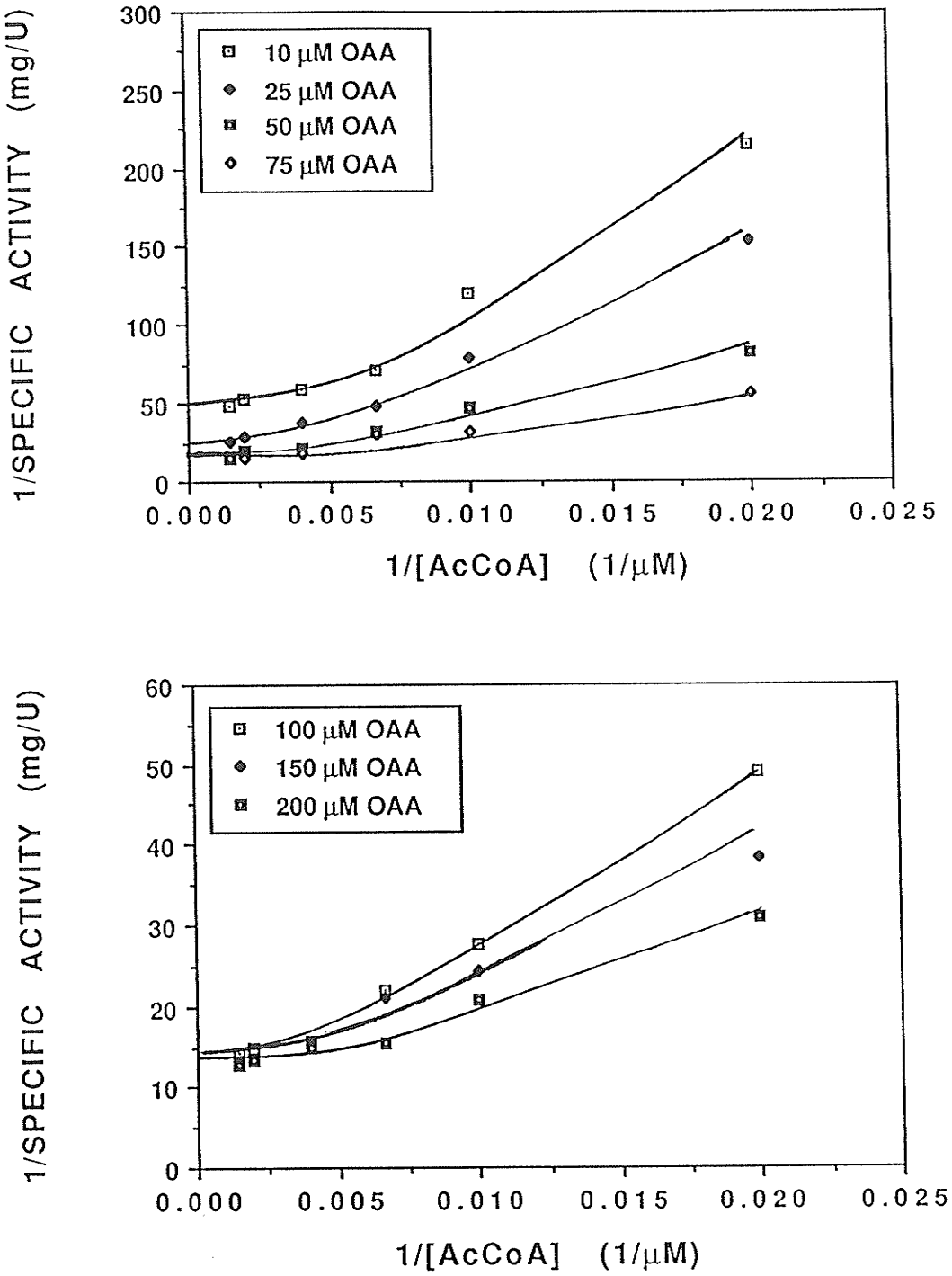

FIGURE 37: LINEWEAVER-BURK PLOTS FOR SPECIFIC ACTIVITY OF CS D362A AS A FUNCTION OF AcCoA CONCENTRATION AT VARIOUS OAA CONCENTRATIONS. KCl PRESENT.

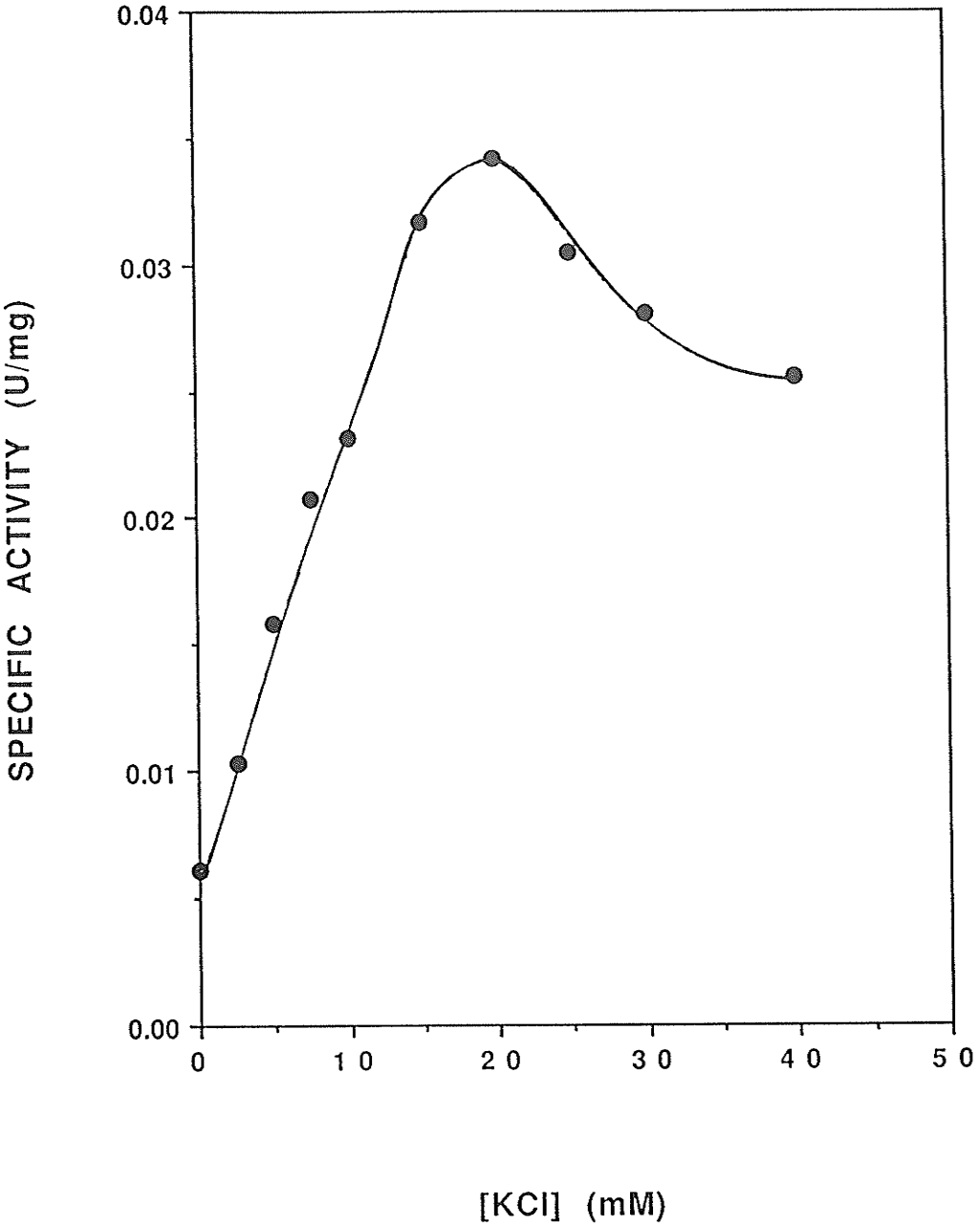

FIGURE 38: KCl SATURATION CURVE FOR CS D362A.

ENZYME	K_D, NADH (μM) (- KCl)	K_D, NADH (μM) (+ KCl)			K_D, KCl
		0.1 M	**0.2 M**	**0.3 M**	
WILD TYPE	1.94±0.07 *0.42-0.74*	3.68±0.05 *0.53±0.03*	6.87±0.16 *0.49±0.01*	11.8±0.50 *0.43±0.01*	90±10
CS D362A	1.72±0.16 *0.62±0.02*	13.46±1.00 *0.68±0.02*	33.59±5.40 *0.63±0.01*	69.71±4.54 *0.57±0.01*	31±5

TABLE 16: CS D362A NADH BINDING RESULTS

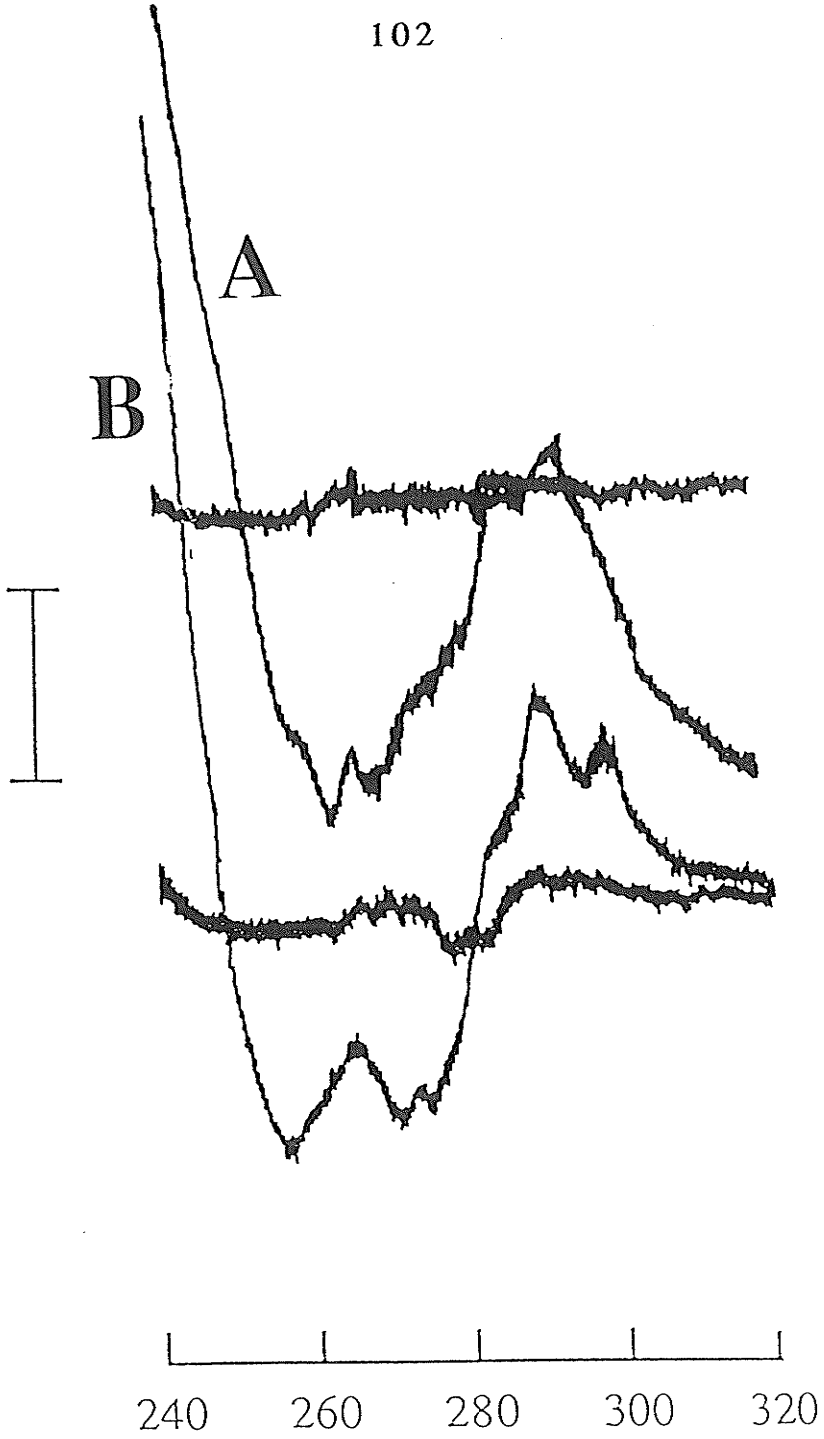

FIGURE 39: DIFFERENCE SPECTRA INDUCED IN CS D362A BY OAA, IN THE ABSENCE (A) AND PRESENCE (B) OF KCl. ENZYME, OAA, AND KCl CONCENTRATIONS WERE 41 μM, 0.91 mM, AND 0.15 M RESPECTIVELY. INCLUDED IN BOTH SPECTRA IS A BASE-LINE, & A VERTICAL BAR REPRESENTING 0.05 ABSORBANCE UNITS. THE BOTTOM SCALE IS WAVELENGTH IN NANOMETERS.

DISCUSSION

The research presented in this thesis was centered around two major objectives. Since the pig heart and *E. coli* citrate synthase amino acid sequences are almost totally conserved in the region of their active sites, the first objective was to mutate the *E. coli* citrate synthase active site residues in order to confirm that their roles were similar to those of their pig heart counterparts. Determining the effect of mutations on the allosteric nature of *E. coli* citrate synthase was the second aim of this research.

EFFECTS ON CATALYSIS

Three mutant *E. coli* citrate synthases, CS R407L, CS H264A, and CS D362A, exhibited striking decreases in their respective kcat values.

Results for CS R407L confirm that removal of this arginine, from the lower OAA-binding layer of the active site, weakens the affinity for OAA. However, the dramatic decrease in the kcat parameter was not expected. When OAA binds to the enzyme, it is possible that the process of Arg-407 and other residues of the second subunit closing around OAA and the active site, may cause a significant conformational rearrangement to occur. Removal of Arg-407 may significantly prevent this "induced fit" from occurring, so that a severe effect on catalysis results.

Since His-264 and Asp-362 are believed to protonate and deprotonate the substrates and their intermediates, as they are converted to products, removal of either of these two residues from the upper enolization layer of the active site should severely retard the enzyme's catalytic efficiency. In fact, for CS H264A, a 620 fold decrease in the kcat parameter resulted in the presence of KCl, while enzyme activity could not be detected in the absence of KCl. In the presence of KCl, a 924 fold decrease in the kcat value for CS D362A resulted.

The effects the H264A and D362A mutations had on substrate binding were minimal. For either mutant enzyme, the Km values for both substrates were either lower than or similar to the wild type values. These findings may be explained by the fact that many amino acids secure and position the substrates for interaction with His-264 and Asp-362, so that removal of His-264 or Asp-362 might have little or no effect on substrate binding, while the effect on catalysis is immense.

In order to fully appreciate the impact the above mutations had on catalysis, a free energy diagram was constructed (see Figure 40) from estimates of free energy changes, in the presence of 0.1 M KCl, for the transition state and intermediate complexes (see Table 17). The standard free energy differences ($\Delta G^{o'}$) between enzyme-substrate complexes (E-S) are determined using equilibrium constants for the association of these complexes. Assuming the Ordered bisubstrate mechanism is obeyed, the symbol ,① on Figure 40, represents the activation free energy value for the formation of E-OAA + AcCoA from free E + OAA + AcCoA, which was calculated from the rate constant of the reaction k_1 or $kcat/K_{OAA}$ (Bell, 1978 - Thesis, Table 5). The $\Delta G^{o'}$ value between the E-OAA complex and free enzyme and OAA (② on Figure 40 and Table 17) is found using the equation, $\Delta G^{o'} = - RT \ln K_{iOAA}$, since K_{iOAA} is the true equilibrium complex for the association of enzyme and OAA. The symbol, ③, on Figure 40, is a maximum value for the activation free energy determined from k_3 $((kcat/K_{AcCoA})(1+k_4/k_5))$, the rate constant for the formation of the E-OAA-AcCoA complex from E-OAA + AcCoA. The k_4 and k_5 constants are defined in Figure 6, and the minimum value of k_3 is $kcat/K_{AcCoA}$. Since the true equilibrium constant for the formation of the E-OAA-AcCoA complex is unknown, K_{AcCoA} is used as an approximation for the determination of $\Delta G^{o'}$ from the equation, $\Delta G^{o'} = -RT \ln K_{AcCoA}$. The standard

free energy difference between the E-OAA-AcCoA complex and free enzyme and substrates (④ on Figure 40 and Table 17) was predicted using the equation, $\Delta G^{o'} = -RT \ln (K_{iOAA} \cdot K_{AcCoA})$. The Eyring equation, $\Delta G^{o'} = RT \ln (Kk_BT/h) - RT \ln kcat$, where K is the "transmission coefficient" for the reaction (usually taken as 1); k_B is the Boltzmann constant; and h represents the Plank's constant, was used to determine the standard free energy of activation for the ternary complex relative to the E-OAA-AcCoA complex (⑥ on Figure 40), while $\Delta G^{o'} = RT \ln (Kk_BT/h) - RT \ln (kcat/K_{iOAA} \cdot K_{AcCoA})$ was used to determine the free energy of activation relative to the free enzyme and substrates (⑤ on Figure 40 and Table 17). The vertical position of the E-CITRATE-CoA complex, on Figure 40, is not known, as indicated by dashed lines. However, it must be at least a few kcal/mol below the E-OAA-AcCoA complex, since the reaction is irreversible. The vertical positions of the transition states for formation of the E-CITRATE and E-CITRATE-CoA complexes from products are also unknown and indicated by dashed lines in Figure 40. However, these values have been estimated to be approximately 8 kcal/mol above their reactants, by analogy with the values for ① and ③. The $\Delta G^{o'}$ of stabilization of the E-CITRATE complex relative to the E + CITRATE + CoA complex (⑦ on Figure 40) was determined using the Ki for citrate as a competitive inhibitor of *E. coli* citrate synthase with respect to OAA, measured by Wright, 1970 (Thesis, page 103), as 4 x 10^3 M. Finally, the $\Delta G^{o'}$ for the overall reaction (-7.16 kcal/mol) accounts for the vertical position of the E + CITRATE + CoA mixture relative to the E + OAA + AcCoA mixture.

Figure 41 compares the effects of the active site mutations on substrate binding (grey and hatched bars) and transition state stabilization (black bars). Since CS F383A did not obey the Michaelis-Menten equation, it was not subjected to the above calculations.

In summary, Figure 41 shows that, as expected, much of the loss of transition state stabilization energy associated with the R407L mutation was accounted for by poorer OAA binding. Despite the fact that the substrate binding energies, for D362A and H264A were close to the wild type values, their transition state destabilization was large.

EFFECTS ON ALLOSTERY

Citrate synthases follow an Ordered Bisubstrate kinetic mechanism. Initially, OAA binds to the enzyme causing the two domains of each subunit to shift to a conformation favoring binding of AcCoA. Subsequently, a further conformational shift results, causing the reaction to occur. For *E. coli* citrate synthase, however, an additional allosteric conformational change, accounting for sigmoid saturation by AcCoA, must be involved. The presence of KCl increases the enzyme's affinity for AcCoA and allows this additional allosteric conformational change to occur more easily, while NADH allosterically inhibits *E. coli* citrate synthases by binding at a site distinct from the active site.

Using the common terminology of Monod et al, (1965), the allosteric nature of *E. coli* citrate synthase is described by a conformational equilibrium in which two conformational states, T and R, exist in equilibrium. The T state binds NADH, while the R state binds substrates well, and is favoured in the presence of KCl.

Using ultraviolet difference spectroscopy, Anderson et al, 1991, demonstrated that both OAA and KCl could induce characteristic spectra for wild type *E. coli* citrate synthase. In this same study, it was found that the OAA induced ultraviolet difference spectrum, for CS R319L, an *E. coli* citrate

synthase mutant, resembled the spectrum induced by OAA in wild type enzyme in the presence of KCl. To account for these observations, it was suggested that wild type *E. coli* citrate synthase exists in equilibrium between the T and R states, where the R state could be converted to another substrate binding state, R', by KCl, and that the allosteric equilibrium of CS R319L was shifted towards the R state, in the absence of ligands. Kinetic evidence, such as lower Km values for both substrates, lower Km for KCl activation, and weaker binding of NADH, also suggested that CS R319L was in a R conformational state before addition of ligands (Anderson et al, 1991).

When three *E. coli* citrate synthase active site residues, His-264, Asp-362, and Phe-383, were mutated to alanine, kinetic and physical studies suggested that their allosteric equilibria were shifted towards the R (CS H264A and CS D362A) and T (CS F383A) states.

As compared to the wild type enzyme, CS H264A steady state kinetics, in the presence of KCl, changed in four ways which could most readily be explained by assuming that its allosteric equilibrium shifted towards the R state. First, the KCl activation ratio for CS H264A was approximately 11 fold lower than the wild type value. In addition, maximum activity occurred in the presence of 20 mM KCl, whereas for the wild type enzyme 100 mM KCl is required. Secondly, Lineweaver-Burk plots for AcCoA saturation of CS H264A were linear in the presence of KCl. Next, Michaelis constants for both substrates, in the presence of KCl, were lower than wild type values by a factor of 3.75. Lastly, binding of NADH to CS H264A was decreased by a factor of 12.

In order to determine whether CS H264A could be converted to a R state, by KCl, ultraviolet difference spectroscopy was used. That OAA induced difference spectra, in the presence and absence of KCl, for CS H264A were

similar in appearance, suggests that CS H264A was in an R state conformation before any ligands were added.

In the case of CS D362A, the allosteric equilibrium is also believed to be shifted to the R state. As with the CS H264A enzyme, the KCl activation ratio is also decreased, however, only a 4.2 fold decrease was observed. Maximum activity occurred in the presence of 20 mM KCl. While the K_{OAA} parameter was found to be similar to the wild type value, K_{AcCoA} was decreased by a factor of 1.5. Kinetic data, determined in the presence of KCl, suggested that the D362A mutation caused a T state stabilizing interaction to be lost. Furthermore, NADH binding to CS D362A was very similar to that of the wild type enzyme, in the absence of KCl, but the ability of 0.3 M KCl to prevent NADH inhibition increased 6 fold.

As with CS H264A, ultraviolet difference spectroscopy was employed to determine whether CS D362A could be converted to an R state conformation, by KCl. The OAA induced difference spectra, in the presence and absence of KCl, were similar, however, the shape of the spectra, in the presence and absence of KCl, resembled the wild type OAA induced spectra in the presence of KCl. This may suggest that before any ligands were added, CS D362A was in an R state conformation which is similar to the R state conformation of the wild type enzyme in the presence of KCl. Since CS H264A spectra do not resemble the wild type OAA induced spectra in the presence of KCl, it may be that the allosteric equilibrium of CS H264A was shifted towards the R state further, in the absence of ligands, than wild type is in the presence of KCl. Therefore, when OAA is bound to CS D362A and CS H264A, the domains of each subunit may shift to an R' state conformation rather than an R state conformation observed for the wild type enzyme. Addition of KCl will not induce a further conformational change.

As stated earlier, CS F383A is a mutant *E. coli* citrate synthase whose allosteric equilibrium is believed to be shifted towards the T state. Steady state kinetics, in the presence of KCl, provide evidence for this T state shift. As compared to the wild type value, a 2 fold increase in the Km, KCl parameter was observed. Lineweaver-Burk plots for AcCoA saturation of CS F383A were sigmoid and associated with a Hill number of 1.85. It was found that OAA induced the wild type and apparently the CS F383A enzymes to shift into R state, however, the 17 fold larger CS F383A K_{AcCoA} value suggests that the R' state may not be attained. Binding of NADH to CS F383A, in the absence of KCl, was similar to wild type, and the presence of 0.3 M KCl did cause a further decrease in NADH binding. These NADH binding results do not coincide with the idea that CS F383A, in the absence of ligands, is in the T state. However, since NADH binds at a site distinct from the active site, it may be that the F383A change has no effect on the NADH binding site, and therefore, the enzyme may still be in a T conformational state. Although the $L_{0.5}$, CoA ANS binding results, in the presence and absence of OAA, were not as high as expected, they are larger than the wild type values, suggesting that CS F383A does not bind AcCoA very well. Collection of steady state kinetic data for AcCoA saturation, in the absence of KCl, was not possible. This finding strongly suggests that CS F383A is in the T state, even in the presence of KCl.

Once again, ultraviolet difference spectroscopy was used to obtain further evidence that CS F383A existed in a T state conformation before addition of ligands. OAA induced ultraviolet difference spectra in the presence and absence of KCl were quite different. Response to KCl was similar to that of the wild type enzyme. The observation that the CS F383A OAA induced spectrum, in the presence of KCl, was similar in appearance to the wild type OAA induced spectrum, in the absence of KCl, suggested that addition of KCl

caused CS F383A to shift from a T state to an R state conformation, similar to the wild type enzyme in the absence of KCl.

FUTURE DIRECTIONS

Unfortunately, the X-ray structure of *E. coli* citrate synthase has not been obtained. Until this problem is solved, insight into what parts of the active site actually undergo rearrangement during the allosteric conformational change can be gained by mutating amino acids in the vicinity of His-264, Asp-362, and Phe-383. Since sigmoidicity of AcCoA saturation is intensified in CS F383A, mutation of neighboring residues in the vicinity of the AcCoA binding site, such as the conserved Leu-259, may exhibit similar kinetic and allosteric effects. Mutation of residues near His-264 and Asp-362, such as the conserved residues, Asn-232 and Ser-234, may also disrupt catalytically important interactions, required for the enolization of AcCoA. Thus, a better understanding of the importance of enzyme structure for the enolization of AcCoA will hopefully be obtained.

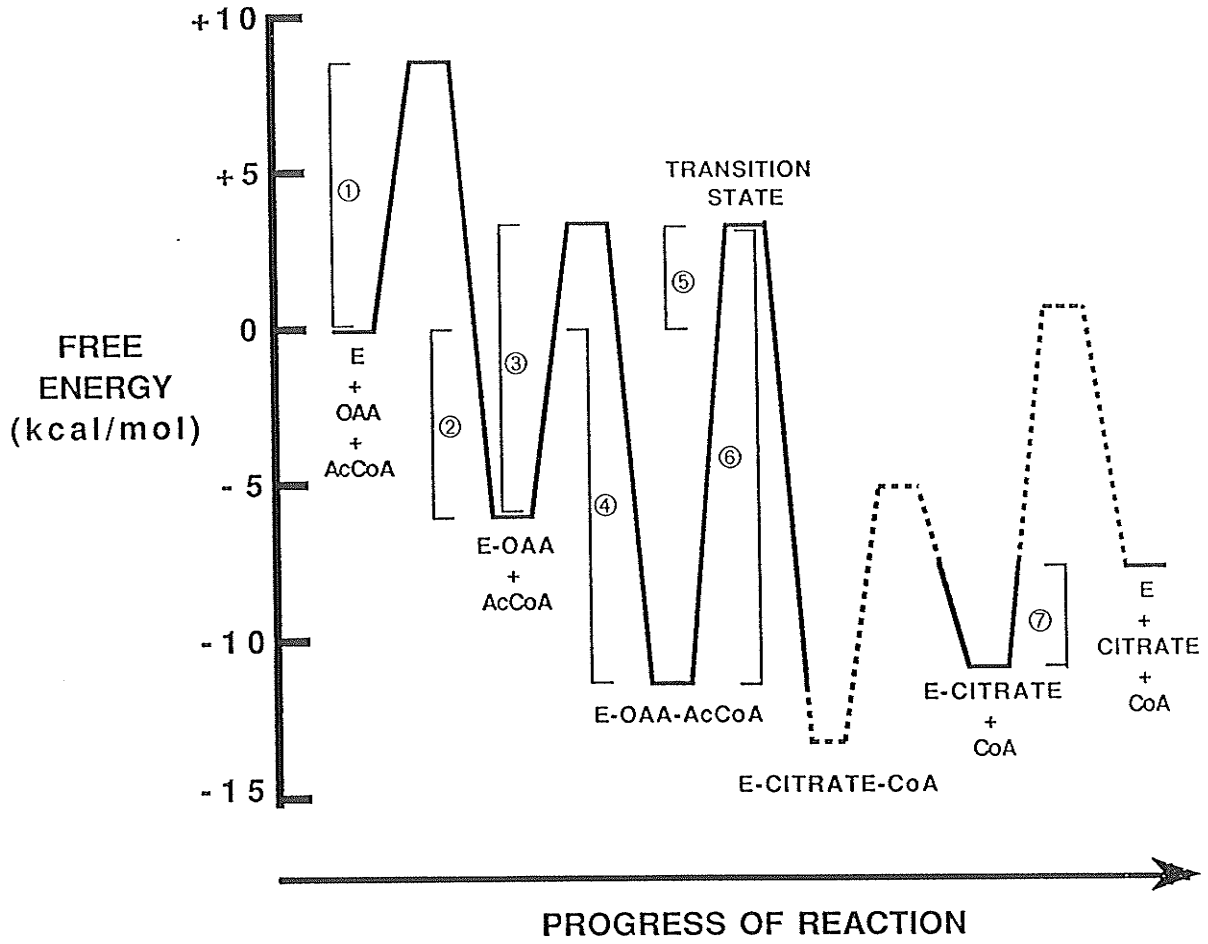

FIGURE 40: FREE ENERGY DIAGRAM FOR WILD TYPE *E. coli* CITRATE SYNTHASE. THE REACTION CATALYZED BY THIS ENZYME BEGINS WITH OAA, AcCoA, AND FREE ENZYME (E) AND FINISHES WITH CITRATE, CoA, AND FREE ENZYME. THE STANDARD FREE ENERGY CHANGES ($\Delta G^{\circ\prime}$) FOR THE FORMATION OF INTERMEDIATE COMPLEXES, REPRESENTED AS CIRCLED NUMBERS, ARE SHOWN (SEE TEXT FOR CALCULATION PROCEDURE). THE SOLID AND DASHED LINES REPRESENT KNOWN AND UNKNOWN $\Delta G^{\circ\prime}$ VALUES, RESPECTIVELY.

TABLE 17: FREE ENERGY PROFILE DATA FOR CATALYSIS BY CITRATE SYNTHASE ACTIVE SITE MUTANTS

MUTANT	$\Delta G^{\circ\prime}$ (E-OAA) (kcal/mol)		$\Delta G^{\circ\prime}$ (E-OAA-AcCoA) (kcal/mol)		$\Delta G^{\ddagger}$ (kcal/mol)	
	ABSOLUTE (represented by ② in Figure 40)	RELATIVE TO WILD TYPE	ABSOLUTE (represented by ④ in Figure 40)	RELATIVE TO WILD TYPE	ABSOLUTE (represented by ⑤ in Figure 40)	RELATIVE TO WILD TYPE
WILD TYPE	-6.01	-	-11.26	-	3.32	-
CS H305A	-4.05	1.96	-10.04	1.22	9.07	5.75
CS R314L	-4.43	1.58	-10.57	0.69	8.57	5.25
CS H226Q	-5.17	0.84	-9.97	1.29	4.50	1.18
CS H229Q	-3.68	2.33	-8.67	2.59	7.17	3.85
CS R407L	-3.97	2.04	-9.18	2.08	7.99	4.67
CS H264A	-5.58	0.43	-11.60	-0.34	6.72	3.40
CS D362A	-5.13	0.88	-10.64	0.62	7.94	4.62
CS R319L *	-7.09	-1.08	-13.26	-2.00	1.62	-1.70

* R319L is not an active site mutation.

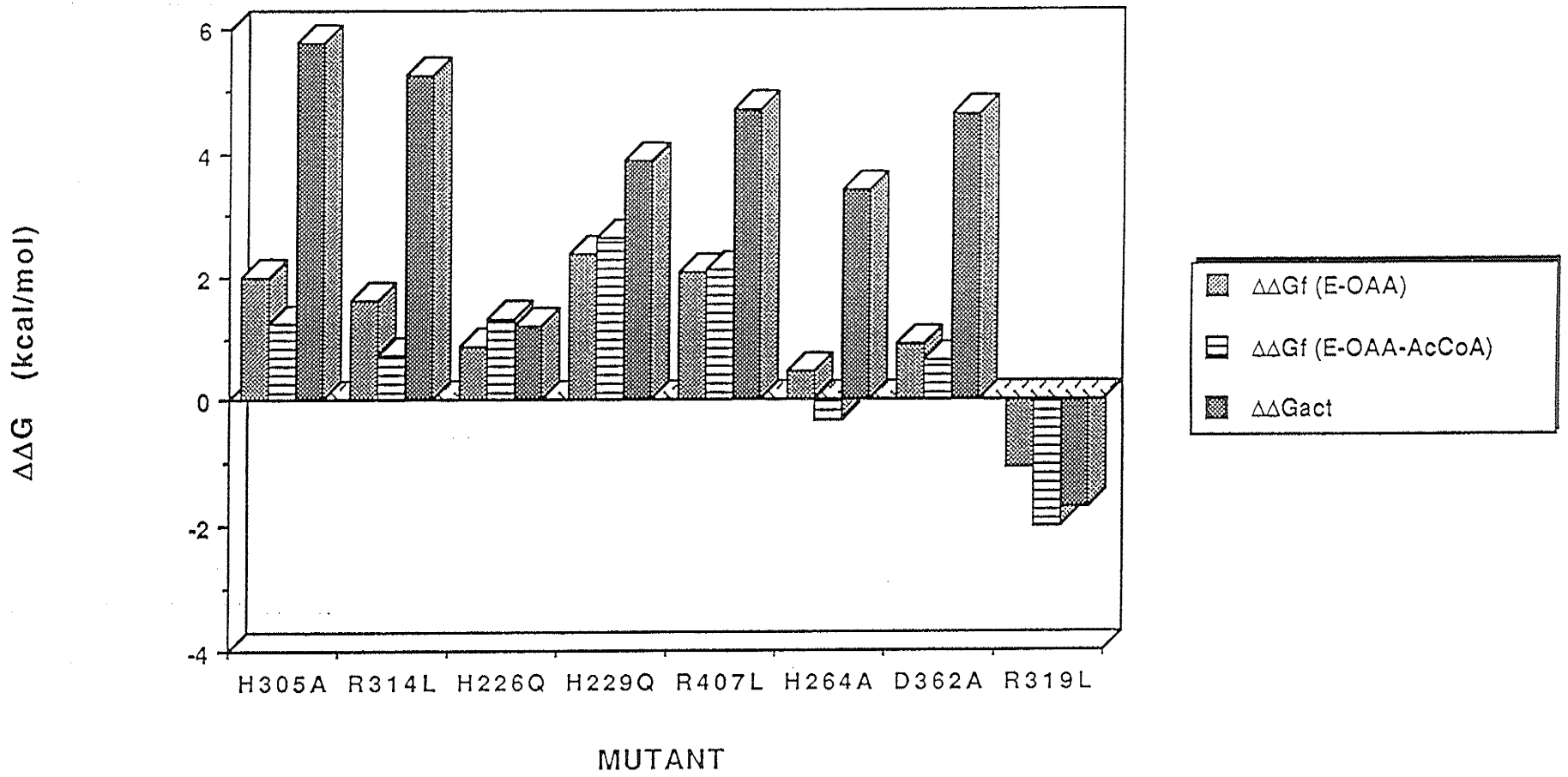

FIGURE 41: THE EFFECTS OF *E. coli* CITRATE SYNTHASE ACTIVE SITE MUTATIONS ON SUBSTRATE BINDING (GREY AND HATCHED BARS) & TRANSITION STATE STABILIZATION (BLACK BARS). THIS GRAPH WAS CREATED FROM DATA ON TABLE 17.

REFERENCES

1) Anderson, DH & Duckworth, HW: Journal of Biological Chemistry 263: 2163-2169, 1988.

2) Anderson, DH & Duckworth, HW: Biochemistry Cell Biology. 67:98-102, 1989.

3) Bayer, E et al: FEBS Letters 127:101-104, 1981.

4) Bell, A et al: Biochemistry 22:3400-3405, 1983.

5) Berger, SA & Evans, PR: Nature 343:575-576, 1990.

6) Birnboim, HC & Doly, J: Nucleic Acids Research 7:1513-1523, 1979.

7) Bloxham, DP et al: PNAS (USA) 78:5381-5385, 1981.

8) Bloxham, DP et al: Biochemistry 21:2028-2036, 1982.

9) Cleland, WW et al: Biochem. Biophys. Acta. 67:104-137, 1963.

10) Danson, MJ et al: European Journal Biochemistry 101:515-521, 1979.

11) DeTar, DF: Computer Programs for Chemistry. 4:71-123, 1972.

12) Donald, LJ & Duckworth, HW: Biochemistry and Cell Biology 65:930-938, 1987.

13) Duckworth, HW, et al: Biochem. Soc. Symp. 54:83-92, 1987.

14) Duckworth, HW & Tong, EK: Biochemistry 15:108-114, 1976.

15) Duckworth, HW & Bell, AW: Canadian Journal Biochemistry 60, 1143-1147, 1982.

16) Eigen, M: Nobel Symposium 5:333, 1967.

17) Ellis, M et al: PNAS (USA) 84:5101-5105, 1987.

18) Else, AJ et al: Biochemical Journal 254:437-442, 1988.

19) Evans, CT et al: Biochem. Biophys. Research Communications 164:1437 1445, 1989.

20) Fairbanks, G et al: Biochemistry 10:2606-2617, 1971.

21) Faloona, GR & Srere PA: Biochemistry 8:4497-4503, 1969.

22) Fersht, A: Enzyme Structure & Mechanism, second edition, W. H. Freeman & Company, New York, New York, 1985.

23) Hammond, DC: Journal Biological Chemistry 261:8424-8428, 1986.

24) Handford, PA et al: Biochimica Biophysica Acta 953:232-240, 1988.

25) Henneke, CM et al: Protein Engineering 2:597-604, 1989.

26) Johansson, CJ & Petterson G: European Journal Biochemistry 42:383-388, 1974.

27) Karpusas, M et al: Biochemistry 29:2213-2219, 1990.

28) Kunkel, TA et al: Methods Enzymology 154:367-382, 1987.

29) Kurz, LC et al: Biochemistry 26:2623-2627, 1987.

30) Laemmli, UK: Nature (London) 227:680-685, 1970.

31) Lehninger, AL: Principles of Biochemistry, Worth Publishers Inc., New York, New York, 1982.

32) Lesk, AM & Chothia C: Journal Molecular Biology 174:175-191, 1984.

33) Maniatis, T: Molecular Cloning: A Laboratory Manual, Cold Spring Harbor Laboratory, Cold Spring Harbor, New York, 1982.

34) Messing, J et al: Nucleic Acids Research 9:309-321, 1983.

35) Mierendorf, RC & Pfeffer, D: Methods Enzymology 152:556-562, 1987.

36) Monod, J, Wyman, J, & Changeaux, JP: Journal Molecular Biology 12:88-118, 1965.

37) Morse, D & Duckworth, HW: Canadian Journal Biochemistry 58:696-709, 1980.

38) Ner, SS et al: Biochemistry 22:5243-5249, 1983.

39) Ouchterlony, O: Acta Path. Microbiol. Scand. 32:231-236, 1953.

40) Remington, S et al: Journal Molecular Biology 158:111-152, 1982.

41) Rosenkranz, MT et al: Molecular and Cell Biology 6:4509-4515, 1986.

42) Sanger, F et al: Journal Molecular Biology 143:161-178, 1981.

43) Sanger, F et al: PNAS (USA) 74:5463-5467, 1977.

44) Srere, PA: Biochim. Biophys. Acta 77:693-696, 1963.

45) Srere, PA: Current Topics Cellular Regulation 5:279-283, 1972.

46) Srere, PA et al: Acta Chem. Scand. 17:S129-S134, 1963.

47) Suissa, M et al: EMBO Journal 3:1773-1781, 1984.

48) Sutherland KJ et al: European Journal Biochemistry 194:3, 1990.

49) Talgoy, M et al: Canadian Journal Biochemistry 57:822-833, 1979.

50) Tong, EK & Duckworth, HW: Biochemistry 14:235-241, 1975.

51) Weitzman, PDJ & Danson, MJ: Current Topics Cellular Regulation 10:161-204, 1976.

52) Weitzman, PDJ & Jones, D: Nature 219:270-272, 1968.

53) Weitzman, PDJ: Biochim. Biophys. Acta 128:213-215, 1966a.

54) Weitzman, PDJ: Biochemical Journal 101:44c-46c, 1966b.

55) Wiegand, G & Remington, SJ: Ann. Rev. Biophys. Biophys. Chem. 15:97-117, 1986.

56) Wiegand, G et al: Journal Molecular Biology 174:205-219, 1984.

57) Wood, DO et al: Journal Bacteriology 169:3564-3572, 1987.

58) Wright, JA et al: Biochem. Biophys. Res. Commun. 29:34-38, 1967.

59) Wu, JY & Yang, JT: Journal Biological Chemistry 245:212-218, 1970.

60) Zoller, MJ & Smith, M: Nucleic Acids Research 10:6487-6500, 1982.

61) Zoller, MJ & Smith,M: Methods Enzymology 100:468-500, 1983.

62) Zoller, MJ & Smith, M: DNA 3:479-488, 1984.